



# Interference Alignment Techniques in Multi-Antenna Wireless Networks

**Author:**

Yang, Lu

**Publication Date:**

2015

**DOI:**

<https://doi.org/10.26190/unsworks/18126>

**License:**

<https://creativecommons.org/licenses/by-nc-nd/3.0/au/>

Link to license to see what you are allowed to do with this resource.

Downloaded from <http://hdl.handle.net/1959.4/54295> in <https://unsworks.unsw.edu.au> on 2024-04-28

# Interference Alignment Techniques in Multi-Antenna Wireless Networks

Lu Yang

A dissertation submitted to the Graduate Research School of  
The University of New South Wales  
in partial fulfillment of the requirements for the degree of

Doctor of Philosophy



School of Electrical Engineering and Telecommunications  
Faculty of Engineering

December 2014

## ABSTRACT

Due to the broadcast nature of wireless networks, users that share the same channel resources may cause severe interference to each other. Such inter-user interference becomes a bottleneck for improving the performance of networks. Recent advances in wireless communication technologies, such as interference alignment, has brought us new insights on interference management in wireless networks. Many new results have been obtained for a variety of networks, especially in terms of degrees of freedom (DoF), which can be seen as an accurate capacity approximation in high signal-to-noise ratio (SNR). However, there are still many important problems remaining unsolved. In this thesis, interference alignment techniques are further investigated in a number of multi-antenna wireless networks, which are multiple-input and multiple-output (MIMO) X channel, MIMO interference channel, and device-to-device (D2D) network.

First, a two-user MIMO X channel is studied. It is known that with conventional spatial interference alignment, i.e., linear interference alignment without symbol extension, the achievable DoF is no more than  $\lfloor D_{outer} \rfloor$ , where  $D_{outer}$  denotes the outer bound of DoF of MIMO X Channels. In this thesis, a spatial interference alignment and zero-forcing framework is proposed in combination with asymmetric complex signaling, which can achieve the DoF of  $\lfloor D_{outer} \rfloor + \frac{1}{2}$  if  $D_{outer} - \lfloor D_{outer} \rfloor \geq \frac{1}{2}$ , and  $\lfloor D_{outer} \rfloor$  otherwise. The result shows that the technique of asymmetric complex signaling, which was originally proposed for single-antenna systems, can be useful for MIMO channels, in particular when

symbol extensions are not allowed.

Second, the DoF region of 3-user MIMO interference channels is studied. The outer-bound of sum DoF of 3-user interference channels has been already known, but the complete DoF region remains unknown. In this thesis, an outer-bound of DoF region of 3-user interference channels is first derived. Then, a linear interference alignment scheme based on spatial interference alignment is proposed that can achieve all integer DoF inside the region. As a result, the region can be seen as both the sufficient and necessary condition for the feasibility of linear interference alignment based on spatial beamforming in 3-user interference channels.

The third work studies a MIMO D2D LAN underlying a MIMO cellular uplink, where multiple D2D users (DUs) intend to communicate with a D2D receiver. Two D2D communication schemes based on interference alignment are proposed to manage the interference between the two networks. In the first scheme, the interference signals from DUs are aligned in the orthogonal signal space of cellular links at the base station. Hence, the links of cellular users are completely free from interference. As a result, the DUs can improve the performance by simply increasing the transmitting power without concerning its impact on the cellular network. In the second scheme, the signals of DUs are allowed to span on some links of cellular users, but the peak interference power on each of the ‘interfered’ links is constrained under a certain threshold. In addition, the scheme can take advantage of multiuser diversity, i.e., the performance of D2D LAN can be improved with the increase of the number of DUs. Performance analysis shows that the interference generated on the cellular links is eliminated or well controlled, while the quality of service of the D2D LAN can also be guaranteed.

## ACKNOWLEDGEMENTS

First and foremost, I would like to express my deepest gratitude to my supervisor, Professor Wei Zhang, for his constant guidance, support, encouragement, and caring. He not only provides me with unreserved support and guidance in research, but also cares about me in other aspects of my life and always tries to help. Without him, I would have never made the academic progress. I feel honored to be one of his students, and feel lucky to have him as a mentor and friend in my life.

I sincerely thank Professor Syed Ali Jafar of University of California, Irvine, for his help and guidance on my work during my visit to his research group. I also would like to thank Professor Pak-Chung Ching of The Chinese University of Hong Kong, for his kind support and critical comments on my work during my visit to his research lab.

My gratitude extends to my friends and colleagues at UNSW. Many thanks to our former group members, Dr. Long Shi, Dr. Yi Lu, Dr. Zhe Wang, and Dr. Chao Zhai, who have helped me a lot when I joined the group. In addition, I would like to thank Rui Ma, Chenxi Liu, Wei Wang, Chiya Zhang, Shihao Yan, Yixuan Xie, Mengyu Huang, Tao Huang, Dr. Tao Yang, and Dr. Nan Yang. The time we spend together is precious and unforgettable. I wish all of them have a successful career and a happy life.

I would like to give my ultimate gratitude and deepest love to my family. I am very grateful to my parents for their unconditional support. They are

always there to encourage me and cheer me up. Finally, the love, understanding, endurance, and support of my wife Chao Zhang were the source of all my achievements.

# Contents

<b>Table of Contents</b>	<b>vii</b>
<b>Abbreviations</b>	<b>ix</b>
<b>List of Notations</b>	<b>x</b>
<b>List of Figures</b>	<b>xi</b>
<b>List of Tables</b>	<b>xii</b>
<b>List of Publications</b>	<b>xiii</b>
<b>1 Introduction</b>	<b>1</b>
1.1 Interference Alignment and Degrees of Freedom . . . . .	2
1.2 Challenges and Motivations . . . . .	5
1.3 Thesis Outline and Contributions . . . . .	7
<b>2 Interference Alignment in Two-User MIMO X Channels</b>	<b>9</b>
2.1 Introduction . . . . .	9
2.2 Main Concepts . . . . .	10
2.2.1 Degrees of Freedom . . . . .	10
2.2.2 Asymmetric Complex Signaling . . . . .	11
2.3 System Model . . . . .	13
2.4 Interference Alignment with Asymmetric Complex Signaling . . . . .	14
2.4.1 Transmit Signals . . . . .	14
2.4.2 Design of Precoding Vectors . . . . .	16
2.4.3 Linear Independence . . . . .	19
2.5 Achievable Degrees of Freedom . . . . .	24
2.6 Summary . . . . .	27
2.7 Appendix A: Proof of Lemma 2.1 . . . . .	28
2.8 Appendix B: Proof of Theorem 2.1 . . . . .	30
2.8.1 $M_1 \geq M_2 \geq N_1 \geq N_2$ . . . . .	30
2.8.2 $M_1 \geq N_1 \geq M_2 \geq N_2$ . . . . .	32
2.8.3 $N_1 \geq M_1 \geq M_2 \geq N_2$ . . . . .	33

<b>3</b>	<b>Interference Alignment in Three-User MIMO Interference Channels</b>	<b>35</b>
3.1	Introduction . . . . .	35
3.2	System Model and Main Result . . . . .	37
3.3	A Beamforming Scheme . . . . .	40
3.3.1	Subspace Alignment Chain [22] . . . . .	40
3.3.2	A Beamforming Scheme . . . . .	42
3.4	Achievable Degrees of Freedom Region . . . . .	51
3.4.1	Bounds of $d_i + d_j + d_k$ . . . . .	52
3.4.2	Bounds of $d_i + d_j$ and $d_i$ . . . . .	53
3.5	Achieving Fractional DoF with Symbol Extension . . . . .	59
3.6	Summary . . . . .	64
3.7	Appendix A: Proof of Theorem 3.1 . . . . .	64
3.8	Appendix B: Derivation of (3.42)-(3.45) . . . . .	68
3.9	Appendix C: Derivation of (3.61) . . . . .	69
3.10	Appendix D: Discussion on achievable DoF region for $\frac{3t-2}{3t-1} \leq \frac{M}{N} < \frac{3t-1}{3t}$ . . . . .	70
3.11	Appendix E: Proof of $\bar{Q}_i \geq 0$ . . . . .	71
3.12	Appendix F: Proof of the redundancy of (3.70) . . . . .	72
<b>4</b>	<b>Device-to-Device LAN Underlying Cellular Network</b>	<b>74</b>
4.1	Introduction . . . . .	74
4.2	System Model . . . . .	77
4.3	Interference-Free IA Scheme . . . . .	79
4.3.1	Design Process . . . . .	79
4.3.2	Performance of Cellular Network . . . . .	82
4.3.3	Performance of D2D LAN . . . . .	83
4.3.4	Discussion . . . . .	84
4.4	Interference-limiting IA scheme . . . . .	85
4.4.1	Design Process . . . . .	85
4.4.2	Performance of Cellular Network . . . . .	86
4.4.3	Performance of D2D LAN . . . . .	87
4.4.4	Discussion . . . . .	88
4.5	Simulation Results . . . . .	88
4.6	Summary . . . . .	92
<b>5</b>	<b>Conclusion and Future Work</b>	<b>96</b>
5.1	Thesis Conclusion . . . . .	96
5.2	Future Work . . . . .	97
	<b>Bibliography</b>	<b>99</b>

# Abbreviations

<b>ACK</b>	Acknowledgement
<b>IA</b>	Interference alignment
<b>DoF</b>	Degrees of freedom
<b>SNR</b>	Signal-to-noise ratio
<b>MIMO</b>	Multiple-input and multiple-output
<b>i.i.d</b>	Independent and identical distribution
<b>D2D</b>	Device-to-device
<b>LAN</b>	Local area network
<b>DU</b>	Device-to-device user
<b>OFDM</b>	Orthogonal frequency division multiplexing
<b>TDMA</b>	Time division multiple access
<b>BS</b>	Base station
<b>eNB</b>	evolved nodeB
<b>CU</b>	cellular user
<b>QoS</b>	Quality of service
<b>SINR</b>	Signal-to-interference-noise ratio
<b>SLNR</b>	Signal-to-leakage-noise ratio
<b>DR</b>	Device-to-device receiver
<b>UE</b>	User equipment
<b>CDF</b>	Cumulative distribution function
<b>PDF</b>	Probability density function
<b>CSI</b>	Channel state information

# List of Notations

$C(\rho)$	sum capacity of the network with signal-to-noise ratio equals $\rho$
$R_m$	the rate of the codeword encoding the message $m$
$\log_2$	logarithm with base two
$\mathbb{C}^{a \times b}$	$a \times b$ matrix with complex entries
$\mathbb{R}^{a \times b}$	$a \times b$ matrix with real entries
$\text{Re}(\cdot)$	real part of a complex number
$\text{Im}(\cdot)$	imaginary part of a complex number
$ \cdot $	determinant of a matrix
$\det\{\cdot\}$	determinant of a matrix
$ \cdot ^2$	inner product of a vector
$(\cdot)^T$	transpose
$(\cdot)^H$	conjugate transpose
$\mathbf{j}$	the imaginary unit $\mathbf{j} = \sqrt{-1}$
$\max\{\cdot\}$	maximization
$\max\{a, b\}$	the maximum number among $a$ and $b$
$\min\{\cdot\}$	minimization
$\min\{a, b\}$	the minimum number among $a$ and $b$
mod	modulo operation
$\text{E}\{\cdot\}$	mathematical expectation

# List of Figures

1.1	TDMA transmission scheme . . . . .	3
1.2	Interference alignment transmission scheme [3] . . . . .	4
2.1	$2 \times 2$ MIMO $X$ channel ( $M_1, M_2, N_1, N_2$ ) . . . . .	13
4.1	D2D LAN underlying a cellular uplink network . . . . .	77
4.2	Outage probability of cellular link with ‘interference-free’ IA scheme. . . . .	89
4.3	Outage probability of D2D link with ‘interference-free’ IA scheme. . . . .	90
4.4	Number of qualified D2D users. . . . .	91
4.5	Outage probability of each interfered cellular link. . . . .	92
4.6	Achievable sum rate of D2D LAN. . . . .	93

# List of Tables

2.1	The achievable DoF for three types of antenna configurations . . . . .	26
2.2	The achievable DoF for other three types of antenna configurations . . . . .	26

# List of Publications

## Journal Papers:

1. **L. Yang** and W. Zhang, "Interference alignment with asymmetric complex signaling on MIMO X channels," *IEEE Trans. on Communications*, vol. 62, no. 10, pp. 3560-3570, Oct. 2014.
2. **L. Yang** and W. Zhang, "On degrees of freedom region of three-user MIMO interference channels," *IEEE Trans. on Signal Processing*, vol. 63, no. 3, pp. 590-603, Feb. 2015.
3. **L. Yang**, W. Zhang and S. Jin, "Interference alignment in device-to-device LAN underlying cellular networks," *IEEE Trans. on Wireless Communications*, accepted for publication.

## Conference Papers:

1. **L. Yang** and W. Zhang, "On design of asymmetric interference alignment and cancelation scheme in MIMO X network," in *Proc. IEEE International Conference on Wireless Communications and Signal Processing (WCSP 2011)*, Nanjing, China, Nov. 9-11, 2011.
2. **L. Yang** and W. Zhang, "Asymmetric interference alignment and cancelation for 3-user MIMO interference channel," in *Proc. IEEE International Conference on Communications (ICC 2012)*, Ottawa, Canada, June 10-15, 2012, pp. 2260-2264.
3. **L. Yang** and W. Zhang, "Opportunistic interference alignment in heterogeneous two-cell uplink network," in *Proc. IEEE International Conference on Communications (ICC 2013)*, Budapest, Hungary, June 9-13, 2013, pp. 5448-5452.
4. **L. Yang**, W. Zhang and S. Jafar, "Degrees of freedom region of 3-user interference channels," in *Proc. IEEE Global Communications Conference (Globecom 2013)*, Atlanta, GA, USA, Dec. 9-13, 2013, pp. 1791-1795.

5. **L. Yang**, W. Zhang, N. Zheng, P. C. Ching, “Opportunistic user scheduling in MIMO cognitive radio networks,” in *Proc. IEEE International Conference on Acoustics, Speech and Signal Processing (ICASSP 2014)*, Florence, Italy, May 4-9, 2014, pp. 7303-7307.
6. **L. Yang** and W. Zhang, “On achievable degrees of freedom of 3-user MIMO interference channels,” in *Proc. IEEE Information Theory Workshop (ITW 2014)*, Hobart, Tasmania, Australia, Nov. 2-5, 2014, pp. 98-102.
7. **L. Yang** and W. Zhang, “Interference alignment in device-to-device LAN underlaying cellular network,” in *Proc. IEEE International Conferences on Communication Systems (ICCS 2014)*, Macau, China, Nov. 19-21, 2014, pp. 21-25.
8. **L. Yang** and W. Zhang, “Degrees of freedom of relay-assisted MIMO interfering broadcast channels,” in *Proc. IEEE Global Communications Conference (Globecom 2014)*, Austin, TX, USA, Dec. 8-12, 2014, pp. 3833-3837.

# Chapter 1

## Introduction

Driven by the increasing demands for high-rate data transmission and high-quality communications, wireless communication technologies has been investigated and advanced for decades. Recently, the fourth generation wireless network has been deployed and almost reached saturation. With advanced technologies such as OFDM, capacity and performance of cellular networks have been largely improved. However, due to the extensive use of smartphones, Tablets, and video streaming, the wireless data explosion will continue, which necessitates the new research and development of more advanced wireless communication schemes and technologies.

One key issue for the development of current and future wireless networks is the high density of wireless devices. With limited radio spectrum, many wireless users are bound to share the same resources in time and/or frequency domain. As a result, the interference among devices becomes inevitable. In fact, such mutual interference is one major bottleneck that limits the capacity of cellular network. Lots of research effort have been made to investigate interference management techniques. Thanks to the use of multiple antennas on devices, beamforming has been shown as an effective technique for interference management, i.e., the direction of transmitted signals is steered so that their negative effect on receivers can be minimized [1,2]. As a typical type of beamforming, interference alignment (IA) has recently been proposed [3,4].

Based on this idea, many surprising results are obtained, especially in terms of degrees of freedom.

In this chapter, the concepts of degrees of freedom and IA are first introduced in Section 1.1. Then, some challenging issues and our motivations are discussed in Section 1.2. Finally, the outline and contribution of the thesis are presented in Section 1.3.

## 1.1 Interference Alignment and Degrees of Freedom

It was known that the capacity of a point-to-point MIMO system with  $M$  inputs and  $N$  outputs increases linearly as  $\min\{M, N\}$  at high signal-to-noise ratio (SNR) [5, 6, 20]. MIMO systems offer the possibility of multiplexing signals in space.

Degrees of freedom (DoF), also known as multiplexing gain, is a fundamental parameter that measures the number of spatial signaling dimensions that are accessible in the network. Theoretically, DoF is defined as [20]

$$d \triangleq \lim_{\rho \rightarrow \infty} \frac{C(\rho)}{\log_2(\rho)} \quad (1.1)$$

where  $C(\rho)$  is the sum capacity of the network with SNR  $\rho$ . As can be seen, DoF provides accurate capacity approximation in high SNR region. For interference networks, where multiple transmitters send signals to their respect receivers simultaneously, the characterization of DoF is very challenging. The emergence of IA brings a new tool to tackle this problem.

We first use an example in [3] to explain the basic concept of IA. Three transmitters,  $T_1$ ,  $T_2$ , and  $T_3$ , communicate with three receivers,  $R_1$ ,  $R_2$ , and  $R_3$ , respectively. The signal from one transmitter constitutes interference on two unintended receivers. Conventionally, orthogonal transmission scheme such as TDMA [7] can be used for medium access, i.e., each transmitter-receiver pair transmits in one third of entire period of time while other two pairs remain silent. As a result, each pair can have

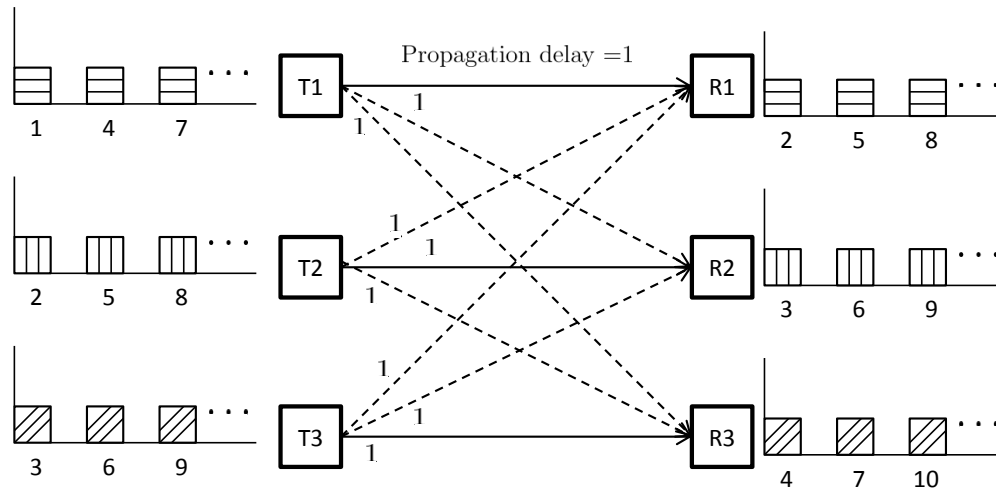


**Figure 1.1** TDMA transmission scheme

one third of the transmission time. The TDMA transmission is shown in Fig. 1.1. Now, it is interesting to know if we can do better than that. In [3], it is assumed that the propagation delay can be controlled so that the delay from one transmitter to the intended receiver is one symbol period, whereas to its unintended receivers is two symbol period. Then, each transmitter only transmits at odd time slots and remains silent at even time slots. Consequently, at each receiver, the desired signal arrives at even time slots while all interference signals are received only at odd time slots, as shown in Fig. 1.2, which is on top of next page. In that case, each transmitter-receiver pair can have half of the degrees of freedom, which is more efficient than TDMA. At each receiver, the two interference signals are aligned at the same time slots, which is referred to as interference alignment. As we can see, the above artificial delay model is not realistic. However, the IA is not limited in time. It can be also implemented in space, frequency, or even signal domains. According to [9], IA is defined as a construction of signals in a way that they cast overlapping shadows at the receivers where they constitute interference, while remaining distinguishable at the receivers where they are desired.

In general, IA schemes can be broadly classified into two categories, which are signal vector space IA [3, 8–10, 18–23, 25, 26] and signal level IA [12–17]. Specifically,

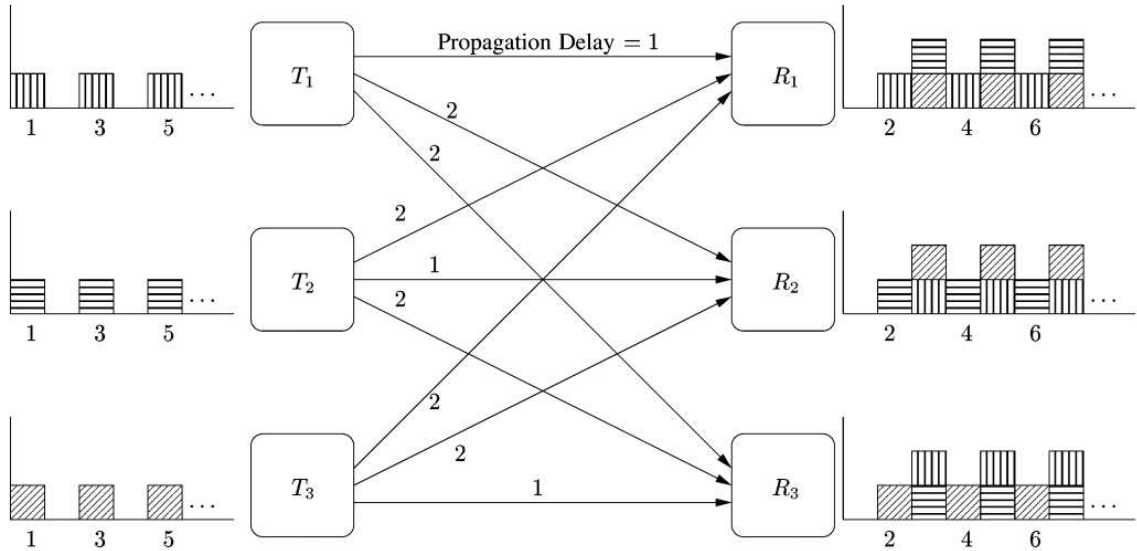


**Figure 1.2** Interference alignment transmission scheme [3]

in signal vector space IA, by exploiting the distinct linear transformation (channel matrix) between each transmitter-receiver pair, the transmitters perform linear precoding to rotate the signal vectors on each link. This type of IA inherits the advantages of linear processing. It is tractable, linearly decodable, and applicable for any channels [10]. On the other hand, signal-level IA uses structured coding to align interference in the signal-level space. The advantage of signal-level IA is that it does not need the distinct rotation of channel matrices, which may not always be available. Since signal-level IA is derived from the deterministic channel model in [11], they are most suitable for channels with real coefficients. Moreover, the decoding methods for signal-level IA are more complicated due to the non-linear effect.

Within the class of signal vector space IA schemes, it can be further divided into two types, which are linear spatial IA with and without symbol extensions. Linear spatial IA refers to alignment based on spatial beamforming through multiple antennas [25], and symbol extension refers to beamforming over multiple channel uses in time or frequency [3]. In spite of the obvious advantage of symbol extension, which is to take advantage of time (or frequency) dimensions, it has its own limitations, such as the added complexity of dealing with block diagonal channel matrices [21], or

the need to “predict” the channel information under time-varying channel scenarios. Therefore, many recent research focused on the design of linear IA schemes based on spatial beamforming only [9, 19, 25–28]. In addition, the DoF achievable through linear spatial IA is referred to as ‘feasibility of IA’ [25].

## 1.2 Challenges and Motivations

In recent years, IA has been widely studied and utilized in the DoF characterization of a variety of networks, including MIMO X networks [4, 8, 9, 18, 19], interference channels [10, 20–29], cellular networks [30–34], cognitive radio networks [35, 36, 38], multi-hop networks [39–42], and storage system [43], etc. Among these networks, the X channels and interference channels are the most elementary and fundamental models, i.e., they are the core networks of many communication networks in practice. Hence, the understanding of X channels and interference channels is of great importance.

A  $K \times L$  X network is defined as a communication network with  $K$  transmitters and  $L$  receivers and a total of  $KL$  independent messages, one from each transmitter to each receiver. As we can see, the X network is the most generalized model as it encompasses all types of networks such as interference channels, broadcast channels, multiple access channels. The DoF characterization of  $2 \times 2$  X channels with  $M$  and  $N$  antennas on each transmitter and receiver, respectively was studied in [8]. Then, the concept of IA in  $2 \times 2$  X channel was crystalized in [4, 9]. The outer bound of DoF of the  $2 \times 2$  X channels with arbitrary number of antennas on each node was derived in [9], and it was also shown to be achievable with linear spatial beamforming in combination with symbol extensions. Meanwhile, the DoF of general  $K \times L$  X networks was investigated in [18, 19], where each node has the same number of antennas. Let us consider the  $2 \times 2$  X channel model. As we can see, even though the outer bound DoF, denoted as  $D_{outer}$ , can be achieved, it requires symbol extensions. When symbol extension is not allowed, the achievable DoF with existing linear spatial IA schemes is not more than  $\lfloor D_{outer} \rfloor$  [4, 9]. It remains unknown if the achievable DoF

can be higher than  $\lfloor D_{outer} \rfloor$ .

A  $K$ -user interference channel is comprised of  $K$  transmitters and  $K$  receivers, where each transmitter has message only for one corresponding receiver, and causes interference to other receivers. Interference channel is the most classic and elementary model. For 2-user interference channels with arbitrary number of antennas on each node, the DoF was fully characterized in [20], i.e., not only the outer bound DoF was derived, but also shown to be achievable with linear spatial beamforming schemes. However, when the number of users is more than 2, i.e.,  $K \geq 3$ , the model becomes too complicated to deal with because of the massive amount of variables associated with signal dimensions. Hence, for  $K \geq 3$ , we only focus on the symmetric scenario where each transmitter and each receiver has  $M_T$  and  $M_R$  antennas, respectively. Even for this setup, the results of general  $K$ -user interference channels are very limited, i.e., it was shown in [21] that if  $\eta = \frac{\max(M_T, M_R)}{\min(M_T, M_R)}$  is an integer, each user can achieve DoF of  $\min(M_T, M_R) \frac{\eta}{\eta+1}$  when  $K > \eta$ . In [22], the outer bound DoF of each user for 3-user interference channels was derived as  $DoF^*$ , where

$$DoF^* = \min\left\{\frac{\kappa}{2\kappa-1}M, \frac{\kappa}{2\kappa+1}N\right\} \quad (1.2)$$

with  $N = \max\{M_T, M_R\}$ ,  $M = \min\{M_T, M_R\}$  and  $\kappa = \lceil \frac{M}{N-M} \rceil$ . Accordingly, the outer-bound of the sum DoF of the network is equal to  $3DoF^*$ . Moreover, in terms of feasibility of IA, it was shown in [22, 29] that if each user has the same DoF  $d$ , IA is feasible if and only if  $d \leq \lfloor DoF^* \rfloor$ .

However, in spite of these achievements, the DoF characterization is still not completed even for 3-user interference channel. The key issue is that the ‘sum’ DoF is not equivalent to the DoF region. If we see the DoF of each user as one coordinate, the DoF region of 3-user interference channel would be a 3-dimensional space that is closed by multiple planes. Let  $d_i$  denote the DoF of user  $i$  ( $i = 1, 2, 3$ ). The outer bound of sum DoF  $\sum_{i=1}^3 d_i = 3DoF^*$  can be seen as one plane, and the space under the plane,  $\sum_{i=1}^3 d_i \leq 3DoF^*$ , can certainly be seen as an outer bound of DoF region. However, this region is too loose. Hence, the DoF region of 3-user interference

channel still remains unknown. Another related problem is the feasibility condition of IA. Although the feasibility condition is known for each user having the same DoF, it is unknown if the users are allowed to have different DoF.

IA is not only a powerful tool for theoretical research, but also has great potential to be applied in modern communication technologies [44–47]. With the 4G networks reaching saturation, the discussion about possible 5G standard has promoted newly emerged communication technologies that could be implemented in 5G networks [48], such as millimeter wave [49–51], massive MIMO [52, 53], and device-to-device (D2D) communications [54–56], etc. Among all these technologies, D2D communication shows great potential to be compatible with IA for two reasons. First, D2D communication is in need of an effective interference management mechanism to coordinate the mutual interference between D2D communication and cellular network [56–58]. Meanwhile, IA is well known for its effectiveness in interference management. Secondly, since D2D communication is also a part of cellular network operation, it can be monitored and controlled with base station (BS) [59, 62]. Hence, the BS can allocate the required information (such as channel state information) to different devices, which facilitates the feasibility of IA.

### 1.3 Thesis Outline and Contributions

This thesis aims to design IA in MIMO X channel and 3-user interference channels. Further, the application of IA in D2D communications is investigated.

In Chapter 2, we investigate the achievable DoF of MIMO X channels. A linear IA scheme based on spatial beamforming is proposed to achieve the DoF of  $\frac{1}{2}\lfloor 2D_{outer} \rfloor$  for arbitrary number of antennas on each node. Note that with conventional spatial beamforming schemes, only  $\lfloor D_{outer} \rfloor$  DoF can be achieved, which is less than or equal to  $\frac{1}{2}\lfloor 2D_{outer} \rfloor$ . The key of our proposed scheme is to transform the generic complex channel matrices into double-sized equivalent real channel matrices with asymmetric complex signaling, which improves the achievable DoF.

In Chapter 3, we study the DoF region of 3-user interference channels. An outer bound DoF region is derived and shown to be tight in terms of integer DoF, i.e., the points with integer coordinates in the region are achievable for sure. In addition, the achievability of fractional DoF is also discussed. Further, according to the definition of feasibility of interference alignment [25], the exact feasibility condition of a 3-user interference channel when each user can have different DoF is in fact equivalent to our derived DoF region, because all the points with integer coordinates in the region can be achieved with a linear scheme based on spatial beamforming only.

In Chapter 4, we explore the possibility of applying IA in D2D communications. We focus on a D2D LAN underlaying a cellular uplink, where multiple D2D users (DUs) intend to communicate with a D2D receiver. Two IA based D2D communication schemes are proposed to manage the interference between two networks. The first scheme is referred as ‘interference-free’ IA scheme, in which the interference signals from DUs are designed to be aligned in the orthogonal signal space of cellular links at the evolved NodeB (eNB), so that the links of cellular users (CUs) are completely free from interference. The second scheme is referred as ‘interference-limiting’ IA scheme. In this scheme, the DUs’ signals are allowed to span on some links of CUs, but the peak interference power on each of the ‘interfered’ links is limited. The application scenarios of these two schemes are complementary to each other. Performance analysis shows that the interference generated on the cellular links is eliminated or well controlled, while the quality of service of the D2D LAN can also be guaranteed.

In Chapter 5, the thesis conclusion and perspectives for future work are presented.

## Chapter 2

# Interference Alignment in Two-User MIMO X Channels

### 2.1 Introduction

The outer bound DoF of  $2 \times 2$  MIMO X channels is shown to be achievable with linear spatial IA in combination with symbol extensions [9]. However, due to the limitations of symbol extensions, it is essential to characterize the achievable DoF based on linear spatial IA only.

The spatial beamforming schemes on MIMO X channels was first studied in [4], in which some linear filters were employed at transmitters and receivers to decompose the system into either two noninterfering multiple-antenna broadcast sub-channels or two noninterfering multiple-antenna multiple-access sub-channels. Then, with the use of spatial interference alignment, some surprisingly high DoF was obtained. In particular, it was shown in [4] that if transmitters 1 and 2 are equipped with  $\lceil \frac{1}{2} \lfloor \frac{4N}{3} \rfloor \rceil$  and  $\lfloor \frac{1}{2} \lfloor \frac{4N}{3} \rfloor \rfloor$  antennas, respectively and each receiver is equipped with  $N$  antennas, the DoF of  $\lfloor \frac{4N}{3} \rfloor$  can be achieved. This spatial IA scheme was then crystalized in [9] to achieve the DoF of  $\lfloor D_{outer} \rfloor$ , where  $D_{outer}$  denotes the outer bound of DoF. As we can see, the DoF achievable through conventional spatial IA schemes is at most

$\lfloor D_{outer} \rfloor$  when symbol extensions are not used. This argument has also been studied as the topic of feasibility of IA in [9, 19].

In this Chapter, we propose a linear interference alignment and zero-forcing framework that is applied for all antenna configurations with complex channel coefficients. The framework utilizes spatial beamforming and *asymmetric complex signaling* [24] and does not need the symbol extension. We show that for all antenna configurations, our proposed scheme is able to achieve the DoF of  $\frac{1}{2} \lfloor 2D_{outer} \rfloor$  without the use of symbol extensions, which is equal to or larger than  $\lfloor D_{outer} \rfloor$ . In addition, one key step in our proposed scheme is to transform the generic complex channel matrices into double-sized equivalent channel matrices with real entries. Because of the use of asymmetric complex signaling, all equivalent real channel matrices must have the same quaternion structure and hence lose the generic nature. We further show that the real equivalent channels created by asymmetric complex signaling can still behave like generic channels when symbol extension is not allowed.

The paper is organized as follows. In Section 2.2, some main concepts incorporated in the scheme are presented. In Section 2.3, the system model is introduced. In Section 2.4, an interference alignment and zero-forcing scheme with asymmetric complex signaling is proposed. In Sections 2.5, the achievable DoF of the MIMO X channels are investigated according to different antenna configurations. Section 2.6 summarizes the chapter.

## 2.2 Main Concepts

### 2.2.1 Degrees of Freedom

The DoF value of a symbol  $m$  transmitted in the system is defined as [18]

$$d_m = \lim_{\rho \rightarrow \infty} \frac{R_m(\rho)}{\log_2 \rho} \quad (2.1)$$

where  $\rho$  denotes the power constraint of the symbol and  $R_m(\rho)$  represents the rate of the codeword encoding the message  $m$ . Consider a single user point-to-point channel

where the transmitted constellation  $\mathcal{U}(-Q, Q)_{\mathbb{Z}} = \{-Q, -Q + 1, \dots, -1, 1, \dots, Q - 1, Q\}$  ( $Q$  is an integer) is used for a single message. Since it is assumed that the additive noise has unit variance and the minimum distance in the received constellation is, the same as transmitted constellation, also one, the noise can be treated as removable [14]. Therefore  $R_m \approx \log_2 2Q$  is achievable for the channel. In addition, the power constraint should be no less than  $Q^2$ . Hence,  $\rho = Q^2$ , and the DoF associated with the symbol can be calculated as

$$d_m = \lim_{Q \rightarrow \infty} \frac{\log_2(2Q)}{\log_2 Q^2} = \frac{1}{2} \quad (2.2)$$

If the symbol ( $m = u + \mathbf{j}v$ ) is modulated with a two-dimensional constellation  $\mathcal{U} = \mathcal{V} = (-Q, Q)_{\mathbb{Z}} = \{-Q, -Q + 1, \dots, -1, 1, \dots, Q - 1, Q\}$ , the rate will be  $R_m = 2 \log_2(2Q)$ . Since the power constraint is  $2Q^2$ , each message carries 1 DoF, i.e.,

$$d_m = \lim_{Q \rightarrow \infty} \frac{2 \log_2(2Q)}{\log_2 2Q^2} = 1 \quad (2.3)$$

In this paper, it is assumed that each symbol has only one dimension (real), which means each symbol contains  $\frac{1}{2}$  DoF.

### 2.2.2 Asymmetric Complex Signaling

In wireless communication, we usually deal with symmetric complex Gaussian random variables such as additive noise, fading channels, and so are the input signals, whose real and imaginary parts are independent of each other. Inspired by [24], we use asymmetric complex signaling in our scheme, in which the input signals are chosen to be complex but not symmetric. By doing so, an  $M$ -dimensional complex system can be transformed into a  $2M$ -dimensional real system.

For instance, we consider a MIMO point-to-point channel with one antenna at each side. Let  $\mathbf{x} \in \mathbb{C}$  denote the transmitted signal which contains two symbols, and let  $\mathbf{y} \in \mathbb{C}$  denote the received signal. We have

$$\mathbf{y} = h^{11} \cdot \underbrace{(v_1 \cdot m_1 + v_2 \cdot m_2)}_{\mathbf{x}} \quad (2.4)$$

where  $v_1 \in \mathbb{C}$  and  $v_2 \in \mathbb{C}$  denote the precoders of  $m_1$  and  $m_2$ , respectively.  $m_1$  and  $m_2$  are both real, and  $h^{ij}$  denotes the complex channel coefficient from the  $j$ th transmit antenna to the  $i$ th receive antenna with phase  $\varphi^{ij}$ , which can be written as

$$h^{ij} = |h^{ij}|(\cos \varphi^{ij} + \mathbf{j} \sin \varphi^{ij}) \quad (2.5)$$

Since  $m_1$  and  $m_2$  are real, (2.4) can be expressed alternatively as a real system, i.e.,

$$\begin{aligned} \bar{\mathbf{y}} &= \begin{bmatrix} \text{Re}(\mathbf{y}) \\ \text{Im}(\mathbf{y}) \end{bmatrix} \\ &= |h^{11}| \begin{bmatrix} \cos \varphi^{11} & -\sin \varphi^{11} \\ \sin \varphi^{11} & \cos \varphi^{11} \end{bmatrix} \times \left( \begin{bmatrix} \text{Re}(v_1) \\ \text{Im}(v_1) \end{bmatrix} m_1 + \begin{bmatrix} \text{Re}(v_2) \\ \text{Im}(v_2) \end{bmatrix} m_2 \right) \end{aligned} \quad (2.6)$$

where  $\text{Re}(v)$  and  $\text{Im}(v)$  denote real and imaginary parts of  $v$ , respectively. It can be seen that the  $1 \times 1$  complex system is turned into a  $2 \times 2$  real system, and both  $m_1$  and  $m_2$  can be linearly decoded from (2.6).

$$\text{Note that for a complex channel matrix } \mathbf{H} \in \mathbb{C}^{n \times m}, \text{ where } \mathbf{H} = \begin{bmatrix} h^{11} & \dots & h^{1m} \\ \vdots & \ddots & \vdots \\ h^{n1} & \dots & h^{nm} \end{bmatrix},$$

its equivalent real channel matrix  $\hat{H}$  can be expressed as follows,

$$\hat{H} = \begin{bmatrix} \hat{h}^{11} & \dots & \hat{h}^{1m} \\ \vdots & \ddots & \vdots \\ \hat{h}^{n1} & \dots & \hat{h}^{nm} \end{bmatrix} \quad (2.7)$$

where  $\hat{h}^{ij} = |h^{ij}| \begin{bmatrix} \cos \varphi^{ij} & -\sin \varphi^{ij} \\ \sin \varphi^{ij} & \cos \varphi^{ij} \end{bmatrix}$  for  $i = 1, 2, \dots, n$  and  $j = 1, 2, \dots, m$ .

Obviously, the equivalent channel matrix  $\hat{H}$  is no longer generic due to its quaternion structure. Hence, some arguments which are suitable for generic channels cannot be applied directly on such channels. For example, under generic channel conditions, if two signals from different transmitters are aligned at one receiver, they are almost surely independent of each other at other receivers because of the random nature

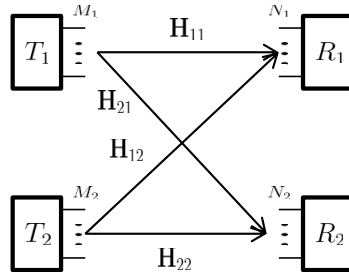


**Figure 2.1**  $2 \times 2$  MIMO X channel  $(M_1, M_2, N_1, N_2)$

of generic channels. However, such argument cannot be used directly if the channel matrices have quaternion structure.

## 2.3 System Model

We consider a  $2 \times 2$  MIMO X channel as depicted in Fig. 2.1. Transmitter  $T_t$  ( $t = 1, 2$ ) is equipped with  $M_t$  antennas and receiver  $R_r$  ( $r = 1, 2$ ) is equipped with  $N_r$  antennas. This configuration of antennas is denoted by  $(M_1, M_2, N_1, N_2)$ . In X channels, each transmitter has messages for both receivers. Without loss of generality, we assume  $M_1 \geq M_2$  and  $N_1 \geq N_2$ .

Let  $h_{rt}^{ij}$  denote the channel gain from the  $j$ th antenna of transmitter  $t$  to the  $i$ th antenna of receiver  $r$ . It can be expressed as

$$h_{rt}^{ij} = |h_{rt}^{ij}|(\cos \varphi_{rt}^{ij} + \mathbf{j} \sin \varphi_{rt}^{ij}) \quad (2.8)$$

where  $\varphi_{rt}^{ij}$  denotes the phase of  $h_{rt}^{ij}$ .

With asymmetric complex signaling, we can let  $\mathbf{H}_{rt}$  denote the channel matrix between transmitter  $t$  and receiver  $r$  and let  $\hat{H}_{rt}$  denote its equivalent form with real quantities. All the channel matrices are sampled from continuous complex Gaussian distributions and each entry of  $\mathbf{H}_{rt}$  is independent and identically distributed (i.i.d.). The global channel information is assumed to be available at all nodes.

Let  $\mathbf{m}_{rt}$  denote the message vector intended for receiver  $r$  from transmitter  $t$ . All elements of  $\mathbf{m}_{rt}$  (i.e., the symbol  $m_{rt}$ ) are set to be real, and then each carries  $\frac{1}{2}$  DoF

according to (2.2).

## 2.4 Interference Alignment with Asymmetric Complex Signaling

In this section, we first present signals design. Then, we investigate the conditions under which the signals are linear independent of each other at both receivers.

### 2.4.1 Transmit Signals

For each link, the transmit signals are divided into three groups. The signals design involves the use of three techniques, which are zero forcing, asymmetric complex signaling, and interference alignment.

There are two message vectors  $\mathbf{m}_{11}$  and  $\mathbf{m}_{21}$  to be sent from  $T_1$ , which are desired signals of  $R_1$  and  $R_2$ , respectively.

For  $\mathbf{m}_{11}$ , it has three blocks  $\mathbf{m}_{11}^1$ ,  $\mathbf{m}_{11}^2$  and  $\mathbf{m}_{11}^3$ , each having length  $L_1$ ,  $L_2$  and  $L_3$ , respectively, i.e.,

$$\mathbf{m}_{11} = \left[ \underbrace{(\mathbf{m}_{11}^1)^T}_{L_1} \quad \underbrace{(\mathbf{m}_{11}^2)^T}_{L_2} \quad \underbrace{(\mathbf{m}_{11}^3)^T}_{L_3} \right]^T \quad (2.9)$$

Further,  $\mathbf{m}_{11}^1$  is precoded with  $[\mathbf{v}_{11}^1 \cdots \mathbf{v}_{11}^{L_1}] \in \mathbb{C}^{M_1 \times L_1}$ ,  $\mathbf{m}_{11}^2$  is precoded with  $[\mathbf{w}_{11}^1 \cdots \mathbf{w}_{11}^{L_2}] \in \mathbb{C}^{M_1 \times L_2}$ , and  $\mathbf{m}_{11}^3$  is precoded with  $[\mathbf{u}_{11}^1 \cdots \mathbf{u}_{11}^{L_3}] \in \mathbb{C}^{M_1 \times L_3}$ . Then, the transmitted signal intended for  $R_1$  from  $T_1$  can be expressed as

$$\begin{aligned} \mathbf{x}_{11} &= \underbrace{\begin{bmatrix} \mathbf{v}_{11}^1 & \cdots & \mathbf{v}_{11}^{L_1} \end{bmatrix}}_{\mathbf{x}_{11}^1} \mathbf{m}_{11}^1 \\ &+ \underbrace{\begin{bmatrix} \mathbf{w}_{11}^1 & \cdots & \mathbf{w}_{11}^{L_2} \end{bmatrix}}_{\mathbf{x}_{11}^2} \mathbf{m}_{11}^2 \\ &+ \underbrace{\begin{bmatrix} \mathbf{u}_{11}^1 & \cdots & \mathbf{u}_{11}^{L_3} \end{bmatrix}}_{\mathbf{x}_{11}^3} \mathbf{m}_{11}^3 \end{aligned} \quad (2.10)$$

Similarly, we divide  $\mathbf{m}_{21}$  into three blocks  $\mathbf{m}_{21}^1$ ,  $\mathbf{m}_{21}^2$ , and  $\mathbf{m}_{21}^3$ , each having length  $K_1$ ,  $K_2$  and  $K_3$ , respectively, i.e.,

$$\mathbf{m}_{21} = \left[ \underbrace{(\mathbf{m}_{21}^1)^T}_{K_1} \quad \underbrace{(\mathbf{m}_{21}^2)^T}_{K_2} \quad \underbrace{(\mathbf{m}_{21}^3)^T}_{K_3} \right]^T \quad (2.11)$$

Furthermore,  $\mathbf{m}_{21}^1$  is precoded with  $[\mathbf{v}_{21}^1 \cdots \mathbf{v}_{21}^{K_1}]$ ,  $\mathbf{m}_{21}^2$  is precoded with  $[\mathbf{w}_{21}^1 \cdots \mathbf{w}_{21}^{K_2}]$ , and  $\mathbf{m}_{21}^3$  is precoded with  $[\mathbf{u}_{21}^1 \cdots \mathbf{u}_{21}^{K_3}]$ , respectively. Then, the transmitted signal intended to  $R_2$  from  $T_1$  can be written as

$$\begin{aligned} \mathbf{x}_{21} &= \underbrace{\left[ \mathbf{v}_{21}^1 \quad \cdots \quad \mathbf{v}_{21}^{K_1} \right]}_{\mathbf{x}_{21}^1} \mathbf{m}_{21}^1 \\ &+ \underbrace{\left[ \mathbf{w}_{21}^1 \quad \cdots \quad \mathbf{w}_{21}^{K_2} \right]}_{\mathbf{x}_{21}^2} \mathbf{m}_{21}^2 \\ &+ \underbrace{\left[ \mathbf{u}_{21}^1 \quad \cdots \quad \mathbf{u}_{21}^{K_3} \right]}_{\mathbf{x}_{21}^3} \mathbf{m}_{21}^3 \end{aligned} \quad (2.12)$$

At  $T_2$ , two message vectors  $\mathbf{m}_{12}$  and  $\mathbf{m}_{22}$  will be sent, which are the desired signals of  $R_1$  and  $R_2$ , respectively.

For  $\mathbf{m}_{12}$ , it is also divided into three blocks  $\mathbf{m}_{12}^1$ ,  $\mathbf{m}_{12}^2$  and  $\mathbf{m}_{12}^3$ , each having length  $J_1$ ,  $J_2$  and  $J_3$  respectively, i.e.,

$$\mathbf{m}_{12} = \left[ \underbrace{(\mathbf{m}_{12}^1)^T}_{J_1} \quad \underbrace{(\mathbf{m}_{12}^2)^T}_{J_2} \quad \underbrace{(\mathbf{m}_{12}^3)^T}_{J_3} \right]^T \quad (2.13)$$

We let  $\mathbf{m}_{12}^1$  be precoded with  $[\mathbf{v}_{12}^1 \cdots \mathbf{v}_{12}^{J_1}]$ ,  $\mathbf{m}_{12}^2$  be precoded with  $[\mathbf{w}_{12}^1 \cdots \mathbf{w}_{12}^{J_2}]$ , and  $\mathbf{m}_{12}^3$  be precoded with  $[\mathbf{u}_{12}^1 \cdots \mathbf{u}_{12}^{J_3}]$ . Then, the transmitted signal from  $T_2$  intended to  $R_1$  can be expressed as

$$\begin{aligned} \mathbf{x}_{12} &= \underbrace{\left[ \mathbf{v}_{12}^1 \quad \cdots \quad \mathbf{v}_{12}^{J_1} \right]}_{\mathbf{x}_{12}^1} \mathbf{m}_{12}^1 \\ &+ \underbrace{\left[ \mathbf{w}_{12}^1 \quad \cdots \quad \mathbf{w}_{12}^{J_2} \right]}_{\mathbf{x}_{12}^2} \mathbf{m}_{12}^2 \\ &+ \underbrace{\left[ \mathbf{u}_{12}^1 \quad \cdots \quad \mathbf{u}_{12}^{J_3} \right]}_{\mathbf{x}_{12}^3} \mathbf{m}_{12}^3 \end{aligned} \quad (2.14)$$

For  $\mathbf{m}_{22}$ , we divide the message vector into three blocks  $\mathbf{m}_{22}^1$ ,  $\mathbf{m}_{22}^2$  and  $\mathbf{m}_{22}^3$ , each having length  $G_1$ ,  $G_2$  and  $G_3$ , respectively, i.e.,

$$\mathbf{m}_{22} = \left[ \underbrace{(\mathbf{m}_{22}^1)^T}_{G_1} \quad \underbrace{(\mathbf{m}_{22}^2)^T}_{G_2} \quad \underbrace{(\mathbf{m}_{22}^3)^T}_{G_3} \right]^T \quad (2.15)$$

We let  $\mathbf{m}_{22}^1$  be precoded with  $[\mathbf{v}_{22}^1 \cdots \mathbf{v}_{22}^{G_1}]$ ,  $\mathbf{m}_{22}^2$  be precoded with  $[\mathbf{w}_{22}^1 \cdots \mathbf{w}_{22}^{G_2}]$ , and  $\mathbf{m}_{22}^3$  be precoded with  $[\mathbf{u}_{22}^1 \cdots \mathbf{u}_{22}^{G_3}]$ , respectively. Then, the transmitted signal intended to  $R_2$  from  $T_2$  can be expressed as

$$\begin{aligned} \mathbf{x}_{22} &= \underbrace{\begin{bmatrix} \mathbf{v}_{22}^1 & \cdots & \mathbf{v}_{22}^{G_1} \end{bmatrix}}_{\mathbf{x}_{22}^1} \mathbf{m}_{22}^1 \\ &+ \underbrace{\begin{bmatrix} \mathbf{w}_{22}^1 & \cdots & \mathbf{w}_{22}^{G_2} \end{bmatrix}}_{\mathbf{x}_{22}^2} \mathbf{m}_{22}^2 \\ &+ \underbrace{\begin{bmatrix} \mathbf{u}_{22}^1 & \cdots & \mathbf{u}_{22}^{G_3} \end{bmatrix}}_{\mathbf{x}_{22}^3} \mathbf{m}_{22}^3 \end{aligned} \quad (2.16)$$

If the desired signals are linear independent of each other at each receiver, the total DoF of the system can be calculated as

$$D_{sum} = \frac{\sum_{\gamma=1}^3 (L_\gamma + K_\gamma + J_\gamma + G_\gamma)}{2} \quad (2.17)$$

## 2.4.2 Design of Precoding Vectors

Next, we present the design of precoding vectors. We first examine the received signals at  $R_1$ . It can be expressed as

$$\begin{aligned} \mathbf{Y}_1 &= \mathbf{H}_{11}(\mathbf{x}_{11}^1 + \mathbf{x}_{11}^2 + \mathbf{x}_{11}^3) + \mathbf{H}_{12}(\mathbf{x}_{12}^1 + \mathbf{x}_{12}^2 + \mathbf{x}_{12}^3) \\ &+ \underbrace{\mathbf{H}_{11}(\mathbf{x}_{21}^1 + \mathbf{x}_{21}^2 + \mathbf{x}_{21}^3) + \mathbf{H}_{12}(\mathbf{x}_{22}^1 + \mathbf{x}_{22}^2 + \mathbf{x}_{22}^3)}_{\text{interference}} + \mathbf{z}_1 \end{aligned} \quad (2.18)$$

where  $\mathbf{z}_r$  denotes the noise vector at receiver  $r$  ( $r = 1, 2$ ).

It can be seen that  $\mathbf{x}_{21}^1$ ,  $\mathbf{x}_{21}^2$ ,  $\mathbf{x}_{21}^3$ , and  $\mathbf{x}_{22}^1$ ,  $\mathbf{x}_{22}^2$ ,  $\mathbf{x}_{22}^3$  are the desired signals for  $R_2$ , but also the interference for  $R_1$ .

In order to cancel the interference  $\mathbf{x}_{21}^1, \mathbf{x}_{21}^2$  and  $\mathbf{x}_{22}^1, \mathbf{x}_{22}^2$  at  $R_1$ , we let

$$\begin{aligned}\mathbf{H}_{11} \begin{bmatrix} \mathbf{v}_{21}^1 & \cdots & \mathbf{v}_{21}^{K_1} \end{bmatrix} &= \mathbf{0} \\ \mathbf{H}_{11} \begin{bmatrix} \mathbf{w}_{21}^1 & \cdots & \mathbf{w}_{21}^{K_2} \end{bmatrix} &= \mathbf{0}\end{aligned}\quad (2.19)$$

and

$$\begin{aligned}\mathbf{H}_{12} \begin{bmatrix} \mathbf{v}_{22}^1 & \cdots & \mathbf{v}_{22}^{G_1} \end{bmatrix} &= \mathbf{0} \\ \mathbf{H}_{12} \begin{bmatrix} \mathbf{w}_{22}^1 & \cdots & \mathbf{w}_{22}^{G_2} \end{bmatrix} &= \mathbf{0}\end{aligned}\quad (2.20)$$

These can be achieved by letting

$$\mathbf{v}_{21}^1, \dots, \mathbf{v}_{21}^{K_1} \subset \text{span}\{\mathbf{P}_{11}\} \quad (2.21)$$

$$\mathbf{w}_{21}^k = \mathbf{j} \cdot \mathbf{v}_{21}^k, \quad k = 1, 2, \dots, K_2. \quad (2.22)$$

$$\mathbf{v}_{22}^1, \dots, \mathbf{v}_{22}^{G_1} \subset \text{span}\{\mathbf{P}_{12}\} \quad (2.23)$$

$$\mathbf{w}_{22}^g = \mathbf{j} \cdot \mathbf{v}_{22}^g, \quad g = 1, 2, \dots, G_2 \quad (2.24)$$

where  $\mathbf{P}_{rt}$  denotes the null space of  $\mathbf{H}_{rt}$ .

For each channel matrix  $\mathbf{H}_{rt}$ , there are  $(M_t - N_r)^+$  independent column vectors in its null space  $\mathbf{P}_{rt}$ . In order to satisfy (2.21)-(2.24), we can set

$$K_2 \leq K_1 \leq (M_1 - N_1)^+ \quad (2.25)$$

$$G_2 \leq G_1 \leq (M_2 - N_1)^+ \quad (2.26)$$

where  $(x)^+ = \max\{x, 0\}$ .

In addition, we want interference  $\mathbf{x}_{21}^3$  to be aligned with interference  $\mathbf{x}_{22}^3$  at  $R_1$ .

If  $N_1 \leq M_1$ , we first design  $\mathbf{u}_{22}$  to satisfy following conditions.

$$\mathbf{u}_{22}^1, \dots, \mathbf{u}_{22}^{\lceil \frac{G_3}{2} \rceil} \not\subset \text{span}\{\mathbf{P}_{12}\} \quad (2.27)$$

$$\mathbf{u}_{22}^{\lceil \frac{G_3}{2} \rceil + e} = \mathbf{j} \cdot \mathbf{u}_{22}^e, \quad e = 1, \dots, \lfloor \frac{G_3}{2} \rfloor \quad (2.28)$$

In the above, Eq. (2.27) guarantees the message signals precoded by  $\mathbf{u}_{22}$  and  $\mathbf{v}_{22}$  (r.f. (2.23)) are not aligned in the same signal space at  $R_2$ . Otherwise, they will not be separated and linearly decoded.

After determining  $\mathbf{u}_{22}$ , we design  $\mathbf{u}_{21}$  as follows.

$$\mathbf{H}_{11}\mathbf{u}_{21}^\epsilon = \mathbf{H}_{12}\mathbf{u}_{22}^\epsilon, \quad \epsilon = 1, \dots, \lceil \frac{K_3}{2} \rceil \quad (2.29)$$

$$\mathbf{u}_{21}^{\lceil \frac{K_3}{2} \rceil + \epsilon} = \mathbf{j} \cdot \mathbf{u}_{21}^\epsilon, \quad \epsilon = 1, \dots, \lfloor \frac{K_3}{2} \rfloor \quad (2.30)$$

$$K_3 \leq G_3 \leq 2N_1 \quad (2.31)$$

where (2.31) ensures that  $\mathbf{u}_{22}^1, \dots, \mathbf{u}_{22}^{\lceil \frac{G_3}{2} \rceil}$  are independent of each other. Note that since  $N_1 \leq M_1$ ,  $\mathbf{u}_{21}^\epsilon$  can be surely found from (2.29). In addition, from (2.28)-(2.30) we can get

$$\mathbf{H}_{11}\mathbf{u}_{21}^{\lceil \frac{K_3}{2} \rceil + \epsilon} = \mathbf{H}_{12}\mathbf{u}_{22}^{\lceil \frac{G_3}{2} \rceil + \epsilon}, \quad \epsilon = 1, \dots, \lfloor \frac{K_3}{2} \rfloor. \quad (2.32)$$

If  $N_1 > M_1$ , we design  $\mathbf{u}_{21}$  and  $\mathbf{u}_{22}$  together by letting them satisfy following conditions,

$$\begin{bmatrix} \mathbf{H}_{11} & -\mathbf{H}_{12} \end{bmatrix} \begin{bmatrix} \mathbf{u}_{21}^\epsilon \\ \mathbf{u}_{22}^\epsilon \end{bmatrix} = \mathbf{0}, \quad \epsilon = 1, \dots, \lceil \frac{K_3}{2} \rceil \quad (2.33)$$

$$K_3 \leq G_3 \leq 2(M_1 + M_2 - N_1)^+ \quad (2.34)$$

and conditions (2.28) and (2.30).

The received signal at  $R_2$  can be expressed as

$$\begin{aligned} \mathbf{Y}_2 &= \mathbf{H}_{21}(\mathbf{x}_{21}^1 + \mathbf{x}_{21}^2 + \mathbf{x}_{21}^3) + \mathbf{H}_{22}(\mathbf{x}_{22}^1 + \mathbf{x}_{22}^2 + \mathbf{x}_{22}^3) \\ &+ \underbrace{\mathbf{H}_{21}(\mathbf{x}_{11}^1 + \mathbf{x}_{11}^2 + \mathbf{x}_{11}^3) + \mathbf{H}_{22}(\mathbf{x}_{12}^1 + \mathbf{x}_{12}^2 + \mathbf{x}_{12}^3)}_{\text{interference}} + \mathbf{z}_2 \end{aligned} \quad (2.35)$$

Similarly, we want to cancel the interference  $\mathbf{x}_{11}^1, \mathbf{x}_{11}^2$  and  $\mathbf{x}_{12}^1, \mathbf{x}_{12}^2$  at  $R_2$ . These can be achieved by letting

$$\mathbf{v}_{11}^1, \dots, \mathbf{v}_{11}^{L_1} \subset \text{span}\{\mathbf{P}_{21}\} \quad (2.36)$$

$$\mathbf{w}_{11}^l = \mathbf{j} \cdot \mathbf{v}_{11}^l, \quad l = 1, 2, \dots, L_2 \quad (2.37)$$

$$\mathbf{v}_{12}^1, \dots, \mathbf{v}_{12}^{J_1} \subset \text{span}\{\mathbf{P}_{22}\} \quad (2.38)$$

$$\mathbf{w}_{12}^\kappa = \mathbf{j} \cdot \mathbf{v}_{12}^\kappa, \quad \kappa = 1, 2, \dots, J_2 \quad (2.39)$$

and

$$L_2 \leq L_1 \leq (M_1 - N_2)^+ \quad (2.40)$$

$$J_2 \leq J_1 \leq (M_2 - N_2)^+ \quad (2.41)$$

Further, we want interference  $\mathbf{x}_{11}^3$  to be aligned with interference  $\mathbf{x}_{12}^3$  at  $R_2$ .

When  $N_2 \leq M_1$ , we let

$$\mathbf{u}_{12}^1, \dots, \mathbf{u}_{12}^{\lceil \frac{J_3}{2} \rceil} \not\subseteq \text{span}\{\mathbf{P}_{22}\} \quad (2.42)$$

$$\mathbf{u}_{12}^{\lceil \frac{J_3}{2} \rceil + \mathbf{a}} = \mathbf{j} \cdot \mathbf{u}_{12}^{\mathbf{a}}, \quad \mathbf{a} = 1, \dots, \lfloor \frac{J_3}{2} \rfloor \quad (2.43)$$

$$\mathbf{H}_{21} \mathbf{u}_{11}^\varepsilon = \mathbf{H}_{22} \mathbf{u}_{12}^\varepsilon, \quad \varepsilon = 1, \dots, \lfloor \frac{L_3}{2} \rfloor \quad (2.44)$$

$$\mathbf{u}_{11}^{\lceil \frac{L_3}{2} \rceil + \mathbf{b}} = \mathbf{j} \cdot \mathbf{u}_{11}^{\mathbf{b}}, \quad \mathbf{b} = 1, \dots, \lfloor \frac{L_3}{2} \rfloor \quad (2.45)$$

$$L_3 \leq J_3 \leq 2N_2 \quad (2.46)$$

which implies that

$$\mathbf{H}_{21} \mathbf{u}_{11}^{\lceil \frac{L_3}{2} \rceil + \mathbf{c}} = \mathbf{H}_{22} \mathbf{u}_{12}^{\lceil \frac{J_3}{2} \rceil + \mathbf{c}}, \quad \mathbf{c} = 1, \dots, \lfloor \frac{L_3}{2} \rfloor \quad (2.47)$$

When  $N_2 > M_1$ ,  $\mathbf{u}_{12}$  and  $\mathbf{u}_{11}$  are designed together to satisfy following conditions,

$$\begin{bmatrix} \mathbf{H}_{21} & -\mathbf{H}_{22} \end{bmatrix} \begin{bmatrix} \mathbf{u}_{11}^\varepsilon \\ \mathbf{u}_{12}^\varepsilon \end{bmatrix} = \mathbf{0}, \quad \varepsilon = 1, \dots, \lfloor \frac{L_3}{2} \rfloor \quad (2.48)$$

$$L_3 \leq J_3 \leq 2(M_1 + M_2 - N_2)^+ \quad (2.49)$$

and the conditions (2.43) and (2.45).

### 2.4.3 Linear Independence

Next, we investigate constraints under which the desired signals on each receiver can be linearly decoded.

First, we examine the received signals on  $R_1$ , which can be expressed as

$$\begin{aligned} \mathbf{Y}_1 &= \mathbf{H}_{11}(\mathbf{x}_{11}^1 + \mathbf{x}_{11}^2 + \mathbf{x}_{11}^3) + \mathbf{H}_{12}(\mathbf{x}_{12}^1 + \mathbf{x}_{12}^2 + \mathbf{x}_{12}^3) \\ &+ \underbrace{\mathbf{H}_{11}\mathbf{x}_{21}^3 + \mathbf{H}_{12}\mathbf{x}_{22}^3}_{\text{interference}} + \mathbf{z}_1 \end{aligned} \quad (2.50)$$

We neglect noise vector and rewrite (2.50) as

$$\begin{aligned}
\mathbf{Y}_1 &= (\mathbf{H}_{11} \underbrace{[\mathbf{v}_{11}^1 \cdots \mathbf{v}_{11}^{L_2}, \mathbf{u}_{11}^1 \cdots \mathbf{u}_{11}^{\lfloor \frac{L_3}{2} \rfloor}]}_{\mathbf{D}_1^1} \mathbf{H}_{12} \underbrace{[\mathbf{v}_{12}^1 \cdots \mathbf{v}_{12}^{J_2}, \mathbf{u}_{12}^1, \cdots, \mathbf{u}_{12}^{\lfloor \frac{J_3}{2} \rfloor}]}_{\mathbf{D}_1^2}) \\
&\quad \underbrace{\mathbf{H}_{12} [\mathbf{u}_{22}^1 \cdots \mathbf{u}_{22}^{\lfloor \frac{G_3}{2} \rfloor}]}_{\mathbf{D}_1^3} \\
&\quad \text{interference dimensions} \\
&\quad \mathbf{H}_{11} \underbrace{[\mathbf{w}_{11}^1 \cdots \mathbf{w}_{11}^{L_2}, \mathbf{u}_{11}^{\lfloor \frac{L_3}{2} \rfloor + 1} \cdots \mathbf{u}_{11}^{L_3}]}_{\mathbf{D}_2^1} \mathbf{H}_{12} \underbrace{[\mathbf{w}_{12}^1 \cdots \mathbf{w}_{12}^{J_2}, \mathbf{u}_{12}^{\lfloor \frac{J_3}{2} \rfloor + 1} \cdots \mathbf{u}_{12}^{J_3}]}_{\mathbf{D}_2^2} \\
&\quad \underbrace{\mathbf{H}_{12} [\mathbf{u}_{22}^{\lfloor \frac{G_3}{2} \rfloor + 1} \cdots \mathbf{u}_{22}^{G_3}]}_{\mathbf{D}_2^3} \\
&\quad \text{(interference dimensions)} \\
&\quad \mathbf{H}_{11} \underbrace{[\mathbf{v}_{11}^{L_2+1} \cdots \mathbf{v}_{11}^{L_1}]}_{\mathbf{D}_3^1} \mathbf{H}_{12} \underbrace{[\mathbf{v}_{12}^{J_2+1} \cdots \mathbf{v}_{12}^{J_1}]}_{\mathbf{D}_3^2} \mathbf{H}_{11} \mathbf{u}_{11}^{\lfloor \frac{L_3}{2} \rfloor} \mathbf{H}_{12} \mathbf{u}_{12}^{\lfloor \frac{J_3}{2} \rfloor} \mathbf{H}_{12} \mathbf{u}_{22}^{\lfloor \frac{G_3}{2} \rfloor}) \mathbf{m}_1
\end{aligned} \tag{2.51}$$

where  $\mathbf{m}_1$  denotes the *real* column vector of all received signals in which some interferences are cancelled due to the precoding and the desired messages and interferences are reordered, and the terms  $\mathbf{H}_{11} \mathbf{u}_{11}^{\lfloor \frac{L_3}{2} \rfloor}$ ,  $\mathbf{H}_{12} \mathbf{u}_{12}^{\lfloor \frac{J_3}{2} \rfloor}$  and  $\mathbf{H}_{12} \mathbf{u}_{22}^{\lfloor \frac{G_3}{2} \rfloor}$  are only shown in (2.51) when  $L_3, J_3, G_3$  are odd, respectively.

According to (2.28), (2.37), (2.39), (2.43) and (2.45), we can get  $\mathbf{D}_2^1 = \mathbf{j} \cdot \mathbf{D}_1^1$ ,  $\mathbf{D}_2^2 = \mathbf{j} \cdot \mathbf{D}_1^2$ ,  $\mathbf{D}_2^3 = \mathbf{j} \cdot \mathbf{D}_1^3$ . Hence,  $\mathbf{Y}_1$  can be expressed as

$$\begin{aligned}
\mathbf{Y}_1 &= \left( \underbrace{[\mathbf{H}_{11} \mathbf{D}_1^1 \mathbf{H}_{12} \mathbf{D}_1^2 \mathbf{H}_{12} \mathbf{D}_1^3]}_{\mathbf{G}_1} \quad \mathbf{j} \underbrace{[\mathbf{H}_{11} \mathbf{D}_1^1 \mathbf{H}_{12} \mathbf{D}_1^2 \mathbf{H}_{12} \mathbf{D}_1^3]}_{\mathbf{G}_2} \right) \\
&\quad \underbrace{[\mathbf{H}_{11} \mathbf{D}_3^1 \mathbf{H}_{12} \mathbf{D}_3^2 \mathbf{H}_{11} \mathbf{u}_{11}^{\lfloor \frac{L_3}{2} \rfloor} \mathbf{H}_{12} \mathbf{u}_{12}^{\lfloor \frac{J_3}{2} \rfloor} \mathbf{H}_{12} \mathbf{u}_{22}^{\lfloor \frac{G_3}{2} \rfloor}]}_{\mathbf{G}_3} \mathbf{m}_1
\end{aligned} \tag{2.52}$$

whose real form can be expressed as

$$\begin{aligned}
\bar{\mathbf{Y}}_1 &= \left( \left[ \hat{H}_{11} \bar{D}_1^1 \hat{H}_{12} \bar{D}_1^2 \hat{H}_{12} \bar{D}_1^3 \right] \left[ \hat{H}_{11} \mathbf{j} \bar{D}_1^1 \hat{H}_{12} \mathbf{j} \bar{D}_1^2 \hat{H}_{12} \mathbf{j} \bar{D}_1^3 \right] \right) \\
&\quad \left( \hat{H}_{11} \bar{D}_3^1 \hat{H}_{12} \bar{D}_3^2 \hat{H}_{11} \overline{U_{11}^{\lfloor \frac{L_3}{2} \rfloor}} \hat{H}_{12} \overline{U_{12}^{\lfloor \frac{J_3}{2} \rfloor}} \hat{H}_{12} \overline{U_{22}^{\lfloor \frac{G_3}{2} \rfloor}} \right) \mathbf{m}_1
\end{aligned} \tag{2.53}$$

where  $\hat{H}$  is the equivalent real form of complex channel matrix  $\mathbf{H}$  as defined in (2.7), and  $\overline{\mathbf{D}}$  denotes the real form of the matrix  $\mathbf{D}$ , which is defined as follows.

Let  $\mathbf{D} \in \mathbb{C}^{n \times m} = \left[ \mathbf{d}_1 \ \cdots \ \mathbf{d}_m \right]$  denote a random complex matrix, where  $\mathbf{d}_p \in \mathbb{C}^{n \times 1} = \left[ \mathbf{d}_p(1) \ \cdots \ \mathbf{d}_p(n) \right]^T$  denotes the  $p$ th column of  $\mathbf{D}$ . Then, we let  $\overline{\mathbf{D}} \in \mathbb{C}^{2n \times m}$  and  $\overline{\mathbf{d}}_p \in \mathbb{C}^{2n \times 1}$  denote the real form of  $\mathbf{D}$  and  $\mathbf{d}_p$ , respectively, i.e.,

$$\overline{\mathbf{D}} = \left[ \overline{\mathbf{d}}_1 \ \cdots \ \overline{\mathbf{d}}_m \right], \text{ where } \overline{\mathbf{d}}_p = \begin{bmatrix} \text{Re}(\mathbf{d}_p(1)) \\ \text{Im}(\mathbf{d}_p(1)) \\ \vdots \\ \text{Re}(\mathbf{d}_p(n)) \\ \text{Im}(\mathbf{d}_p(n)) \end{bmatrix} \quad (2.54)$$

Since  $\hat{H}\overline{\mathbf{D}} = \overline{H\mathbf{D}}$ , (2.53) can be written as

$$\overline{\mathbf{Y}}_1 = \left[ \overline{\mathbf{G}}_1 \ \overline{\mathbf{G}}_2 \ \overline{\mathbf{G}}_3 \right] \mathbf{m}_1 = \left[ \overline{\mathbf{G}}' \ \overline{\mathbf{G}}_3 \right] \mathbf{m}_1 \quad (2.55)$$

where  $\overline{\mathbf{G}}_1$ ,  $\overline{\mathbf{G}}_2$  and  $\overline{\mathbf{G}}_3$  are the real form of  $\mathbf{G}_1$ ,  $\mathbf{G}_2$  and  $\mathbf{G}_3$  in (2.52), respectively, and  $\overline{\mathbf{G}}'$  is the real form of  $\mathbf{G}' = \left[ \mathbf{G}_1 \ \mathbf{G}_2 \right] = \left[ \mathbf{G}_1 \ \mathbf{j}\mathbf{G}_1 \right]$ .

Next, we shall show that under some constraints,  $\overline{\mathbf{Y}}_1$  has full column rank almost surely. First, we introduce two Lemmas.

**Lemma 2.1** *For random  $\alpha^{ij}$  and  $\beta^{ij}$ ,  $i = 1, 2, \dots, n$  and  $j = 1, 2, \dots, m$ , a matrix  $\mathbf{Q}$  with the quaternion structure as*

$$\mathbf{Q} \in \mathbb{R}^{2n \times 2m} = \begin{bmatrix} \mathbf{q}^{11} & \cdots & \mathbf{q}^{1m} \\ \vdots & \ddots & \vdots \\ \mathbf{q}^{n1} & \cdots & \mathbf{q}^{nm} \end{bmatrix}$$

$$\text{where } \mathbf{q}^{ij} = \begin{bmatrix} \alpha^{ij} & -\beta^{ij} \\ \beta^{ij} & \alpha^{ij} \end{bmatrix} \quad (2.56)$$

has full column rank almost for sure if  $m \leq n$ .

*Proof:* The proof is given in Appendix A.

**Lemma 2.2** Let  $\mathbf{G} \in \mathbb{C}^{n \times m}$  be a random matrix ( $m \leq n$ ), and  $\mathbf{G}' = \begin{bmatrix} \mathbf{G} & \mathbf{jG} \end{bmatrix} \in \mathbb{C}^{n \times 2m}$ . Then, the real matrix  $\overline{\mathbf{G}'} \in \mathbb{R}^{2n \times 2m}$  as defined in (2.54) has full column rank almost for sure.

Proof of Lemma 2.2 is given as below.

*Proof:* First, we let  $\mathbf{g}_p$  denote the  $p$ th column of complex random matrix  $\mathbf{G}$  and define

$$\mathbf{G}'_X = \begin{bmatrix} \mathbf{g}_1 & \mathbf{jg}_1 & \cdots & \mathbf{g}_m & \mathbf{jg}_m \end{bmatrix}.$$

Note that  $\overline{\mathbf{G}'_X}$  has quaternion structure according to (2.54). Hence,  $\overline{\mathbf{G}'_X}$  has full column rank almost for sure according to Lemma 2.1.

Further, note that  $\mathbf{G}'_X$  is generated via column permutation of the matrix  $\mathbf{G}' = \begin{bmatrix} \mathbf{G} & \mathbf{jG} \end{bmatrix}$ . According to (2.54), the real matrix  $\overline{\mathbf{G}'}$  can be expressed as

$$\overline{\mathbf{G}'} = \overline{\mathbf{G}'_X} \cdot C$$

where  $C \in \mathbb{R}^{2m \times 2m}$  is a column permutation matrix. As the permutation of a matrix does not change the rank of the matrix,  $\overline{\mathbf{G}'}$  also has full column rank almost surely.

Note that the precoding vectors in  $\mathbf{G}_1$  are designed according to (2.36), (2.38), (2.42) and (2.44) or (2.48). Since the channels are all generic in complex level,  $\mathbf{G}_1 \in \mathbb{C}^{N_1 \times (L_2 + \lfloor \frac{L_3}{2} \rfloor + J_2 + \lfloor \frac{J_3}{2} \rfloor + \lfloor \frac{G_3}{2} \rfloor)}$  has full column rank for sure as long as

$$L_2 + \lfloor \frac{L_3}{2} \rfloor + J_2 + \lfloor \frac{J_3}{2} \rfloor + \lfloor \frac{G_3}{2} \rfloor \leq N_1. \quad (2.57)$$

For  $\mathbf{G}' = \begin{bmatrix} \mathbf{G}_1 & \mathbf{jG}_1 \end{bmatrix}$ ,  $\overline{\mathbf{G}'}$  must have full rank according to Lemma 2.2.

Next, in order to guarantee that  $\overline{\mathbf{Y}}_1$  has full column rank, two conditions must be satisfied. First,  $\overline{\mathbf{Y}}_1 \in \mathbb{C}^{2N_1 \times (\sum_{\gamma=1}^3 (L_\gamma + J_\gamma) + G_3)}$  must be a square or “thin” matrix, which means

$$\sum_{\gamma=1}^3 (L_\gamma + J_\gamma) + G_3 \leq 2N_1 \quad (2.58)$$

Secondly, we need to ensure that the columns in  $\mathbf{G}_3$  are completely independent of each other and also independent of the columns in  $\mathbf{G}_1$ . From (2.52) we can see

that the signals in  $\mathbf{H}_{11}\mathbf{D}_1^1$ ,  $\mathbf{H}_{11}\mathbf{D}_3^1$  (and  $\mathbf{H}_{11}\mathbf{u}_{11}^{\lceil \frac{L_3}{2} \rceil}$ ) are sent through the same channel  $\mathbf{H}_{11}$ , i.e.,

$$\begin{bmatrix} \mathbf{H}_{11}\mathbf{D}_1^1 & \mathbf{H}_{11}\mathbf{D}_3^1 & \mathbf{H}_{11}\mathbf{u}_{11}^{\lceil \frac{L_3}{2} \rceil} \end{bmatrix} = \mathbf{H}_{11}[\mathbf{v}_{11}^1 \cdots \mathbf{v}_{11}^{L_2}, \mathbf{u}_{11}^1 \cdots \mathbf{u}_{11}^{\lceil \frac{L_3}{2} \rceil}, \mathbf{v}_{11}^{L_2+1} \cdots \mathbf{v}_{11}^{L_1}, \mathbf{u}_{11}^{\lceil \frac{L_3}{2} \rceil}] \quad (2.59)$$

In order to guarantee that  $\begin{bmatrix} \mathbf{H}_{11}\mathbf{D}_1^1 & \mathbf{H}_{11}\mathbf{D}_3^1 & \mathbf{H}_{11}\mathbf{u}_{11}^{\lceil \frac{L_3}{2} \rceil} \end{bmatrix}$  has full column rank, we let

$$L_1 + \lceil \frac{L_3}{2} \rceil \leq \min\{N_1, M_1\} \quad (2.60)$$

which is equivalent to

$$2L_1 + L_3 \leq \min\{2N_1, 2M_1\} \quad (2.61)$$

Further, in (2.52) some signals in  $\mathbf{G}_1$  and  $\mathbf{G}_3$  are sent through the same channel  $\mathbf{H}_{12}$ , which are  $\begin{bmatrix} \mathbf{H}_{12}\mathbf{D}_1^2 & \mathbf{H}_{12}\mathbf{D}_3^2 & \mathbf{H}_{12}\mathbf{u}_{12}^{\lceil \frac{J_3}{2} \rceil} & \mathbf{H}_{12}\mathbf{u}_{22}^{\lceil \frac{G_3}{2} \rceil} & \mathbf{H}_{12}\mathbf{D}_1^3 \end{bmatrix}$ . First, similar to (2.59)-(2.61), to guarantee that  $\begin{bmatrix} \mathbf{H}_{12}\mathbf{D}_1^2 & \mathbf{H}_{12}\mathbf{D}_3^2 & \mathbf{H}_{12}\mathbf{u}_{12}^{\lceil \frac{J_3}{2} \rceil} \end{bmatrix}$  has full column rank, we must let

$$2J_1 + J_3 \leq \min\{2N_1, 2M_2\}. \quad (2.62)$$

Then, since the design of  $\mathbf{u}_{22}$  is completely unrelated to  $\mathbf{v}_{12}$  and  $\mathbf{u}_{12}$ , the signals in  $\begin{bmatrix} \mathbf{H}_{12}\mathbf{u}_{22}^{\lceil \frac{G_3}{2} \rceil} & \mathbf{H}_{12}\mathbf{D}_1^3 \end{bmatrix}$  must be independent of  $\begin{bmatrix} \mathbf{H}_{12}\mathbf{D}_1^2 & \mathbf{H}_{12}\mathbf{D}_3^2 & \mathbf{H}_{12}\mathbf{u}_{12}^{\lceil \frac{J_3}{2} \rceil} \end{bmatrix}$ . Due to channel randomness, the signals that are sent through different channels are independent of each other almost surely. Hence, it is ensured that the columns in  $\mathbf{G}_3$  are independent of each other and also independent of the columns in  $\mathbf{G}_1$ .

Finally, with (2.58), (2.61) and (2.62) being satisfied,  $\overline{\mathbf{Y}}_1$  can have full column rank almost for sure.

Likewise, the received signals on  $R_2$  can be expressed as

$$\begin{aligned}
\mathbf{Y}_2 &= (\mathbf{H}_{21}[\mathbf{v}_{21}^1 \cdots \mathbf{v}_{21}^{K_2}, \mathbf{u}_{21}^1 \cdots \mathbf{u}_{21}^{\lfloor \frac{K_3}{2} \rfloor}]) \mathbf{H}_{22}[\mathbf{v}_{22}^1 \cdots \mathbf{v}_{22}^{G_2}, \mathbf{u}_{22}^1, \dots, \mathbf{u}_{22}^{\lfloor \frac{G_3}{2} \rfloor}] \\
&\quad \underbrace{\mathbf{H}_{22}[\mathbf{u}_{12}^1 \cdots \mathbf{u}_{12}^{\lfloor \frac{J_3}{2} \rfloor}]}_{\text{(interference dimensions)}} \\
&\quad \mathbf{H}_{21}[\mathbf{w}_{21}^1 \cdots \mathbf{w}_{21}^{K_2}, \mathbf{u}_{21}^{\lfloor \frac{K_3}{2} \rfloor + 1} \cdots \mathbf{u}_{21}^{K_3}] \mathbf{H}_{22}[\mathbf{w}_{22}^1 \cdots \mathbf{w}_{22}^{L_{22}^2}, \mathbf{u}_{22}^{\lfloor \frac{G_3}{2} \rfloor + 1} \cdots \mathbf{u}_{22}^{G_3}] \\
&\quad \underbrace{\mathbf{H}_{22}[\mathbf{u}_{12}^{\lfloor \frac{J_3}{2} \rfloor + 1} \cdots \mathbf{u}_{12}^{J_3}]}_{\text{(interference dimensions)}} \\
&\quad \mathbf{H}_{21}[\mathbf{v}_{21}^{K_2+1} \cdots \mathbf{v}_{21}^{K_1}] \mathbf{H}_{22}[\mathbf{v}_{22}^{G_2+1} \cdots \mathbf{v}_{22}^{G_1}] \mathbf{H}_{21} \mathbf{u}_{21}^{\lfloor \frac{K_3}{2} \rfloor} \mathbf{H}_{22} \mathbf{u}_{22}^{\lfloor \frac{G_3}{2} \rfloor} \mathbf{H}_{22} \mathbf{u}_{12}^{\lfloor \frac{J_3}{2} \rfloor}) \mathbf{m}_2
\end{aligned} \tag{2.63}$$

With the same approach, we can show that  $\overline{\mathbf{Y}}_2$  has full column rank almost for sure if the following three constraints are satisfied,

$$\sum_{\gamma=1}^3 (K_\gamma + G_\gamma) + J_3 \leq 2N_2 \tag{2.64}$$

$$2K_1 + K_3 \leq \min\{2N_2, 2M_1\} \tag{2.65}$$

$$2G_1 + G_3 \leq \min\{2N_2, 2M_2\} \tag{2.66}$$

## 2.5 Achievable Degrees of Freedom

In this section, we investigate the achievable DoF of our proposed scheme.

**Theorem 2.1** *In  $2 \times 2$  MIMO X channels with  $M_t$  antennas at transmitter  $t$  and  $N_r$  antennas at receiver  $r$ , based on the proposed scheme of interference alignment and nulling with asymmetric complex signaling, the achievable DoF equals  $\frac{1}{2} \lfloor 2D_{outer} \rfloor$ ,*

where  $D_{outer}$  denotes the outer bound of sum DoF [20], i.e.,

$$D_{outer} = \min \left\{ \begin{array}{l} M_1 + M_2, N_1 + N_2 \\ \frac{\max\{M_1, N_1\} + \max\{M_1, N_2\} + M_2}{2}, \\ \frac{\max\{M_2, N_1\} + \max\{M_2, N_2\} + M_1}{2}, \\ \frac{\max\{M_1, N_1\} + \max\{M_2, N_1\} + N_2}{2}, \\ \frac{\max\{M_1, N_2\} + \max\{M_2, N_2\} + N_1}{2}, \\ \frac{\max\{M_1, N_1\} + \max\{M_1, N_2\} + \max\{M_2, N_1\} + \max\{M_2, N_2\}}{3} \end{array} \right.$$

The exact value of achievable DoF in different cases are shown in Table 2.1 and 2.2.

*Proof:* According to (2.17), the optimal achievable DoF is obtained by maximizing  $\sum_{\gamma=1}^3 (L_\gamma + K_\gamma + J_\gamma + G_\gamma)$  under the constraints that ensure the linear independence. It is equivalent to solving the following linear optimization problem,

$$\begin{aligned} & \max \sum_{\gamma=1}^3 (L_\gamma + K_\gamma + J_\gamma + G_\gamma) \quad (2.67) \\ \text{st. } & \sum_{\gamma=1}^3 (L_\gamma + J_\gamma) \leq 2N_1 - G_3 \quad (2.58), \quad \sum_{\gamma=1}^3 (K_\gamma + G_\gamma) \leq 2N_2 - J_3 \quad (2.64). \\ & 2L_1 + L_3 \leq \min\{2N_1, 2M_1\} \quad (2.61), \quad 2J_1 + J_3 \leq \min\{2N_1, 2M_2\} \quad (2.62). \\ & 2K_1 + K_3 \leq \min\{2N_2, 2M_1\} \quad (2.65), \quad 2G_1 + G_3 \leq \min\{2N_2, 2M_2\} \quad (2.66). \\ & K_2 \leq K_1 \leq (M_1 - N_1)^+ \quad (2.25), \quad G_2 \leq G_1 \leq (M_2 - N_1)^+ \quad (2.26). \\ & J_2 \leq J_1 \leq (M_2 - N_2)^+ \quad (2.41), \quad L_2 \leq L_1 \leq (M_1 - N_2)^+ \quad (2.40) \\ & K_3 \leq G_3 \leq 2N_1 \text{ when } N_1 \leq M_1 \quad (2.31). \\ & K_3 \leq G_3 \leq 2(M_1 + M_2 - N_1)^+ \text{ when } N_1 > M_1 \quad (2.34). \\ & L_3 \leq J_3 \leq 2N_2 \text{ when } N_2 \leq M_1 \quad (2.46). \\ & L_3 \leq J_3 \leq 2(M_1 + M_2 - N_2)^+ \text{ when } N_2 > M_1 \quad (2.49). \end{aligned}$$

The detailed calculation is given in Appendix B.

Finally, we use a simple example to elaborate the design process and show the advantage of the proposed scheme. We assume that  $M_1 = M_2 = N_1 = 2$ ,  $N_2 = 1$ . By

**Table 2.1** The achievable DoF for three types of antenna configurations

$M_1 \geq M_2 \geq N_1 \geq N_2$			
	$M_1 + M_2 \geq 2N_1 + N_2$	$3N_2 \leq M_1 + M_2 < 2N_1 + N_2$	$M_1 + M_2 < 3N_2$
Achievable DoF	$N_1 + N_2$	$\frac{M_1 + M_2 + N_2}{2}$	$\frac{1}{2} \lfloor \frac{4}{3}(M_1 + M_2) \rfloor$
Outer bound DoF [9]	$N_1 + N_2$	$\frac{M_1 + M_2 + N_2}{2}$	$\frac{2}{3}(M_1 + M_2)$
$M_1 \geq N_1 \geq M_2 \geq N_2$			
	$M_1 \geq N_1 + N_2$	$N_1 + 3N_2 \leq M_1 + 2M_2 < N_1 + N_2 + 2M_2$	$M_1 + 2M_2 < N_1 + 3N_2$
Achievable DoF	$N_1 + N_2$	$\frac{M_1 + N_1 + N_2}{2}$	$\frac{1}{2} \lfloor \frac{2(2M_1 + N_1 + M_2)}{3} \rfloor$
Outer bound DoF [9]	$N_1 + N_2$	$\frac{M_1 + N_1 + N_2}{2}$	$\frac{2M_1 + N_1 + M_2}{3}$
$N_1 \geq M_1 \geq M_2 \geq N_2$			
	$2(M_1 + M_2) \geq 2N_1 + 3N_2$	$2N_1 \leq 2(M_1 + M_2) < 2N_1 + 3N_2$	$M_1 + M_2 \leq N_1$
Achievable DoF	$\frac{2N_1 + N_2}{2}$	$\frac{1}{2} \lfloor \frac{2(2N_1 + M_1 + M_2)}{3} \rfloor$	$M_1 + M_2$
Outer bound DoF [9]	$\frac{2N_1 + N_2}{2}$	$\frac{2N_1 + M_1 + M_2}{3}$	$M_1 + M_2$

**Table 2.2** The achievable DoF for other three types of antenna configurations

$N_1 \geq N_2 \geq M_1 \geq M_2$			
	$N_1 + N_2 \geq 2M_1 + M_2$	$3M_2 \leq N_1 + N_2 < 2M_1 + M_2$	$N_1 + N_2 < 3M_2$
Achievable DoF	$M_1 + M_2$	$\frac{N_1 + N_2 + M_2}{2}$	$\frac{1}{2} \lfloor \frac{4}{3}(N_1 + N_2) \rfloor$
Outer bound DoF [9]	$M_1 + M_2$	$\frac{N_1 + N_2 + M_2}{2}$	$\frac{2}{3}(N_1 + N_2)$
$N_1 \geq M_1 \geq N_2 \geq M_2$			
	$N_1 \geq M_1 + M_2$	$M_1 + 3M_2 \leq N_1 + 2N_2 < M_1 + M_2 + 2N_2$	$N_1 + 2N_2 < M_1 + 3M_2$
Achievable DoF	$M_1 + M_2$	$\frac{M_1 + N_1 + M_2}{2}$	$\frac{1}{2} \lfloor \frac{2(2N_1 + M_1 + N_2)}{3} \rfloor$
$M_1 \geq N_1 \geq N_2 \geq M_2$			
	$2(N_1 + N_2) \geq 2M_1 + 3M_2$	$2M_1 \leq 2(N_1 + N_2) < 2M_1 + 3M_2$	$N_1 + N_2 \leq M_1$
Achievable DoF	$\frac{2M_1 + M_2}{2}$	$\frac{1}{2} \lfloor \frac{2(2M_1 + N_1 + N_2)}{3} \rfloor$	$N_1 + N_2$
Outer bound DoF [9]	$\frac{2M_1 + M_2}{2}$	$\frac{2M_1 + N_1 + N_2}{3}$	$N_1 + N_2$

solving (2.67), we can get  $L_1 = J_1 = J_2 = G_3 = K_3 = 1$  and other parameters equal zero. (The solution can be found in (2.71)). Hence, the transmitted signals can be expressed as follows,

$$\begin{aligned}\mathbf{x}_{11} &= \mathbf{v}_{11}^1 m_{11}^1; \mathbf{x}_{21} = \mathbf{u}_{21}^1 m_{21}^3 \\ \mathbf{x}_{12} &= \mathbf{v}_{12}^1 m_{12}^1 + \mathbf{w}_{12}^1 m_{12}^2; \mathbf{x}_{22} = \mathbf{u}_{22}^1 m_{22}^3\end{aligned}$$

where the messages are all real and the designs of precoding vectors are elaborated in Section 2.4.2.

As a result, the received signals on each receiver is

$$\begin{aligned}\mathbf{Y}_1 &= \underbrace{\mathbf{H}_{11} \begin{bmatrix} \mathbf{v}_{11}^1 & \mathbf{u}_{21}^1 \end{bmatrix}}_{\mathbf{A} \in \mathbb{C}^{(2 \times 2)}} \begin{bmatrix} m_{11}^1 \\ m_{21}^3 + m_{22}^3 \end{bmatrix} + \underbrace{\mathbf{H}_{12} \begin{bmatrix} \mathbf{v}_{12}^1 & \mathbf{j} \cdot \mathbf{v}_{12}^1 \end{bmatrix}}_{\mathbf{B} \in \mathbb{C}^{(2 \times 2)}} \begin{bmatrix} m_{12}^1 \\ m_{12}^2 \end{bmatrix} \\ \mathbf{Y}_2 &= \underbrace{\begin{bmatrix} \mathbf{H}_{21} \mathbf{u}_{21}^1 & \mathbf{H}_{22} \mathbf{u}_{22}^1 \end{bmatrix}}_{\mathbf{C} \in \mathbb{C}^{(1 \times 2)}} \begin{bmatrix} m_{21}^3 \\ m_{22}^3 \end{bmatrix}\end{aligned}$$

After transforming the system into real form, we have

$$\begin{aligned}\bar{\mathbf{Y}}_1 &= \begin{bmatrix} \bar{\mathbf{A}} & \bar{\mathbf{B}} \end{bmatrix} \begin{bmatrix} m_{11}^1 & m_{21}^3 + m_{22}^3 & m_{12}^1 & m_{12}^2 \end{bmatrix}^T \\ \bar{\mathbf{Y}}_2 &= \bar{\mathbf{C}} \begin{bmatrix} m_{21}^3 & m_{22}^3 \end{bmatrix}^T\end{aligned}$$

Since  $\begin{bmatrix} \bar{\mathbf{A}} & \bar{\mathbf{B}} \end{bmatrix} \in \mathbb{R}^{(4 \times 4)}$  and  $\bar{\mathbf{C}} \in \mathbb{R}^{(2 \times 2)}$  both have full rank almost surely,  $R_1$  and  $R_2$  can decode  $m_{11}^1, m_{12}^1, m_{12}^2$  and  $m_{21}^3, m_{22}^3$ , respectively. Hence, the total DoF of  $\frac{5}{2}$  is achieved, which equals the outer-bound. Note that with conventional scheme, only DoF of 2 is achievable.

## 2.6 Summary

In this chapter, we investigate the achievable DoF of MIMO X channels based on linear spatial beamforming schemes. While conventional schemes can achieve no more than  $\lfloor D_{outer} \rfloor$  DoF, we show that the DoF of  $\lfloor D_{outer} \rfloor + \frac{1}{2}$  can be achieved if

$D_{outer} - \lfloor D_{outer} \rfloor \geq \frac{1}{2}$ , and  $\lfloor D_{outer} \rfloor$  can be achieved otherwise. The improvement is realized by combining asymmetric complex signaling with interference alignment framework. The results indicate that the technique of asymmetric complex signaling, which was originally proposed for single-antenna systems, can provide DoF benefit for MIMO systems as well when symbol extensions are not allowed.

## 2.7 Appendix A: Proof of Lemma 2.1

Note that if we can prove  $\mathbf{Q} \in \mathbb{R}^{2n \times 2m}$  has full rank when  $m = n$ , then  $\mathbf{Q}$  would have full column rank for sure if  $m < n$ . Hence, we focus on showing that the matrix  $\mathbf{Q}$  in (2.56) has full rank when  $m = n$ , i.e., the determinant of  $\mathbf{Q}$  is non-zero. The argument will be proved recursively.

When  $m = 1$ , we have  $|\mathbf{Q}| = |\mathbf{q}^{11}| = (\alpha^{11})^2 + (\beta^{11})^2$ , which is non-zero almost for sure. When  $m = 2$ , we have

$$\begin{aligned} \mathbf{Q} &= \begin{bmatrix} \mathbf{q}^{11} & \mathbf{q}^{12} \\ \mathbf{q}^{21} & \mathbf{q}^{22} \end{bmatrix} \\ &= \begin{bmatrix} \mathbf{q}^{11} & \mathbf{0} \\ \mathbf{q}^{21} & \mathbf{I} \end{bmatrix} \cdot \begin{bmatrix} \mathbf{I} & (\mathbf{q}^{11})^{-1}\mathbf{q}^{12} \\ \mathbf{0} & \mathbf{q}^{22} - \mathbf{q}^{21}(\mathbf{q}^{11})^{-1}\mathbf{q}^{12} \end{bmatrix} \end{aligned}$$

which means

$$\begin{aligned} |\mathbf{Q}| &= \left| \begin{bmatrix} \mathbf{q}^{11} & \mathbf{0} \\ \mathbf{q}^{21} & \mathbf{I} \end{bmatrix} \right| \cdot \left| \begin{bmatrix} \mathbf{I} & (\mathbf{q}^{11})^{-1}\mathbf{q}^{12} \\ \mathbf{0} & \mathbf{q}^{22} - \mathbf{q}^{21}(\mathbf{q}^{11})^{-1}\mathbf{q}^{12} \end{bmatrix} \right| \\ &= |\mathbf{q}^{11}| \cdot |\mathbf{q}^{22} - \mathbf{q}^{21}(\mathbf{q}^{11})^{-1}\mathbf{q}^{12}| \end{aligned}$$

Since  $\mathbf{q}^{21}(\mathbf{q}^{11})^{-1}\mathbf{q}^{12}$  and  $\mathbf{q}^{22}$  are both full rank quaternion structured matrices and completely random with respect to each other,  $\mathbf{q}' = \mathbf{q}^{22} - \mathbf{q}^{21}(\mathbf{q}^{11})^{-1}\mathbf{q}^{12}$  is also a quaternion structured matrix with  $m = 1$ , which was already proved to have full rank almost surely. Therefore, both  $|\mathbf{q}^{11}|$  and  $|\mathbf{q}'|$  are non-zero almost surely. Finally, we can get that  $|\mathbf{Q}|$  is non-zero almost for sure.

Next, assuming  $\mathbf{Q}$  is full rank when  $m = q$ , we show that  $\mathbf{Q}$  is also full rank when  $m = q + 1$ . First of all, we denote  $\mathbf{Q}_1$  and  $\mathbf{Q}_2$  as the matrices  $\mathbf{Q} \in \mathbb{R}^{2q \times 2q}$  and  $\mathbf{Q} \in \mathbb{R}^{2(q+1) \times 2(q+1)}$ , respectively. Then, we have

$$\begin{aligned}
\mathbf{Q}_2 &= \begin{bmatrix} & & & \mathbf{q}^{1(q+1)} \\ & \mathbf{Q}_1 & & \vdots \\ & & & \mathbf{q}^{q(q+1)} \\ \mathbf{q}^{(q+1)1} & \dots & \mathbf{q}^{(q+1)q} & \mathbf{q}^{(q+1)(q+1)} \end{bmatrix} \\
&= \begin{bmatrix} & & & & & \alpha^{1(q+1)} & -\beta^{1(q+1)} \\ & & & & & \beta^{1(q+1)} & \alpha^{1(q+1)} \\ & & & & & \vdots & \vdots \\ & & \mathbf{Q}_1 & & & \alpha^{q(q+1)} & -\beta^{q(q+1)} \\ & & & & & \beta^{q(q+1)} & \alpha^{q(q+1)} \\ \alpha^{(q+1)1} & -\beta^{(q+1)1} & \dots & \alpha^{(q+1)q} & -\beta^{(q+1)q} & \alpha^{(q+1)(q+1)} & -\beta^{(q+1)(q+1)} \\ \hline \beta^{(q+1)1} & \alpha^{(q+1)1} & \dots & \beta^{(q+1)q} & \alpha^{(q+1)q} & \beta^{(q+1)(q+1)} & \alpha^{(q+1)(q+1)} \end{bmatrix} \\
&= \begin{bmatrix} \mathbf{\Omega} & W \\ Z & \alpha^{(q+1)(q+1)} \end{bmatrix} = \begin{bmatrix} \mathbf{\Omega} & \mathbf{0} \\ Z & \mathbf{I} \end{bmatrix} \cdot \begin{bmatrix} \mathbf{I} & \mathbf{\Omega}^{-1}W \\ \mathbf{0} & \alpha^{(q+1)(q+1)} - Z\mathbf{\Omega}^{-1}W \end{bmatrix} \quad (2.68)
\end{aligned}$$

It is obvious that  $\mathbf{\Omega} \in \mathbb{R}^{(2q+1) \times (2q+1)}$  has full rank for sure because it is  $\mathbf{Q}_1$  added with one random column and row. Hence, the determinant of  $\mathbf{Q}_2$  can be calculated as follows,

$$|\mathbf{Q}_2| = \det\{\mathbf{\Omega}\} \cdot \det\{\alpha^{(q+1)(q+1)} - Z\mathbf{\Omega}^{-1}W\} \quad (2.69)$$

Since  $\mathbf{\Omega}$  has full rank,  $\det\{\mathbf{\Omega}\}$  is nonzero for sure. Further, since  $Z$ ,  $\mathbf{\Omega}^{-1}$  and  $W$  are all random matrix or vectors with respect to  $\alpha^{(q+1)(q+1)}$ , we can get that  $Z\mathbf{\Omega}^{-1}W \neq \alpha^{(q+1)(q+1)}$  almost for sure, which means  $\det\{\alpha^{(q+1)(q+1)} - Z\mathbf{\Omega}^{-1}W\}$  is also non-zero almost surely. Hence,  $\mathbf{Q}_2$  is proved to have full rank almost for sure.

## 2.8 Appendix B: Proof of Theorem 2.1

As can be seen from Table 2.1 and Table 2.2, the network can be divided into six cases according to different antenna configurations. Further, note that the three cases in Table 2.2,  $N_1 \geq N_2 \geq M_1 \geq M_2$ ,  $N_1 \geq M_1 \geq N_2 \geq M_2$ , and  $M_1 \geq N_1 \geq N_2 \geq M_2$ , are just the reciprocal of the three cases in Table 2.1,  $M_1 \geq M_2 \geq N_1 \geq N_2$ ,  $M_1 \geq N_1 \geq M_2 \geq N_2$  and  $N_1 \geq M_1 \geq M_2 \geq N_2$ , respectively. Hence, we only focus on the cases in Table 2.1.

### 2.8.1 $M_1 \geq M_2 \geq N_1 \geq N_2$

As can be seen from Table 2.1, we further divide this case into three sub-cases, i.e.,  $M_1 + M_2 \geq 2N_1 + N_2$ ,  $3N_2 \leq M_1 + M_2 < 2N_1 + N_2$ , and  $M_1 + M_2 < 3N_2$ .

• **When  $M_1 + M_2 \geq 2N_1 + N_2$**

Since  $M_1 + M_2 \geq 2N_1 + N_2$ , we have  $(M_1 - N_1) + (M_2 - N_1) \geq N_2$  and  $(M_1 - N_2) + (M_2 - N_2) \geq N_1$ , which means there always exists  $L_1, L_2, K_1, K_2, J_1, J_2, G_1, G_2$  that can satisfy the equalities of (2.58) and (2.64), with  $L_3 = J_3 = K_3 = G_3 = 0$ . There are many possible solutions for the values of each parameter. We present one solution as follows,

$$\begin{cases} G_1 = G_2 = \min\{M_2 - N_1, N_2\}, G_3 = 0 \\ K_1 = K_2 = \max\{N_1 + N_2 - M_2, 0\}, K_3 = 0 \\ J_1 = J_2 = \min\{M_2 - N_2, N_1\}, J_3 = 0 \\ L_1 = L_2 = \max\{N_1 + N_2 - M_2, 0\}, L_3 = 0 \end{cases} \quad (2.70)$$

As a result,  $\sum_{\gamma=1}^3 (L_\gamma + K_\gamma + J_\gamma + G_\gamma)$  is maximized as  $2N_1 + 2N_2$ , which leads to the achievable DoF  $N_1 + N_2$ .

• **When  $3N_2 \leq M_1 + M_2 < 2N_1 + N_2$**

First of all, to maximize  $\sum_{\gamma=1}^3 (L_\gamma + K_\gamma + J_\gamma + G_\gamma)$ , we let the equalities hold for both (2.58) and (2.64). Then, we maximize  $K_1, K_2$  and  $G_1, G_2$  as  $M_1 - N_1, M_2 - N_1$ , respectively, which gives  $K_3 + G_3 + J_3 = 2(2N_1 + N_2 - M_1 - M_2)$ . Note

that  $G_3 + J_3$  should be minimized as it denotes the number of interference dimensions on two receivers. First, since  $K_3 \leq G_3$ , we minimize  $G_3 + J_3$  by letting  $K_3 = G_3$ , i.e.,  $G_3 + J_3 = 2(2N_1 + N_2 - M_1 - M_2) - G_3$ . Further, we can see that  $G_3 + J_3$  is minimized if  $G_3$  is maximized. Hence, we let  $K_3 = G_3 = 2N_1 + N_2 - M_1 - M_2$  and  $J_3 = 0$ . Moreover, since  $3N_2 \leq M_1 + M_2$ , there exists  $L_1, L_2, J_1, J_2$  that can satisfy the equality of (2.58) for sure.

Finally, one of many possible solutions is given as follows,

$$\begin{cases} G_1 = G_2 = M_2 - N_1, & G_3 = 2N_1 + N_2 - M_1 - M_2 \\ K_1 = K_2 = M_1 - N_1, & K_3 = 2N_1 + N_2 - M_1 - M_2 \\ J_1 = J_2 = M_2 - N_2, & J_3 = 0 \\ L_1 = \lceil \frac{M_1 + N_2 - M_2}{2} \rceil, & L_2 = \lfloor \frac{M_1 + N_2 - M_2}{2} \rfloor, & L_3 = 0 \end{cases} \quad (2.71)$$

Hence, the achievable DoF in this scenario can be calculated as  $\frac{M_1 + M_2 + N_2}{2}$ .

• **When**  $M_1 + M_2 < 3N_2$

First, we let the equalities hold for both (2.58) and (2.64). Then, we maximize  $L_1, L_2$  and  $J_1, J_2$  as  $M_1 - N_2$  and  $M_2 - N_2$ , respectively; maximize  $K_1, K_2$  and  $G_1, G_2$  as  $M_1 - N_1$  and  $M_2 - N_1$ , respectively. As a result, we have  $L_3 + J_3 + G_3 = 2(N_1 + 2N_2 - M_1 - M_2)$  and  $K_3 + G_3 + J_3 = 2(2N_1 + N_2 - M_1 - M_2)$ , which means

$$K_3 + L_3 + 2(J_3 + G_3) = 6N_1 + 6N_2 - 4(M_1 + M_2) \quad (2.72)$$

To minimize the number of interference dimensions, i.e.,  $J_3 + G_3$ , we should maximize  $K_3 + L_3$ . Further, we should note that  $K_3 \leq G_3$  and  $L_3 \leq J_3$ , which means  $K_3 + L_3 \leq G_3 + J_3$ . Hence, we let

$$K_3 + L_3 = J_3 + G_3 - x, \text{ where } x = (M_1 + M_2) \pmod{3} \quad (2.73)$$

which implies that

$$J_3 + G_3 = 2(N_1 + N_2) - \lfloor \frac{4(M_1 + M_2)}{3} \rfloor \quad (2.74)$$

As can be seen, the achievable DoF can be calculated as  $\frac{1}{2}(2N_1 + 2N_2 - J_3 - G_3) = \frac{1}{2} \lfloor \frac{4(M_1 + M_2)}{3} \rfloor$ . As for the exact values of  $K_3, L_3, J_3, G_3$ , one possible solution of  $J_3$  and

$G_3$  is given as follows,

$$G_3 = 2N_1 - \lfloor \frac{2(M_1 + M_2)}{3} \rfloor, J_3 = 2N_2 - \lfloor \frac{2(M_1 + M_2) + 1}{3} \rfloor$$

Then, the value of  $K_3$  and  $L_3$  can be easily obtained according to (2.73).

### 2.8.2 $M_1 \geq N_1 \geq M_2 \geq N_2$

The optimization process of this case is similar to the case of  $M_1 \geq M_2 \geq N_1 \geq N_2$ , except  $G_1 = G_2 = 0$ . Hence, we directly provide the results for different antenna configurations.

- **When  $M_1 \geq N_1 + N_2$**

$$\begin{cases} G_1 = G_2 = G_3 = 0 \\ K_1 = K_2 = N_2, K_3 = 0 \\ J_1 = J_2 = \min\{M_2 - N_2, N_1\}, J_3 = 0 \\ L_1 = L_2 = \max\{N_1 + N_2 - M_2, 0\}, L_3 = 0 \end{cases} \quad (2.75)$$

The achievable DoF equals  $N_1 + N_2$ .

- **When  $N_1 + 3N_2 \leq M_1 + 2M_2 < N_1 + N_2 + 2M_2$**

$$\begin{cases} G_1 = G_2 = 0, G_3 = N_1 + N_2 - M_1 \\ K_1 = K_2 = M_1 - N_1, K_3 = N_1 + N_2 - M_1 \\ J_1 = J_2 = M_2 - N_2, J_3 = N_1 - M_2 \\ L_1 = \lceil \frac{M_1 + N_2 - N_1}{2} \rceil, L_2 = \lfloor \frac{M_1 + N_2 - N_1}{2} \rfloor, \\ L_3 = N_1 - M_2 \end{cases} \quad (2.76)$$

The achievable DoF equals  $\frac{M_1 + N_1 + N_2}{2}$ .

- **When  $M_1 + 2M_2 < N_1 + 3N_2$**

$$\begin{cases} G_1 = G_2 = 0, K_1 = K_2 = M_1 - N_1 \\ J_1 = J_2 = M_2 - N_2, L_1 = L_2 = M_1 - N_2 \\ G_3 = N_1 + N_2 - \lfloor \frac{2M_1 + N_1 + M_2}{3} \rfloor \\ J_3 = N_1 + N_2 - \lfloor \frac{2M_1 + N_1 + M_2 + 1}{3} \rfloor \end{cases} \quad (2.77)$$

and

$$K_3 + L_3 = J_3 + G_3 - y \text{ where } y = 2(2M_1 + N_1 + M_2) \pmod{3} \quad (2.78)$$

The achievable DoF equals  $\frac{1}{2} \lfloor \frac{2(2M_1 + N_1 + M_2)}{3} \rfloor$ .

### 2.8.3 $N_1 \geq M_1 \geq M_2 \geq N_2$

Note that in this scenario,  $K_1 = K_2 = G_1 = G_2 = 0$ .

- **When**  $2(M_1 + M_2) \geq 2N_1 + 3N_2$

According to (2.64), we have  $K_3 + J_3 + G_3 = 2N_2$ . In order to minimize the number of interference dimensions,  $G_3 + J_3$ , we first maximize  $K_3$  by letting  $K_3 = G_3$ , which means  $G_3 + J_3 = 2N_2 - G_3$ . Hence, we minimize  $G_3 + J_3$  by maximizing  $G_3$ , i.e., we let  $G_3 = N_2$  and  $J_3 = 0$ . Further, since  $2(M_1 + M_2) \geq 2N_1 + 3N_2$ , it can be proved that there exists  $L_1, L_2, J_1, J_2$  that can satisfy the equality of (2.58) for sure. One possible solution is  $L_1 = \lceil 2N_1 + N_2 - 2M_2 \rceil$ ,  $L_2 = \lfloor 2N_1 + N_2 - 2M_2 \rfloor$ , and  $J_1 = J_2 = M_2 - N_2$ .

As a result, the achievable DoF equals  $\frac{2N_1 + 2N_2 - N_2}{2} = \frac{2N_1 + N_2}{2}$ .

- **When**  $2N_1 \leq 2(M_1 + M_2) < 2N_1 + 3N_2$

We first let  $L_1 = L_2 = M_1 - N_2$  and  $J_1 = J_2 = M_2 - N_2$ , which implies that  $L_3 + J_3 + G_3 = 2(N_1 + 2N_2 - M_1 - M_2)$ . In addition, we have  $K_3 + J_3 + G_3 = 2N_2$ . Similar to (2.73) and (2.74), we let

$$K_3 + L_3 = J_3 + G_3 - z, \text{ where } z = 2(M_1 + M_2 - N_1) \pmod{3} \quad (2.79)$$

which implies that

$$J_3 + G_3 = 2N_2 + \lceil \frac{2N_1 - 2M_1 - 2M_2}{3} \rceil \quad (2.80)$$

The value of  $G_3$  and  $J_3$  can be set as

$$G_3 = \lceil \frac{M_1 + M_2 - N_1}{3} \rceil, \quad J_3 = 2N_2 + N_1 - M_1 - M_2$$

As a result, the achievable DoF equals  $2N_1 + 2N_2 - J_3 - G_3 = \frac{1}{2} \lfloor \frac{2(2N_1 + M_1 + M_2)}{3} \rfloor$ .

- **When**  $M_1 + M_2 \leq N_1$

---

Since  $M_1 + M_2 \leq N_1$ , we have  $K_3 = G_3 = 0$ . First, we let  $L_1 = L_2 = M_1 - N_2$  and  $J_1 = J_2 = M_2 - N_2$ , which means  $J_3 = L_3 = 2N_2$ . As a result, the achievable DoF equals  $M_1 + M_2$ . Note that in this case, the equalities should hold for (2.64) and (2.61).

## Chapter 3

# Interference Alignment in Three-User MIMO Interference Channels

### 3.1 Introduction

In this chapter, we study 3-user MIMO interference channels, with  $M_T$  and  $M_R$  antennas on each transmitter and each receiver, respectively. The optimal sum DoF for this model was solved in [22], where the idea of subspace alignment chain was introduced and the outer-bound of sum DoF was derived. According to [22], the outer-bound DoF of each link of 3-user interference channels equals  $DoF^*$ , which is given in (1.2). Hence, the outer-bound of the sum DoF of the network is equal to  $3DoF^*$ . Feasibility of interference alignment studies the achievability of DoF obtained by linear interference alignment based on spatial beamforming, i.e., without the need for symbol extensions. This problem was first studied in [?], where iterative algorithms were proposed to test the feasibility of desired alignments. Then, [25] proposed to determine feasibility of alignment by counting the number of equations and comparing them with the number of variables. In [25], an interference alignment problem is

defined as “proper” if and only if the number of variables in every set of equations is not less than the number of equations in that set. Moreover, it is conjectured in [25] that proper systems are likely to be feasible and improper systems to be infeasible. This conjecture is confirmed on one hand, i.e., the improper systems are infeasible [26, 28]. On the other hand, it has been shown that the proper systems are feasible for sure if  $M_T = M_R$  [28] and/or both  $M_T$  and  $M_R$  are divisible by  $d$ , where  $d$  denotes the DoF of each user [26]. For the scenarios where each user can have different DoF, it was shown in [27] that if each user is equipped more than two antennas, the problem of checking the achievability of a given tuple of DoF is NP-hard. For 3-user MIMO interference channels, it was shown in [22, 29] that when each user has the same DoF  $d$ , the interference alignment is feasible if and only if  $(2r + 1)d \leq \max(rN, (r + 1)M)$ , where  $N = \max\{M_T, M_R\}$ ,  $M = \min\{M_T, M_R\}$ , for all integers  $r \geq 0$ , which also proves that some proper systems are not feasible.

Let  $d_i$  denote the DoF of user  $i$  and  $D = d_1 + d_2 + d_3$ . It was shown in [22] that the outer bound of *sum DoF* of 3-user interference channel is  $D \leq 3DoF^*$ . In addition, if the DoF of each user denotes one coordinate, the DoF region of 3-user interference channel would be a 3-dimensional space that is closed by multiple planes. As we can see, the sum DoF  $D = 3DoF^*$  can be seen as one plane, and the space under the plane,  $D \leq 3DoF^*$ , can certainly be seen as an outer bound of DoF region. However, this region is too loose to be considered as tight. In this paper, we derive an outer bound DoF region and show that it is tight in terms of integer DoF, i.e., the points with integer coordinates in the region are achievable for sure. Furthermore, the achievability of fractional DoF is also discussed. While there is lack of a systematic approach to prove that all fractional DoF inside the region can be achieved for sure, we introduce some methods that can examine and confirm the achievability of each individual case.

Another unsettled issue is the feasibility of linear interference alignment. It was already known that in general the “proper” system is not equivalent to “feasible” system [29]. It was also known that if each user has the same DoF  $d$ , the feasibility

condition is  $d \leq \lfloor \text{DoF}^* \rfloor$  [22]. The achievability is based on a novel technique called ‘subspace alignment chain’. However, when each user can have different DoF, the feasibility condition remains unknown. According to the definition of feasibility of interference alignment [25], the exact feasibility condition of a 3-user interference channel is in fact equivalent to our derived DoF region, because all the points with integer coordinates in the region can be achieved with a linear beamforming scheme proposed in this paper, without the need of symbol extension in time, frequency, or space.

The rest of the paper is organized as follows. In Section 3.2, the system model is introduced and the outer bound of DoF region is given. In Section 3.3, a beamforming scheme is proposed based on the concept of interference alignment chain. In Section 3.4, the achievable DoF region of the beamforming scheme is derived. In Section 3.5, with the combination of the beamforming scheme and symbol extension, the achievability of fractional DoF inside the outer bound DoF region is discussed. Section 3.6 summarizes the chapter.

## 3.2 System Model and Main Result

We consider a fully connected 3-user MIMO interference channel with  $M_T$  and  $M_R$  antennas at each transmitter and each receiver, respectively. Transmitter  $i$  transmits messages intended to receiver  $i$  ( $i = 1, 2, 3$ ) and causes interference to other two receivers. Let  $N = \max\{M_R, M_T\}$  and  $M = \min\{M_R, M_T\}$ . Note that when  $\frac{M}{N} \leq \frac{1}{2}$ , the DoF region is just the combination of single user and/or cooperation DoF outer bounds [20, 22], which can be trivially achieved. Moreover, interference alignment is irrelevant when  $\frac{M}{N} \leq \frac{1}{2}$ . Hence, in this paper, we focus on the region  $\frac{1}{2} < \frac{M}{N} < 1$ , where the DoF region remains an open problem.

Let  $\mathbf{H}_{ji} \in \mathbb{C}^{M_R \times M_T}$  denote the channel matrix between transmitter  $i$  and receiver  $j$ . We assume that all channel matrices are sampled from continuous complex Gaussian distributions and each entry of  $\mathbf{H}_{ij}$  is independent and identically distributed

(i.i.d.). The received signals on receiver  $j$  can be expressed as

$$\mathbf{y}_j = \sum_{i=1}^3 \mathbf{H}_{ji} \mathbf{B}_i \mathbf{m}_i + \mathbf{z}_j \quad (3.1)$$

where  $\mathbf{y}_j \in \mathbb{C}^{M_R \times 1}$  denotes the received signal,  $\mathbf{B}_i \in \mathbb{C}^{M_T \times d_i}$  denotes the beamforming matrix of transmitter  $i$ ,  $\mathbf{m}_i \in \mathbb{C}^{d_i \times 1}$  denotes the original message vector from transmitter  $i$ , and  $\mathbf{z}_j \in \mathbb{C}^{M_R \times 1}$  denotes the white Gaussian noise at receiver  $j$ .

In addition, in the case of  $M_T > M_R$  (i.e.,  $N = M_T$  and  $M = M_R$ ), each channel matrix has a  $(N - M)$ -dimensional null space. Let  $\text{nullspace}\{\mathbf{H}_{ij}\}$  denote the span of the null space of  $\mathbf{H}_{ij}$ . The following conditions are satisfied almost surely because the channels are generic and  $N \leq 2M$ .

$$\text{nullspace}\{\mathbf{H}_{21}\} \cap \text{nullspace}\{\mathbf{H}_{31}\} = \emptyset \quad (3.2)$$

$$\text{nullspace}\{\mathbf{H}_{12}\} \cap \text{nullspace}\{\mathbf{H}_{32}\} = \emptyset \quad (3.3)$$

$$\text{nullspace}\{\mathbf{H}_{13}\} \cap \text{nullspace}\{\mathbf{H}_{23}\} = \emptyset \quad (3.4)$$

Let  $\rho$  denote the power constraints on each transmitter and  $\mathbf{R}_i(\rho)$  denote the achievable rate of user  $i$ . The DoF of user  $i$  is defined as  $\lim_{\rho \rightarrow \infty} \frac{\mathbf{R}_i(\rho)}{\log(\rho)}$ , which can be interpreted as the number of independent signaling dimensions or streams available for user  $i$ . Further, note that  $d_i$  is the number of signals sent by transmitter  $i$ . If the desired signals on each receiver can be linearly decoded,  $d_i$  would be equal to the DoF of link  $i$ . Then, the sum DoF of the network can be calculated as  $D = \sum_{i=1}^3 d_i$ .

The main results of this paper are given in the following two theorems.

**Theorem 3.1** *In 3-user interference channels where each transmitter is equipped with  $M_T$  antennas and each receiver is equipped with  $M_R$  antennas, the outer bound of DoF region,  $\mathbf{R}(d_1, d_2, d_3)$ , is*

$$\left\{ \begin{array}{l} 2td_i + 2td_j + (2t - 1)d_k \leq (3t - 1)N \\ (2t - 1)d_i + 2(t - 1)d_j + 2(t - 1)d_k \leq (3t - 2)M \\ (2t - 1)d_i + (2t - 1)d_j + (2t - 1)d_k \leq (3t - 1)M \\ d_i + d_j \leq N \end{array} \right. \quad (3.5)$$

for  $\frac{M}{N} \in [\frac{3t-2}{3t-1}, \frac{3t-1}{3t})$ , ( $t = 1, 2, \dots, \infty$ )

$$\begin{cases} 2td_i + 2td_j + (2t-1)d_k \leq 3tM \\ (2t+1)d_i + 2td_j + 2td_k \leq 3tN \\ d_i + d_j \leq N \end{cases} \quad (3.6)$$

for  $\frac{M}{N} \in [\frac{3t-1}{3t}, \frac{3t}{3t+1})$ , and

$$\begin{cases} (2t+1)d_i + 2td_j + 2td_k \leq (3t+1)M \\ (2t+1)d_i + (2t+1)d_j + (2t+1)d_k \leq (3t+1)N \\ d_i + d_j \leq N \end{cases} \quad (3.7)$$

for  $\frac{M}{N} \in [\frac{3t}{3t+1}, \frac{3t+1}{3t+2})$ , where  $N = \max\{M_T, M_R\}$ ,  $M = \min\{M_T, M_R\}$ ,  $i, j, k = 1, 2, 3$  and  $i \neq j \neq k$ .

*Proof:* The proof is presented in Appendix A.

**Theorem 3.2** For the 3-user MIMO interference channels with  $M_T$  and  $M_R$  antennas on each transmitter and receiver, respectively and  $\frac{1}{2} \leq \frac{\min\{M_T, M_R\}}{\max\{M_T, M_R\}} < 1$ , the DoF of user  $i$ ,  $d_i$  (where  $i = 1, 2, 3$  and  $d_i$  is integer), is feasible with linear interference alignment if and only if (3.5)-(3.7) are satisfied.

The converse proof follows directly from *Theorem 1*, i.e., any DoF that does not satisfy (3.5)-(3.7) cannot be achieved for sure as (3.5)-(3.7) is outer bound. The achievability proof is given in Sections 3.3-3.4. Specifically, we first propose a linear beamforming scheme in Section 3.3. Then, Section 3.4 shows that the achievable DoF region of the proposed scheme is the same as (3.5)-(3.7) with  $d_i$  being an integer.

**Remark 3.1** Now, we compare our results with existing ones based on the example of  $M = 4, N = 7$ . According to our result, the DoF region of this setup is (3.5) with  $t = 1$ , i.e.,

$$\begin{cases} 2d_i + 2d_j + d_k \leq 14 \\ d_i \leq 4 \\ d_i + d_j + d_k \leq 8 \\ d_i + d_j \leq N \end{cases} \quad (3.8)$$

Whereas based on the results in [20, 22], the DoF region is

$$\begin{cases} d_i \leq 4 \\ d_i + d_j + d_k \leq 8 \\ d_i + d_j \leq N \end{cases} \quad (3.9)$$

As we can see, (3.8) has one more constraint than (3.9), which makes our result a ‘tighter’ DoF region. For instance, the DoF tuple  $(d_1 = 4, d_2 = 3, d_3 = 1)$  satisfies (3.9), but not (3.8), which means it is in fact outside the region and cannot be achieved at all.

Moreover, Theorem 3.2 shows that any (integer) DoF tuple inside (3.8) can be achieved with a linear beamforming scheme. This finding is not available in previous works.

Finally, if we let  $d_i = d_j = d_k = d$ , (3.8) and (3.9) will both become the same as the result in [22], i.e.,  $d \leq \frac{8}{3}$ .

### 3.3 A Beamforming Scheme

In this section, we propose a spatial beamforming scheme that can achieve all the integer DoF within the outer bound region  $R(d_1, d_2, d_3)$ . First, we review the concept of the subspace alignment chain in [22]. Then, the designs of beamforming matrices based on subspace alignment chain are elaborated. At last, we discuss how to ensure the signals are linearly decoded at each receiver. In the following discussion, we assume  $M_T > M_R$ . Then,  $N = M_T$ ,  $M = M_R$ . Note that due to the reciprocity of linear scheme, the same DoF region can be achieved with  $M_T < M_R$  for sure.

#### 3.3.1 Subspace Alignment Chain [22]

Two ends of an alignment chain correspond to the signals that are nulled at one unintended receiver and cause interference at the other. For the signals in between, each of which is aligned with another interference signal at each of those undesired

receivers. The length of each chain is defined as the number of signals that participate in it.

Let  $\mathbf{V}_{i(n)}^j \in \mathbb{C}^{N \times Q_j}$  denote the  $s$ th  $Q_j$ -dimensional subspace transmitted by transmitter  $i$  which participates in the chain that originates from transmitter  $j$ . Consider one alignment chain originating from transmitter 1, where  $\mathbf{V}_{1(1)}^1$  is nulled at receiver 2 but causes an interference dimension at receiver 3. The second signal,  $\mathbf{V}_{2(1)}^1$  from transmitter 2, should be aligned with  $\mathbf{V}_{1(1)}^1$  on receiver 3, so that no more interference dimension is generated on receiver 3. Then, if  $\mathbf{V}_{2(1)}^1$  can be nulled at receiver 1, the chain is finished. Otherwise, transmitter 3 should send a vector,  $\mathbf{V}_{3(1)}^1$ , which is aligned with  $\mathbf{V}_{2(1)}^1$  on receiver 1. The chain will keep going until the zero-forcing can be achieved. Mathematically, it can be expressed as follows,

$$\underbrace{\begin{bmatrix} \mathbf{H}_{21} & 0 & \cdots & \cdots & 0 \\ \mathbf{H}_{31} & -\mathbf{H}_{32} & 0 & \cdots & 0 \\ 0 & \mathbf{H}_{12} & -\mathbf{H}_{13} & 0 & \cdots \\ \vdots & \ddots & \cdots & & \\ 0 & \cdots & \cdots & \mathbf{H}_{ri} & -\mathbf{H}_{rj} \\ 0 & 0 & \cdots & 0 & \mathbf{H}_{ij} \end{bmatrix}}_{\mathbf{H} \in \mathbb{C}^{M(S+1) \times S \cdot N}} \underbrace{\begin{bmatrix} \mathbf{V}_{1(1)}^1 \\ \mathbf{V}_{2(1)}^1 \\ \mathbf{V}_{3(1)}^1 \\ \mathbf{V}_{1(2)}^1 \\ \vdots \\ \mathbf{V}_{i(n)}^1 \\ \mathbf{V}_{j(n)}^1 \end{bmatrix}}_{\mathbf{V} \in \mathbb{C}^{S \cdot N \times Q_1}} = \mathbf{0} \quad (3.10)$$

where  $S$  is the length of the chain, which equals the number of subspaces,  $\mathbf{V}_{i(n)}^1$ , that participate in the chain.

As can be seen, zero-forcing can be performed at the end of chain when the matrix  $\mathbf{H}$  turns into a “fat” matrix, i.e.,  $S \cdot N > (S+1)M \Rightarrow S > \frac{M}{N-M}$ . Hence, the length of the shortest chain can be expressed as

$$S = \begin{cases} \lceil \frac{M}{N-M} \rceil + 1 & \text{when } \frac{M}{N} = \frac{p}{p+1} \\ \lceil \frac{M}{N-M} \rceil & \text{when } \frac{M}{N} \neq \frac{p}{p+1} \end{cases} \quad (3.11)$$

where  $p = 1, 2, 3, \dots, +\infty$ . Note that for any chain that is longer than  $S$ ,  $\mathbf{H}$  will always be a “fat” matrix, which means for each antenna configuration, there exist multiple chains with length equal to  $S, S+1, \dots$ .

The chains with the length of  $S$  are referred to as the *original* alignment chains. It can be seen there are three *original* chains. Each chain originates from one transmitter, i.e.,  $j = 1, 2, 3$ . The three *original* chains can be expressed as follows

$$\begin{aligned}
\mathbf{0} &\xleftrightarrow{R_2} \mathbf{V}_{1(1)}^1 \xleftrightarrow{R_3} \mathbf{V}_{2(1)}^1 \xleftrightarrow{R_1} \mathbf{V}_{3(1)}^1 \xleftrightarrow{R_2} \mathbf{V}_{1(2)}^1 \cdots \mathbf{0} \\
\mathbf{0} &\xleftrightarrow{R_3} \mathbf{V}_{2(1)}^2 \xleftrightarrow{R_1} \mathbf{V}_{3(1)}^2 \xleftrightarrow{R_2} \mathbf{V}_{1(1)}^2 \xleftrightarrow{R_3} \mathbf{V}_{2(2)}^2 \cdots \mathbf{0} \\
\mathbf{0} &\xleftrightarrow{R_1} \mathbf{V}_{3(1)}^3 \xleftrightarrow{R_2} \mathbf{V}_{1(1)}^3 \xleftrightarrow{R_3} \mathbf{V}_{2(1)}^3 \xleftrightarrow{R_1} \mathbf{V}_{3(2)}^3 \cdots \mathbf{0}
\end{aligned} \tag{3.12}$$

where  $\mathbf{V}_{1(1)}^1 \xleftrightarrow{R_3} \mathbf{V}_{2(1)}^1$  means that the interference generated by transmitter 1  $\mathbf{V}_{1(1)}^1$  and the one generated by transmitter 2  $\mathbf{V}_{2(1)}^1$  are aligned at receiver 3, i.e.,  $\mathbf{H}_{31} \mathbf{V}_{1(1)}^1 = \mathbf{H}_{32} \mathbf{V}_{2(1)}^1$ , as shown in (3.10).

### 3.3.2 A Beamforming Scheme

In [22], the *original* chain (3.12) is designed to achieve the point with coordinates  $([DoF^*], [DoF^*], [DoF^*])$  in the space of DoF region. However, there are some points in the region that cannot be achieved with the scheme in [22]. This is because those points have unequal values of  $d_1, d_2$  and  $d_3$ , which means the signal spaces on the users are unbalanced, and *original* chain itself does not have enough flexibility to distribute the signal space accordingly. Next, we propose a beamforming scheme design based on three types of chains: *original* chains, long chains (with length  $\bar{S} = S + 1$ ), and null space of interference channels. Note that in theory, the length of each chain can be arbitrarily long. Hence, it is not trivial to select the chains that only with length of  $S$  and  $S + 1$ .

The beamforming matrix of transmitter  $i$  is designed as

$$\mathbf{B}_i = \begin{bmatrix} \mathbf{V}_i & \bar{\mathbf{V}}_i & \mathbf{U}_i \end{bmatrix} \tag{3.13}$$

where  $\mathbf{V}_i$  is composed of all the subspaces from transmitter  $i$  that participate in the *original* chains (as shown in (3.12)), i.e.,

$$\mathbf{V}_i = \begin{bmatrix} \mathbf{V}_{i(1)}^1 & \mathbf{V}_{i(2)}^1 & \cdots & \mathbf{V}_{i(1)}^2 & \mathbf{V}_{i(2)}^2 & \cdots & \mathbf{V}_{i(1)}^3 & \mathbf{V}_{i(2)}^3 & \cdots \end{bmatrix} \tag{3.14}$$

and  $\bar{\mathbf{V}}_i$  is composed of all the subspaces from transmitter  $i$  that participate in long chains (which is similar to (3.12) but with one more subspace at the end of each chain), i.e.,

$$\bar{\mathbf{V}}_i = \left[ \bar{\mathbf{V}}_{i(1)}^1 \quad \bar{\mathbf{V}}_{i(2)}^1 \quad \cdots \quad \bar{\mathbf{V}}_{i(1)}^2 \quad \bar{\mathbf{V}}_{i(2)}^2 \quad \cdots \quad \bar{\mathbf{V}}_{i(1)}^3 \quad \bar{\mathbf{V}}_{i(2)}^3 \quad \cdots \right] \quad (3.15)$$

where  $\bar{\mathbf{V}}_{i(\bar{n})}^j \in \mathbb{C}^{N \times \bar{Q}_j}$ .

In addition,  $\mathbf{U}_i = \left[ \mathbf{U}_i^1 \quad \mathbf{U}_i^2 \right] \in \mathbb{C}^{M \times q_i}$ , which is designed as follows

$$\begin{aligned} \mathbf{H}_{21} \mathbf{U}_1^1 &= \mathbf{0}, \quad \mathbf{H}_{31} \mathbf{U}_1^2 = \mathbf{0} \\ \mathbf{H}_{12} \mathbf{U}_2^1 &= \mathbf{0}, \quad \mathbf{H}_{32} \mathbf{U}_2^2 = \mathbf{0} \\ \mathbf{H}_{13} \mathbf{U}_3^1 &= \mathbf{0}, \quad \mathbf{H}_{23} \mathbf{U}_3^2 = \mathbf{0} \end{aligned} \quad (3.17)$$

Each part of  $\mathbf{U}_i$  is nulled at one of the unintended receivers and causes interference to the other. Let  $q_{ji}$  denote the number of interference dimensions generated on receiver  $j$  by  $\mathbf{U}_i$ . We have  $\mathbf{U}_1^1 \in \mathbb{C}^{N \times q_{31}}$ ,  $\mathbf{U}_1^2 \in \mathbb{C}^{N \times q_{21}}$ ,  $\mathbf{U}_2^1 \in \mathbb{C}^{N \times q_{32}}$ ,  $\mathbf{U}_2^2 \in \mathbb{C}^{N \times q_{12}}$ ,  $\mathbf{U}_3^1 \in \mathbb{C}^{N \times q_{23}}$ , and  $\mathbf{U}_3^2 \in \mathbb{C}^{N \times q_{13}}$ .

In summary, all the beamforming subspaces of three transmitters can be designed as follows,

$$\begin{aligned} \mathbf{0} &\xleftrightarrow{R_2} \mathbf{V}_{1(1)}^1 \xleftrightarrow{R_3} \mathbf{V}_{2(1)}^1 \xleftrightarrow{R_1} \mathbf{V}_{3(1)}^1 \xleftrightarrow{R_2} \mathbf{V}_{1(2)}^1 \cdots \mathbf{V}_{i(\lceil \frac{S}{3} \rceil)}^1 \xleftrightarrow{R_k} \mathbf{0} \quad (a) \\ \mathbf{0} &\xleftrightarrow{R_3} \mathbf{V}_{2(1)}^2 \xleftrightarrow{R_1} \mathbf{V}_{3(1)}^2 \xleftrightarrow{R_2} \mathbf{V}_{1(1)}^2 \xleftrightarrow{R_3} \mathbf{V}_{2(2)}^2 \cdots \mathbf{V}_{j(\lceil \frac{S}{3} \rceil)}^2 \xleftrightarrow{R_i} \mathbf{0} \quad (b) \\ \mathbf{0} &\xleftrightarrow{R_1} \mathbf{V}_{3(1)}^3 \xleftrightarrow{R_2} \mathbf{V}_{1(1)}^3 \xleftrightarrow{R_3} \mathbf{V}_{2(1)}^3 \xleftrightarrow{R_1} \mathbf{V}_{3(2)}^3 \cdots \mathbf{V}_{k(\lceil \frac{S}{3} \rceil)}^3 \xleftrightarrow{R_j} \mathbf{0} \quad (c) \\ \mathbf{0} &\xleftrightarrow{R_2} \bar{\mathbf{V}}_{1(1)}^1 \xleftrightarrow{R_3} \bar{\mathbf{V}}_{2(1)}^1 \xleftrightarrow{R_1} \bar{\mathbf{V}}_{3(1)}^1 \xleftrightarrow{R_2} \bar{\mathbf{V}}_{1(2)}^1 \cdots \bar{\mathbf{V}}_{i(\lceil \frac{S}{3} \rceil)}^1 \xleftrightarrow{R_k} \bar{\mathbf{V}}_{j(\lceil \frac{S+1}{3} \rceil)}^1 \xleftrightarrow{R_i} \mathbf{0} \quad (d) \\ \mathbf{0} &\xleftrightarrow{R_3} \bar{\mathbf{V}}_{2(1)}^2 \xleftrightarrow{R_1} \bar{\mathbf{V}}_{3(1)}^2 \xleftrightarrow{R_2} \bar{\mathbf{V}}_{1(1)}^2 \xleftrightarrow{R_3} \bar{\mathbf{V}}_{2(2)}^2 \cdots \bar{\mathbf{V}}_{j(\lceil \frac{S}{3} \rceil)}^2 \xleftrightarrow{R_i} \bar{\mathbf{V}}_{k(\lceil \frac{S+1}{3} \rceil)}^2 \xleftrightarrow{R_j} \mathbf{0} \quad (e) \\ \mathbf{0} &\xleftrightarrow{R_1} \bar{\mathbf{V}}_{3(1)}^3 \xleftrightarrow{R_2} \bar{\mathbf{V}}_{1(1)}^3 \xleftrightarrow{R_3} \bar{\mathbf{V}}_{2(1)}^3 \xleftrightarrow{R_1} \bar{\mathbf{V}}_{3(2)}^3 \cdots \bar{\mathbf{V}}_{k(\lceil \frac{S}{3} \rceil)}^3 \xleftrightarrow{R_j} \bar{\mathbf{V}}_{i(\lceil \frac{S+1}{3} \rceil)}^3 \xleftrightarrow{R_k} \mathbf{0} \quad (f) \\ \mathbf{0} &\xleftrightarrow{R_2} \mathbf{U}_1^1, \quad \mathbf{0} \xleftrightarrow{R_3} \mathbf{U}_2^2, \quad \mathbf{0} \xleftrightarrow{R_1} \mathbf{U}_3^1; \mathbf{U}_1^2 \xleftrightarrow{R_3} \mathbf{0}, \quad \mathbf{U}_2^2 \xleftrightarrow{R_1} \mathbf{0}, \quad \mathbf{U}_3^2 \xleftrightarrow{R_2} \mathbf{0}; \quad (g) \end{aligned} \quad (3.18)$$

**Remark 3.2** Note that although  $\mathbf{V}_{i(\bar{n})}^j$  and  $\bar{\mathbf{V}}_{i(\bar{n})}^j$  are designed in the similar way, they are in fact independent of each other almost for sure. For example, let  $\mathbf{V}_{i(1)}^1$  and  $\mathbf{V}_{i(2)}^1$

are designed from the original chain with  $S = 4$ , i.e.,

$$\mathbf{0} \xleftrightarrow{R_2} \mathbf{V}_{1(1)}^1 \xleftrightarrow{R_3} \mathbf{V}_{2(1)}^1 \xleftrightarrow{R_1} \mathbf{V}_{3(1)}^1 \xleftrightarrow{R_2} \mathbf{V}_{1(2)}^1 \xleftrightarrow{R_3} \mathbf{0} \quad (3.19)$$

and  $\bar{\mathbf{V}}_{i(1)}^1, \bar{\mathbf{V}}_{i(2)}^1$  are designed from the long chain as follows,

$$\mathbf{0} \xleftrightarrow{R_2} \bar{\mathbf{V}}_{1(1)}^1 \xleftrightarrow{R_3} \bar{\mathbf{V}}_{2(1)}^1 \xleftrightarrow{R_1} \bar{\mathbf{V}}_{3(1)}^1 \xleftrightarrow{R_2} \bar{\mathbf{V}}_{1(2)}^1 \xleftrightarrow{R_3} \bar{\mathbf{V}}_{2(2)}^1 \xleftrightarrow{R_1} \mathbf{0} \quad (3.20)$$

(3.19) shows that  $\mathbf{V}_{1(2)}^1$  is nulled on receiver 3, i.e.,  $\mathbf{H}_{13}\mathbf{V}_{1(2)}^1 = \mathbf{0}$ , whereas  $\bar{\mathbf{V}}_{1(2)}^1$  in (3.20) is not nulled on receiver 3, i.e.,  $\mathbf{H}_{13}\bar{\mathbf{V}}_{1(2)}^1 \neq \mathbf{0}$ , which means  $\mathbf{V}_{1(2)}^1$  and  $\bar{\mathbf{V}}_{1(2)}^1$  are independent of each other for sure. Accordingly, it can be easily proved that  $\mathbf{V}_{3(1)}^1$  and  $\bar{\mathbf{V}}_{3(1)}^1$  are independent of each other. Hence, it can be seen that based on this design,  $\mathbf{V}_{i(\bar{n})}^j$  and  $\bar{\mathbf{V}}_{i(\bar{n})}^j$  are independent of each other.

Although these subspaces are designed, the scheme is not feasible unless the desired signals can be linearly decoded. In the following, we show that the scheme is feasible for sure under some conditions.

**Theorem 3.3** *In 3-user interference channels with  $M_T \geq M_R$ , for the proposed beamforming design in (3.13)-(3.18), the desired signals on each receiver can be linearly decoded for sure if the following conditions are satisfied.*

$$Q_j \leq S \cdot N - (S + 1)M, \quad j = 1, 2, 3 \quad (3.21)$$

$$\bar{Q}_j \leq (S + 1) \cdot N - (S + 2)M, \quad j = 1, 2, 3 \quad (3.22)$$

$$Q_1 + \bar{Q}_1 + q_{31} \leq N - M \quad (3.23)$$

$$Q_2 + \bar{Q}_2 + q_{12} \leq N - M \quad (3.24)$$

$$Q_3 + \bar{Q}_3 + q_{23} \leq N - M \quad (3.25)$$

$$Q_l + \bar{Q}_j + q_{jm} \leq N - M, \quad j = 1, 2, 3, \quad \text{when } a = 2 \quad (3.26)$$

$$Q_l + \bar{Q}_j + q_{lj} \leq N - M, \quad j = 1, 2, 3, \quad \text{when } a = 0 \quad (3.27)$$

$$Q_j + \bar{Q}_m + q_{lj} \leq N - M, \quad j = 1, 2, 3, \quad \text{when } a = 1 \quad (3.28)$$

$$d_1 + P_1 + q_{12} + q_{13} \leq M \quad (3.29)$$

$$d_2 + P_2 + q_{21} + q_{23} \leq M \quad (3.30)$$

$$d_3 + P_3 + q_{31} + q_{32} \leq M \quad (3.31)$$

where  $l = (j \bmod 3) + 1$ ,  $m = (l \bmod 3) + 1$ ,  $a = S \bmod 3$ ,  $M = M_R$ ,  $N = M_T$ , and  $P_i$  denotes the number of interference dimensions that are generated by the six alignment chains, (3.18a)-(3.18f), on receiver  $i$ .

**Remark 3.3** Note that the value of  $P_i$  is various with different length of the alignment chains. Take  $P_1$  for example. Assuming  $S = 2$ , for the three original chains, only the one that originates from transmitter 2 will generate  $Q_2$  interference dimensions on receiver 1. For the long chains ( $\bar{S} = 3$ ), the ones originate from transmitters 1 and 2 will generate  $\bar{Q}_1$  and  $\bar{Q}_2$  interference dimensions on receiver 1, respectively. Hence, in this case  $P_1 = Q_2 + \bar{Q}_1 + \bar{Q}_2$ .

*Proof of Theorem 3.3:* The proof involves two steps. First, on the receiver side, we need to show that the desired signal space does not overlap the interference space on each receiver. Then, on the transmitter side, each beamforming matrix,  $\mathbf{B}_i$ , must have full column rank.

First, as can be seen, (3.29)-(3.31) ensure that the sum dimensions of the desired signals and interference does not exceed the total number of dimensions on each receiver. Take receiver 1 for example, the number of desired signals and interference dimensions are  $d_1$  and  $P_1 + q_{12} + q_{13}$ , respectively. Since there are total  $M$  dimensions on the receiver, constraint (3.29) must be satisfied. Further, we shall note that the direct channel matrices,  $\mathbf{H}_{11}$ ,  $\mathbf{H}_{22}$  and  $\mathbf{H}_{33}$ , are not used in the design of beamforming subspaces. Hence, due to channel randomness, the desired signal space does not overlap the interference space on each receiver almost surely.

Next, we show that each beamforming matrix  $\mathbf{B}_i$  must have full column rank for sure if (3.21)-(3.28) are satisfied.

The beamforming matrix of transmitter  $i$  is composed of all the subspaces from transmitter  $i$  that participate in (3.18). Accordingly, we define the subspaces in the same position of each chain (starting from the left) to be one layer. Also, let  $\mathbf{U}_1^1$ ,  $\mathbf{U}_2^2$ , and  $\mathbf{U}_3^3$  belong to the first layer, and  $\mathbf{U}_1^2$ ,  $\mathbf{U}_2^1$ ,  $\mathbf{U}_3^2$  belong to the last layer. Hence, the first layer has  $\mathbf{V}_{1(1)}^1, \mathbf{V}_{2(1)}^2, \mathbf{V}_{3(1)}^3, \bar{\mathbf{V}}_{1(1)}^1, \bar{\mathbf{V}}_{2(1)}^2, \bar{\mathbf{V}}_{3(1)}^3, \mathbf{U}_1^1, \mathbf{U}_2^2, \mathbf{U}_3^3$ . Further, we can see

that the subspaces in the same layer belong to different transmitters. For example, in the first layer, the subspaces that belong to  $\mathbf{B}_1$ ,  $\mathbf{B}_2$  and  $\mathbf{B}_3$  are  $\begin{bmatrix} \mathbf{V}_{1(1)}^1 & \bar{\mathbf{V}}_{1(1)}^1 & \mathbf{U}_1^1 \end{bmatrix}$ ,  $\begin{bmatrix} \mathbf{V}_{2(1)}^2 & \bar{\mathbf{V}}_{2(1)}^2 & \mathbf{U}_2^2 \end{bmatrix}$ , and  $\begin{bmatrix} \mathbf{V}_{3(1)}^3 & \bar{\mathbf{V}}_{3(1)}^3 & \mathbf{U}_3^1 \end{bmatrix}$ , respectively.

In order to prove  $\mathbf{B}_i$  is full rank, we shall prove each beamforming matrix has full column rank layer by layer. Take  $\mathbf{B}_1$  for example, we first show that the subspaces of  $\mathbf{B}_1$  in the first layer,  $\begin{bmatrix} \mathbf{V}_{1(1)}^1 & \bar{\mathbf{V}}_{1(1)}^1 & \mathbf{U}_1^1 \end{bmatrix}$ , has full column rank. Next, we show that the subspaces of  $\mathbf{B}_1$  in the first two layers, i.e.,

$\begin{bmatrix} \mathbf{V}_{1(1)}^1 & \bar{\mathbf{V}}_{1(1)}^1 & \mathbf{U}_1^1 & \mathbf{V}_{1(1)}^3 & \bar{\mathbf{V}}_{1(1)}^3 \end{bmatrix}$ , has full column rank. Then, the rest of layers is proved recursively. Assuming the subspaces of  $\mathbf{B}_i$  in the first  $n$  layers have column rank, we will show that the subspaces in the first  $n + 1$  layers also have full column rank for sure. Since  $\mathbf{B}_i$  has totally  $S + 1$  layers, the problem is divided into two cases, i.e., the  $(n + 1)$ th layer is not the last layer ( $n + 1 < S + 1$ ) and the  $(n + 1)$ th layer is the last layer ( $n + 1 = S + 1$ ). Moreover, the case of  $n + 1 = S + 1$  is further divided into 3 subcases according to the value of  $S \bmod 3$ .

In the following, we mainly focus on proving the full column rank of  $\mathbf{B}_1$ , because  $\mathbf{B}_2$  and  $\mathbf{B}_3$  can be proved in the same way.

- *The subspaces of  $\mathbf{B}_i$  in the first layer.*

As mentioned before, the subspaces that belong to  $\mathbf{B}_1$  in the first layer is  $\begin{bmatrix} \mathbf{V}_{1(1)}^1 & \bar{\mathbf{V}}_{1(1)}^1 & \mathbf{U}_1^1 \end{bmatrix}$ , which is in the null space of  $\mathbf{H}_{21}$ . Hence, to ensure it has full column rank, the number of its column vectors cannot be more than the nullity of  $\mathbf{H}_{21}$ , which is guaranteed by (3.23). Further, as one of the subspaces in (3.18a),  $\mathbf{V}_{1(1)}^1 \in \mathbb{C}^{M_T \times Q_1}$  is also part of the null space of  $\mathbf{H}$  in (3.10). As we can see, to ensure  $\mathbf{V}_{1(1)}^1$  has full column rank,  $Q_1$  must be smaller than the nullity of  $\mathbf{H}$ , which is guaranteed by (3.21) with  $j = 1$ . Similarly, the full rank of  $\bar{\mathbf{V}}_{1(1)}^1 \in \mathbb{C}^{M_T \times \bar{Q}_1}$  that belongs to (3.18d) is guaranteed by (3.22) with  $j = 1$ . As a result,  $\begin{bmatrix} \mathbf{V}_{1(1)}^1 & \bar{\mathbf{V}}_{1(1)}^1 & \mathbf{U}_1^1 \end{bmatrix}$  must have full column rank if (3.21)-(3.23) are satisfied.

Similarly, for transmitters 2 and 3, the full rank of  $\begin{bmatrix} \mathbf{V}_{2(1)}^2 & \bar{\mathbf{V}}_{2(1)}^2 & \mathbf{U}_2^2 \end{bmatrix}$  and  $\begin{bmatrix} \mathbf{V}_{3(1)}^3 & \bar{\mathbf{V}}_{3(1)}^3 & \mathbf{U}_3^1 \end{bmatrix}$  can be guaranteed by (3.24), (3.21), (3.22) and (3.25), (3.21), (3.22), respectively.

- *The subspaces of  $\mathbf{B}_i$  in the first two layers.*

The beamforming subspaces of  $\mathbf{B}_1$  in the second layer is  $\left[ \mathbf{V}_{1(1)}^3 \quad \bar{\mathbf{V}}_{1(1)}^3 \right]$ . Now, we need to show that the subspaces of  $\mathbf{B}_1$  in the first two layers,  $\left[ \mathbf{V}_{1(1)}^1 \quad \bar{\mathbf{V}}_{1(1)}^1 \quad \mathbf{U}_1^1 \quad \mathbf{V}_{1(1)}^3 \quad \bar{\mathbf{V}}_{1(1)}^3 \right]$ , has full column rank. It is equivalent to proving that there exists no nonzero solutions of following equation,

$$\left[ \mathbf{V}_{1(1)}^1 \quad \bar{\mathbf{V}}_{1(1)}^1 \quad \mathbf{U}_1^1 \quad \mathbf{V}_{1(1)}^3 \quad \bar{\mathbf{V}}_{1(1)}^3 \right] \begin{bmatrix} \alpha_1 \\ \vdots \\ \alpha_l \end{bmatrix} = \mathbf{0} \quad (3.32)$$

Note that (3.32) can be written as

$$\left[ \mathbf{V}_{1(1)}^1 \quad \bar{\mathbf{V}}_{1(1)}^1 \quad \mathbf{U}_1^1 \right] \begin{bmatrix} \alpha_1 \\ \vdots \\ \alpha_s \end{bmatrix} = - \left[ \mathbf{V}_{1(1)}^3 \quad \bar{\mathbf{V}}_{1(1)}^3 \right] \begin{bmatrix} \alpha_{s+1} \\ \vdots \\ \alpha_l \end{bmatrix} \quad (3.33)$$

By left-multiplying  $\mathbf{H}_{21}$  on both sides of (3.33), we get

$$\mathbf{H}_{21} \left[ \mathbf{V}_{1(1)}^3 \quad \bar{\mathbf{V}}_{1(1)}^3 \right] \begin{bmatrix} \alpha_{s+1} \\ \vdots \\ \alpha_l \end{bmatrix} = \mathbf{0} \quad (3.34)$$

According to (3.18c) and (3.18f), we have  $\mathbf{H}_{21} \left[ \mathbf{V}_{1(1)}^3 \quad \bar{\mathbf{V}}_{1(1)}^3 \right] = \mathbf{H}_{23} \left[ \mathbf{V}_{3(1)}^3 \quad \bar{\mathbf{V}}_{3(1)}^3 \right]$ , which means

$$\mathbf{H}_{23} \left[ \mathbf{V}_{3(1)}^3 \quad \bar{\mathbf{V}}_{3(1)}^3 \right] \begin{bmatrix} \alpha_{s+1} \\ \vdots \\ \alpha_l \end{bmatrix} = \mathbf{0} \quad (3.35)$$

Note that  $\left[ \mathbf{V}_{3(1)}^3 \quad \bar{\mathbf{V}}_{3(1)}^3 \right]$  has been proved to have full column rank and is in the null space of  $\mathbf{H}_{13}$ . Hence, based on (3.4),  $\left[ \alpha_{s+1} \quad \cdots \quad \alpha_l \right]^T$  must be all-zero to satisfy (3.35). Then, we substitute this result into (3.33). Since  $\left[ \mathbf{V}_{1(1)}^1 \quad \bar{\mathbf{V}}_{1(1)}^1 \quad \mathbf{U}_1^1 \right]$  from the first layer has full column rank, it can be seen that  $\left[ \alpha_1 \quad \cdots \quad \alpha_s \right]^T$  must

be an all-zero vector. Therefore, we prove the subspaces of  $\mathbf{B}_1$  in the first two layers have full column rank.

Similarly, the beamforming subspaces of  $\mathbf{B}_2$  and  $\mathbf{B}_3$  in the first two layers also have full column rank.

- *The subspaces of  $\mathbf{B}_i$  in the first  $n + 1$  layers.*

Next, we show that the subspaces of  $\mathbf{B}_1$  in the first  $n + 1$  layers have full column rank provided that the subspaces of  $\mathbf{B}_i$  in the first  $n$  layers have full column rank for sure.

*Case 1:  $n < S$ .*

We first discuss the case in which the  $(n + 1)$ th layer is not the last layer, i.e.,  $n < S$ . According to (3.18), the subspaces of  $\mathbf{B}_1$  in the first  $(n + 1)$  layers are  $\left[ \mathbf{V}_{1(1)}^1 \quad \bar{\mathbf{V}}_{1(1)}^1 \quad \mathbf{U}_1^1 \quad \mathbf{V}_{1(1)}^3 \quad \bar{\mathbf{V}}_{1(1)}^3 \quad \cdots \quad \mathbf{V}_{1(\lceil \frac{n+1}{3} \rceil)}^\iota \quad \bar{\mathbf{V}}_{1(\lceil \frac{n+1}{3} \rceil)}^\iota \right]$  where  $\iota = 1, 3, 2$  for  $n + 1 \bmod 3 = 1, 2, 0$ , respectively. Hence, we shall prove that all-zero vector is the only solution for  $\left[ \beta_1 \quad \cdots \quad \beta_q \right]^T$  in the following equation,

$$\left[ \mathbf{V}_{1(1)}^1 \quad \bar{\mathbf{V}}_{1(1)}^1 \quad \mathbf{U}_1^1 \quad \mathbf{V}_{1(1)}^3 \quad \bar{\mathbf{V}}_{1(1)}^3 \quad \cdots \quad \mathbf{V}_{1(\lceil \frac{n+1}{3} \rceil)}^\iota \quad \bar{\mathbf{V}}_{1(\lceil \frac{n+1}{3} \rceil)}^\iota \right] \begin{bmatrix} \beta_1 \\ \vdots \\ \beta_q \end{bmatrix} = \mathbf{0} \quad (3.36)$$

By left multiplying  $\mathbf{H}_{21}$  on both sides of (3.36), we can get

$$\mathbf{H}_{21} \left[ \mathbf{V}_{1(1)}^3 \quad \bar{\mathbf{V}}_{1(1)}^3 \quad \cdots \quad \mathbf{V}_{1(\lceil \frac{n+1}{3} \rceil)}^\iota \quad \bar{\mathbf{V}}_{1(\lceil \frac{n+1}{3} \rceil)}^\iota \right] \begin{bmatrix} \beta_{s+1} \\ \vdots \\ \beta_q \end{bmatrix} = \mathbf{0} \quad (3.37)$$

According to (3.18), each subspace in (3.37) is aligned with one subspace of  $\mathbf{B}_3$  in previous layers on  $R_2$ . Hence, (3.37) is equivalent to

$$\mathbf{H}_{23} \left[ \mathbf{V}_{3(1)}^3 \quad \bar{\mathbf{V}}_{3(1)}^3 \quad \cdots \quad \mathbf{V}_{3(\lceil \frac{n}{3} \rceil)}^\iota \quad \bar{\mathbf{V}}_{3(\lceil \frac{n}{3} \rceil)}^\iota \right] \begin{bmatrix} \beta_{s+1} \\ \vdots \\ \beta_q \end{bmatrix} = \mathbf{0} \quad (3.38)$$

First of all, since  $\left[ \mathbf{V}_{3(1)}^3 \quad \bar{\mathbf{V}}_{3(1)}^3 \quad \cdots \quad \mathbf{V}_{3(\lceil \frac{n}{3} \rceil)}^\iota \quad \bar{\mathbf{V}}_{3(\lceil \frac{n}{3} \rceil)}^\iota \right]$  are in the first  $n$  layers, it has full column rank for sure. In addition, since  $n < S$ , the chain cannot end at the  $n$ th

layer, which implies that  $\left[ \mathbf{V}_{3(1)}^3 \quad \bar{\mathbf{V}}_{3(1)}^3 \quad \cdots \quad \mathbf{V}_{3(\lceil \frac{n}{3} \rceil)}^\iota \quad \bar{\mathbf{V}}_{3(\lceil \frac{n}{3} \rceil)}^\iota \right] \cap \text{nullspace}\{\mathbf{H}_{23}\} = \emptyset$  for sure. Hence, we can get  $\left[ \beta_{s+1} \quad \cdots \quad \beta_q \right]^T$  in (3.38) must be an all-zero vector. Then, by substituting the results into (3.36), we have

$$\left[ \mathbf{V}_{1(1)}^1 \quad \bar{\mathbf{V}}_{1(1)}^1 \quad \mathbf{U}_1^1 \right] \cdot \begin{bmatrix} \beta_1 \\ \vdots \\ \beta_s \end{bmatrix} = \mathbf{0}$$

Since it is already proved that  $\left[ \mathbf{V}_{1(1)}^1 \quad \bar{\mathbf{V}}_{1(1)}^1 \quad \mathbf{U}_1^1 \right]$  has full column rank, we can get  $\left[ \beta_1 \quad \cdots \quad \beta_s \right]^T = \mathbf{0}$  for sure. Therefore, we proved that the subspaces of  $\mathbf{B}_1$  in the first  $n + 1$  layers have full column rank for sure. Similarly, the subspaces of  $\mathbf{B}_2$  and  $\mathbf{B}_3$  in the first  $n + 1$  layers also have full column rank.

*Case 2:  $n = S$ .*

When  $n = S$ , the  $(n + 1)$ th layer is the last layer. Since the original chains end at the  $n$ th layer, the subspaces of  $\mathbf{B}_1$  in the  $(n + 1)$ th layer would be  $\bar{\mathbf{V}}_{1(\lceil \frac{n+1}{3} \rceil)}^\iota$  and  $\mathbf{U}_1^2$ . Hence, the subspaces of  $\mathbf{B}_1$  in all  $(n + 1)$  layers are  $\left[ \mathbf{V}_{1(1)}^1 \quad \bar{\mathbf{V}}_{1(1)}^1 \quad \mathbf{U}_1^1 \quad \cdots \quad \mathbf{V}_{1(\lceil \frac{n}{3} \rceil)}^\tau \quad \bar{\mathbf{V}}_{1(\lceil \frac{n}{3} \rceil)}^\tau \quad \bar{\mathbf{V}}_{1(\lceil \frac{n+1}{3} \rceil)}^\iota \quad \mathbf{U}_1^2 \right]$ , where  $\tau = (\iota \bmod 3) + 1$ . Similarly, we shall prove that all-zero vector is the only solution for  $\left[ \epsilon_1 \quad \cdots \quad \epsilon_z \right]^T$  in the following equation

$$\left[ \mathbf{V}_{1(1)}^1 \quad \bar{\mathbf{V}}_{1(1)}^1 \quad \mathbf{U}_1^1 \quad \cdots \quad \mathbf{V}_{1(\lceil \frac{n}{3} \rceil)}^\tau \quad \bar{\mathbf{V}}_{1(\lceil \frac{n}{3} \rceil)}^\tau \quad \bar{\mathbf{V}}_{1(\lceil \frac{n+1}{3} \rceil)}^\iota \quad \mathbf{U}_1^2 \right] \begin{bmatrix} \epsilon_1 \\ \vdots \\ \epsilon_z \end{bmatrix} = \mathbf{0} \quad (3.39)$$

Since the  $n$ th layer and the  $(n + 1)$ th layer is the last layer of original chain and long chain, respectively, both  $\mathbf{V}_{1(\lceil \frac{n}{3} \rceil)}^\tau$  and  $\bar{\mathbf{V}}_{1(\lceil \frac{n+1}{3} \rceil)}^\iota$  are in the null space of  $\mathbf{H}_{31}$ . i.e.,  $\left[ \mathbf{V}_{1(\lceil \frac{n}{3} \rceil)}^\tau \quad \bar{\mathbf{V}}_{1(\lceil \frac{n+1}{3} \rceil)}^\iota \quad \mathbf{U}_1^2 \right] \subset \text{nullspace}\{\mathbf{H}_{31}\}$ . Hence, by left multiplying  $\mathbf{H}_{31}$  on both side of (3.39), we have

$$\mathbf{H}_{31} \left[ \mathbf{V}_{1(1)}^1 \quad \bar{\mathbf{V}}_{1(1)}^1 \quad \mathbf{U}_1^1 \quad \cdots \quad \mathbf{V}_{1(\lceil \frac{n-1}{3} \rceil)}^\kappa \quad \bar{\mathbf{V}}_{1(\lceil \frac{n-1}{3} \rceil)}^\kappa \quad \bar{\mathbf{V}}_{1(\lceil \frac{n}{3} \rceil)}^\tau \right] \begin{bmatrix} \epsilon_1 \\ \vdots \\ \epsilon_w \end{bmatrix} = \mathbf{0} \quad (3.40)$$

where  $\kappa = \tau \bmod 3 + 1$ .

Since  $\left[ \mathbf{V}_{1(1)}^1 \bar{\mathbf{V}}_{1(1)}^1 \mathbf{U}_1^1 \cdots \mathbf{V}_{1(\lceil \frac{n-1}{3} \rceil)}^\kappa \bar{\mathbf{V}}_{1(\lceil \frac{n-1}{3} \rceil)}^\kappa \bar{\mathbf{V}}_{1(\lceil \frac{n}{3} \rceil)}^\tau \right]$  are all in the first  $n$  layers, it has full column rank for sure. Then, proving  $\left[ \epsilon_1 \cdots \epsilon_w \right]^T = \mathbf{0}$  is equivalent to proving that  $\left[ \mathbf{V}_{1(1)}^1 \bar{\mathbf{V}}_{1(1)}^1 \mathbf{U}_1^1 \cdots \mathbf{V}_{1(\lceil \frac{n-1}{3} \rceil)}^\kappa \bar{\mathbf{V}}_{1(\lceil \frac{n-1}{3} \rceil)}^\kappa \bar{\mathbf{V}}_{1(\lceil \frac{n}{3} \rceil)}^\tau \right] \cap \text{nullspace}\{\mathbf{H}_{31}\} = \emptyset$ . First, note that  $\left[ \mathbf{V}_{1(1)}^1 \bar{\mathbf{V}}_{1(1)}^1 \mathbf{U}_1^1 \right] \cap \text{nullspace}\{\mathbf{H}_{31}\} = \emptyset$  (based on (3.2)). Then, we show that  $\left[ \mathbf{V}_{1(1)}^3 \bar{\mathbf{V}}_{1(1)}^3 \cdots \mathbf{V}_{1(\lceil \frac{n-1}{3} \rceil)}^\kappa \bar{\mathbf{V}}_{1(\lceil \frac{n-1}{3} \rceil)}^\kappa \bar{\mathbf{V}}_{1(\lceil \frac{n}{3} \rceil)}^\tau \right] \cap \text{nullspace}\{\mathbf{H}_{31}\} = \emptyset$ . Since  $\left[ \mathbf{V}_{1(1)}^3 \bar{\mathbf{V}}_{1(1)}^3 \cdots \mathbf{V}_{1(\lceil \frac{n-1}{3} \rceil)}^\kappa \bar{\mathbf{V}}_{1(\lceil \frac{n-1}{3} \rceil)}^\kappa \right]$  are the subspaces in the first  $n-1$  layers and the chain cannot end before the  $n$ th layer, we have  $\left[ \mathbf{V}_{1(1)}^3 \bar{\mathbf{V}}_{1(1)}^3 \cdots \mathbf{V}_{1(\lceil \frac{n-1}{3} \rceil)}^\kappa \bar{\mathbf{V}}_{1(\lceil \frac{n-1}{3} \rceil)}^\kappa \right] \cap \text{nullspace}\{\mathbf{H}_{31}\} = \emptyset$  for sure. Next, for  $\bar{\mathbf{V}}_{1(\lceil \frac{n}{3} \rceil)}^\tau$ , we have  $\bar{\mathbf{V}}_{1(\lceil \frac{n}{3} \rceil)}^\tau = \mathbf{H}_{32} \bar{\mathbf{V}}_{2(\lceil \frac{n+1}{3} \rceil)}^\tau$ . Note that  $\bar{\mathbf{V}}_{2(\lceil \frac{n+1}{3} \rceil)}^\tau \subset \text{nullspace}\{\mathbf{H}_{12}\}$  and  $\bar{\mathbf{V}}_{2(\lceil \frac{n+1}{3} \rceil)}^\tau \cap \text{nullspace}\{\mathbf{H}_{32}\} = \emptyset$  (based on (3.3)), we can get  $\bar{\mathbf{V}}_{1(\lceil \frac{n}{3} \rceil)}^\tau \cap \text{nullspace}\{\mathbf{H}_{31}\} = \emptyset$  for sure. Now, we have shown that  $\left[ \mathbf{V}_{1(1)}^1 \bar{\mathbf{V}}_{1(1)}^1 \mathbf{U}_1^1 \cdots \mathbf{V}_{1(\lceil \frac{n-1}{3} \rceil)}^\kappa \bar{\mathbf{V}}_{1(\lceil \frac{n-1}{3} \rceil)}^\kappa \bar{\mathbf{V}}_{1(\lceil \frac{n}{3} \rceil)}^\tau \right]$  has full rank and all of its columns are not in  $\text{nullspace}\{\mathbf{H}_{31}\}$ . Further, according to (3.29) we can see that the column rank of  $\left[ \mathbf{V}_{1(1)}^1 \bar{\mathbf{V}}_{1(1)}^1 \mathbf{U}_1^1 \cdots \mathbf{V}_{1(\lceil \frac{n-1}{3} \rceil)}^\kappa \bar{\mathbf{V}}_{1(\lceil \frac{n-1}{3} \rceil)}^\kappa \bar{\mathbf{V}}_{1(\lceil \frac{n}{3} \rceil)}^\tau \right]$  is equal to or less than  $M$ . Hence, due to channel randomness, the matrix  $\mathbf{H}_{31} \left[ \mathbf{V}_{1(1)}^1 \bar{\mathbf{V}}_{1(1)}^1 \mathbf{U}_1^1 \cdots \mathbf{V}_{1(\lceil \frac{n-1}{3} \rceil)}^\kappa \bar{\mathbf{V}}_{1(\lceil \frac{n-1}{3} \rceil)}^\kappa \bar{\mathbf{V}}_{1(\lceil \frac{n}{3} \rceil)}^\tau \right]$  has full column rank almost for sure, which is equivalent to  $\left[ \mathbf{V}_{1(1)}^1 \bar{\mathbf{V}}_{1(1)}^1 \mathbf{U}_1^1 \cdots \mathbf{V}_{1(\lceil \frac{n-1}{3} \rceil)}^\kappa \bar{\mathbf{V}}_{1(\lceil \frac{n-1}{3} \rceil)}^\kappa \bar{\mathbf{V}}_{1(\lceil \frac{n}{3} \rceil)}^\tau \right] \cap \text{nullspace}\{\mathbf{H}_{31}\} = \emptyset$ . As a result, we have proved that  $\left[ \epsilon_1 \cdots \epsilon_w \right]^T$  is an all-zero vector almost surely. After substituting this result into (3.39), we have

$$\left[ \mathbf{V}_{1(\lceil \frac{n}{3} \rceil)}^\tau \quad \bar{\mathbf{V}}_{1(\lceil \frac{n+1}{3} \rceil)}^\iota \quad \mathbf{U}_1^2 \right] \begin{bmatrix} \epsilon_w \\ \vdots \\ \epsilon_z \end{bmatrix} = \mathbf{0}$$

which means we need to show that  $\left[ \mathbf{V}_{1(\lceil \frac{n}{3} \rceil)}^\tau \quad \bar{\mathbf{V}}_{1(\lceil \frac{n+1}{3} \rceil)}^\iota \quad \mathbf{U}_1^2 \right]$  has full column rank. First, it can be proved that  $\left[ \mathbf{V}_{1(\lceil \frac{n}{3} \rceil)}^\tau \quad \bar{\mathbf{V}}_{1(\lceil \frac{n+1}{3} \rceil)}^\iota \right]$  has full column rank for sure with the same approach as (3.36)-(3.38). Then, since  $\left[ \mathbf{V}_{1(\lceil \frac{n}{3} \rceil)}^\tau \quad \bar{\mathbf{V}}_{1(\lceil \frac{n+1}{3} \rceil)}^\iota \quad \mathbf{U}_1^2 \right] \in \mathbb{C}^{N \times (Q_\tau + \bar{Q}_\iota + q_{21})}$  is in the null space of  $\mathbf{H}_{31}$ , the following constraint must be satisfied

to ensure the full column rank,

$$Q_\tau + \bar{Q}_\iota + q_{21} \leq N - M \quad (3.41)$$

When  $S \bmod 3 = 2$ , we can get that  $\tau = 3$  and  $\iota = 2$  (recall that  $\iota = 1, 3, 2$  for  $n + 1 \bmod 3 = 1, 2, 0$ , respectively,  $\tau = \iota \bmod 3 + 1$  and  $n = S$ ), which implies that (3.41) becomes (3.26) with  $j = 2$ , i.e.,  $Q_3 + \bar{Q}_2 + q_{21} \leq N - M$ . Hence, we have proved that when  $S \bmod 3 = 2$ , the subspaces of  $\mathbf{B}_1$  have full column rank for sure under the constraint of (3.26) with  $j = 2$ .

With the same approach, we can prove that when  $S \bmod 3 = 2$ , the subspaces of  $\mathbf{B}_2$  and  $\mathbf{B}_3$  will both have full column rank under the constraint of (3.26) with  $j = 3$  and  $j = 1$ , respectively, i.e.,

$$\begin{aligned} Q_1 + \bar{Q}_3 + q_{32} &\leq N - M \\ Q_2 + \bar{Q}_1 + q_{13} &\leq N - M \end{aligned}$$

When  $S \bmod 3 = 0$ , we have  $\tau = 2$  and  $\iota = 1$ , which means (3.41) becomes (3.27) with  $j = 1$ . Accordingly, when  $S \bmod 3 = 0$ , the subspaces of  $\mathbf{B}_1$ ,  $\mathbf{B}_2$  and  $\mathbf{B}_3$  will have full column rank under the constraints of (3.27) with  $j = 1$ ,  $j = 2$  and  $j = 3$ , respectively.

When  $S \bmod 3 = 1$ , we have  $\tau = 1$  and  $\iota = 3$ , which means (3.41) becomes (3.28) with  $j = 1$ . Hence, when  $S \bmod 3 = 0$ , the subspaces of  $\mathbf{B}_1$ ,  $\mathbf{B}_2$  and  $\mathbf{B}_3$  will have full column rank under the constraints of (3.28) with  $j = 1$ ,  $j = 2$  and  $j = 3$ , respectively.

### 3.4 Achievable Degrees of Freedom Region

In this section, we characterize the achievable (integer) DoF region of the proposed beamforming scheme based on the conditions in *Theorem 3.3*. Since the 3-user interference network region we are interested in is  $\frac{1}{2} < \frac{M}{N} < 1$ , it can be divided into three regions, i.e.,  $[\frac{3t-2}{3t-1}, \frac{3t-1}{3t})$ ,  $[\frac{3t-1}{3t}, \frac{3t}{3t+1})$ , and  $[\frac{3t}{3t+1}, \frac{3t+1}{3t+2})$ , where  $t = 1, 2, \dots, \infty$ . The

achievable DoF region is studied for each region. Further, note that the achievable DoF region of 3-user  $(i, j, k)$  interference networks is the combination of the bounds of  $D = d_i + d_j + d_k$  (sum DoF),  $d_i + d_j$ , and  $d_i$ . For any integer DoF tuples satisfying these bounds, there exists linear precoding schemes such that the desired signals can be decoded.

We first derive the bounds of sum DoF as they are the same for all three regions. Then, we investigate the bounds of  $d_i + d_j$  and  $d_i$  in different regions, respectively. Note that the bounds of  $d_i + d_j$  and  $d_i$  are studied in the context of three-user interference channel, which means they are all related to  $D$ . Hence, they are completely different with the bounds of two-user interference channel or point-to-point channel.

### 3.4.1 Bounds of $d_i + d_j + d_k$

The bounds of sum DoF are obtained based on the following three inequalities, whose derivations are given in Appendix B.

$$Q_s + \bar{Q}_s \geq 2D - 3M \quad (3.42)$$

$$Q_s \geq [(2S + 1)D - 3(S + 1)M]^+ \quad (3.43)$$

$$Q_i \geq [(2S + 1)D - (S + 1)M - 2SN]^+ \quad (3.44)$$

$$\bar{Q}_s \geq [2D - 3SN + 3SM]^+ \quad (3.45)$$

where  $[A]^+ = \max\{A, 0\}$ .

Note that (3.42) and (3.43) are the lower bounds of  $Q_s + \bar{Q}_s$  and  $Q_s$  for a given  $D$ , respectively. Since  $\bar{Q}_s \geq 0$ , the lower bound of  $Q_s + \bar{Q}_s$  cannot be less than that of  $Q_s$ , i.e.,

$$2D - 3M \geq [(2S + 1)D - 3(S + 1)M]^+$$

It can be written as

$$\begin{cases} 2D - 3M \geq 0 & \text{if } D \leq \frac{3(S+1)M}{2S+1} \\ (2S - 1)D \leq 3SM & \text{if } D > \frac{3(S+1)M}{2S+1} \end{cases} \quad (3.46)$$

Further, it has

$$\frac{3M}{2} \leq D \leq \frac{3SM}{2S-1}$$

which leads to

$$D = d_1 + d_2 + d_3 \leq \frac{3SM}{2S-1} \quad (3.47)$$

Next, since  $Q_i \leq S \cdot N - (S+1)M$  (from (3.21)) and  $[(2S+1)D - (S+1)M - 2SN]^+ \leq Q_i$  (from (3.44)), we can get

$$S \cdot N - (S+1)M \geq [(2S+1)D - (S+1)M - 2SN]^+$$

It can be derived as

$$\begin{cases} (S+1)M < S \cdot N & \text{if } D < \frac{2SN+(S+1)M}{2S+1} \\ (2S+1)D \leq 3SN & \text{if } D \geq \frac{2SN+(S+1)M}{2S+1} \end{cases}$$

which leads to

$$D \leq \frac{3SN}{2S+1} \quad (3.48)$$

where  $(S+1)M < S \cdot N$  is proved in Section 3.3.1.

(3.47) and (3.48) are the two bounds of  $D$  that are applied to all cases. As we can see, these two bounds are in fact the  $M$ -bound and  $N$ -bound of sum DoF derived in [22], respectively.

### 3.4.2 Bounds of $d_i + d_j$ and $d_i$

Next, we investigate the bounds of  $d_i + d_j$  and  $d_i$  for different cases. Since each link has the same antenna configurations, the user indices are interchangeable. Hence, the bound of one link can be extended to general. This fact can also be applied to the constraints. We can see that constraints (3.23)-(3.25) have the same form, only with different indices (so is (3.26), (3.27), (3.28) and (3.29)-(3.31)), which implies that each constraint contains the bounds of certain links, and the bounds of each link would be

the same. Hence, in the following, we only study the bounds of  $d_1 + d_2$  and  $d_2$ , and show two bounds for  $d_1 + d_2$  and one bound for  $d_2$ , respectively.

- For  $\frac{3t-2}{3t-1} \leq \frac{M}{N} < \frac{3t-1}{3t}$  ( $S = 3t - 1$ )

The DoF of each link can be calculated as

$$\begin{cases} d_1 = t \cdot Q_s - Q_2 + t \cdot \bar{Q}_s + q_1 \\ d_2 = t \cdot Q_s - Q_3 + t \cdot \bar{Q}_s + q_2 \\ d_3 = t \cdot Q_s - Q_1 + t \cdot \bar{Q}_s + q_3 \end{cases} \quad (3.49)$$

where  $q_1 = q_{21} + q_{31}$ ,  $q_2 = q_{12} + q_{32}$ ,  $q_3 = q_{13} + q_{23}$ .

(3.49) is explained as follows. Since  $S = 3t - 1$ , the subspaces in three original chains can be expressed as

$$\begin{cases} \mathbf{V}_{1(1)}^1 & \mathbf{V}_{2(1)}^1 & \mathbf{V}_{3(1)}^1 & \cdots & \mathbf{V}_{1(t-1)}^1 & \mathbf{V}_{2(t-1)}^1 & \mathbf{V}_{3(t-1)}^1 & \mathbf{V}_{1(t)}^1 & \mathbf{V}_{2(t)}^1 & (3.50a) \\ \mathbf{V}_{2(1)}^2 & \mathbf{V}_{3(1)}^2 & \mathbf{V}_{1(1)}^2 & \cdots & \mathbf{V}_{2(t-1)}^2 & \mathbf{V}_{3(t-1)}^2 & \mathbf{V}_{1(t-1)}^2 & \mathbf{V}_{2(t)}^2 & \mathbf{V}_{3(t)}^2 & (3.50b) \\ \mathbf{V}_{3(1)}^3 & \mathbf{V}_{1(1)}^3 & \mathbf{V}_{2(1)}^3 & \cdots & \mathbf{V}_{3(t-1)}^3 & \mathbf{V}_{1(t-1)}^3 & \mathbf{V}_{2(t-1)}^3 & \mathbf{V}_{3(t)}^3 & \mathbf{V}_{1(t)}^3 & (3.50c) \end{cases} \quad (3.50)$$

where the notation is the same as (3.18).

Take  $d_1$  for example, which is equal to the number of signals sent by transmitter 1. As can be seen, there are  $t$ ,  $t-1$  and  $t$  subspaces belonging to transmitter 1 in (3.50a), (3.50b) and (3.50c), respectively. Since each subspace has  $Q_i$  dimensions, the number of signals in the original chains that belong to transmitter 1 equals  $t \cdot Q_1 + (t-1) \cdot Q_2 + t \cdot Q_3 = t \cdot Q_s - Q_2$ . Then, for the long chains whose length equals  $S + 1 = 3t$ , each contains  $t$  subspaces that belong to transmitter 1. Similarly, the number of signals in the long chain that belong to transmitter 1 equals  $t \cdot (\bar{Q}_1 + \bar{Q}_2 + \bar{Q}_3)$ . Since  $\mathbf{U}_1$  contains  $q_1$  signals, we have  $d_1 = t \cdot Q_s - Q_2 + t \cdot \bar{Q}_s + q_1$ . Likewise,  $d_2$  and  $d_3$  can be calculated.

We first characterize the bounds of  $d_1 + d_2$ . Accordingly, we have

$$\begin{aligned} d_1 + d_2 &= (2t - 1) \cdot Q_s + 2t\bar{Q}_s + Q_1 + q_s - q_3 \\ &= D - (t - 1)(Q_s + \bar{Q}_s) - (Q_s + \bar{Q}_s - Q_1) - q_3 \end{aligned} \quad (3.51)$$

where  $q_s = q_1 + q_2 + q_3$  and  $D = \sum_{i=1}^3 d_i = (3t - 1)Q_s + 3t \cdot \bar{Q}_s + q_s$ .

Since  $Q_s + \bar{Q}_s \geq 2D - 3M$  (from (3.42)),  $Q_1 \leq (3t - 1)N - 3tM$  (from (3.21)) and  $q_3 \geq 0$ , (3.51) can be written as

$$d_1 + d_2 \leq D - (t - 1)(2D - 3M) - [2D - 3M - (3t - 1)N + 3tM]^+$$

It is equivalent to

$$d_1 + d_2 \leq \min\{(3t - 3)M - (2t - 3)D, (3t - 1)N - (2t - 1)D\}$$

which further leads to

$$2(t - 1)d_i + 2(t - 1)d_j + (2t - 3)d_k \leq 3(t - 1)M \quad (3.52)$$

$$2td_i + 2td_j + (2t - 1)d_k \leq (3t - 1)N \quad (3.53)$$

Another bound of  $d_1 + d_2$  can be derived based on (3.23) and (3.30). First, from (3.30) we can get

$$d_2 + p_2 \leq M - q_{21} - q_{23} \leq M \quad (3.54)$$

Since in this case  $d_2 = t \cdot Q_s - Q_3 + t \cdot \bar{Q}_s + q_2$  and  $P_2 = (t - 1) \cdot Q_s + Q_3 + t \cdot \bar{Q}_s - \bar{Q}_1$ , (3.54) can be written as

$$(2t - 1)Q_s + 2t \cdot \bar{Q}_s + q_2 - \bar{Q}_1 \leq M \quad (3.55)$$

Then, since  $D = (3t - 1)Q_s + 3t \cdot \bar{Q}_s + q_s$ , (3.55) can be expressed as

$$D - t(Q_s + \bar{Q}_s) - \bar{Q}_1 - q_s + q_2 \leq M \quad (3.56)$$

Further, note that (3.23) implies that

$$M \leq N - Q_1 - \bar{Q}_1 - q_{31} \quad (3.57)$$

By taking (3.57) into (3.56), we can get

$$D - t(Q_s + \bar{Q}_s) + Q_1 - q_s + q_2 + q_{31} \leq N \quad (3.58)$$

Since  $d_1 + d_2 = D - t(Q_s + \bar{Q}_s) + Q_1 + q_3$  (according (3.51)), (3.58) is equivalent to

$$d_1 + d_2 \leq N + q_s - q_2 - q_{31} - q_3$$

which can be guaranteed by letting

$$d_1 + d_2 \leq N \Rightarrow d_i + d_j \leq N \quad (3.59)$$

Note that by following the exact procedure of (3.54)-(3.59), same bound can be obtained from (3.26) with  $j = 3$  and (3.29).

Next, we derive the bound of  $d_2$  based on (3.54), which is derived from (3.30). Specifically, (3.54) can be expressed as

$$\begin{aligned} d_2 &\leq M - (t-1)Q_s - t \cdot \bar{Q}_s - Q_3 + \bar{Q}_1 \\ &= M - t(Q_s + \bar{Q}_s) + Q_1 + Q_2 + \bar{Q}_1 \\ &= M - (t-1)(Q_s + \bar{Q}_s) - (Q_s + \bar{Q}_s - (Q_1 + Q_2 + \bar{Q}_1)) \end{aligned} \quad (3.60)$$

which can lead to

$$d_i \leq \begin{cases} (9t-2)N - 6tM - 2tD \\ (3t-2)M - 2(t-1)D \\ (6t-2)(N+M) - (8t-3)D \end{cases} \quad (3.61)$$

The derivation of (3.61) is shown in Appendix C.

Finally, the achievable DoF region for  $\frac{3t-2}{3t-1} \leq \frac{M}{N} < \frac{3t-1}{3t}$  can be summarized as (3.47), (3.48), (3.52), (3.53), (3.59) and (3.61). Further, since (3.48), (3.52), the first and third terms of (3.61) are included in other bounds (the proof is in Appendix D), the exact achievable DoF region is composed of (3.47), (3.53), (3.59) and the second term of (3.61), which are the same as (3.5).

- For  $\frac{3t-1}{3t} \leq \frac{M}{N} < \frac{3t}{3t+1}$  ( $S = 3t$ )

In this case, we have  $d_i = t \cdot Q_s + t \cdot \bar{Q}_s + \bar{Q}_i + q_i$ . The derivation of the bounds of  $d_i + d_j$  and  $d_i$  will be the same as the previous case. First, we have

$$\begin{aligned} d_1 + d_2 &= 2tQ_s + (2t+1)\bar{Q}_s - \bar{Q}_3 + q_s - q_3 \\ &= D - t(Q_s + \bar{Q}_s) - \bar{Q}_3 - q_3 \end{aligned} \quad (3.62)$$

Since  $\bar{Q}_3 \geq 0$  (from (3.94) in Appendix E),  $q_3 \geq 0$  and  $Q_s + \bar{Q}_s \geq 2D - 3M$ , we can get

$$d_1 + d_2 \leq D - t(Q_s + \bar{Q}_s) \leq 3tM - (2t - 1)D \quad (3.63)$$

which leads to

$$2td_i + 2td_j + (2t - 1)d_k \leq 3tM \quad (3.64)$$

Then, note that in this case  $d_2 = t(Q_s + \bar{Q}_s) + \bar{Q}_2 + q_2$  and  $P_2 = t \cdot (Q_s + \bar{Q}_s) - Q_1$ . With the same approach as (3.54)-(3.59), the following bound can be obtained based on (3.23) and (3.30) (or based on (3.27) with  $j = 2$  and (3.29)),

$$d_1 + d_2 \leq N \Rightarrow d_i + d_j \leq N \quad (3.65)$$

Next, to obtain the bound of  $d_i$ , (3.54) is written as

$$d_2 \leq M - t(Q_s + \bar{Q}_s) + Q_1 \quad (3.66)$$

Since  $Q_s + \bar{Q}_s \geq 2D - 3M$  and  $Q_1 \leq 3tN - (3t + 1)M$ , we have

$$d_2 \leq 3tN - 2tD \quad (3.67)$$

which leads to

$$(2t + 1)d_i + 2td_j + 2td_k \leq 3tN \quad (3.68)$$

Finally, by combining (3.47), (3.48), (3.64), (3.65) and (3.68), the achievable DoF region for  $\frac{3t-1}{3t} \leq \frac{N}{M} < \frac{3t}{3t+1}$  is the same as (3.6). (Note that in (3.6) the two bounds derived from (3.47) and (3.48) are both included.)

- For  $\frac{3t}{3t+1} \leq \frac{M}{N} < \frac{3t+1}{3t+2}$  ( $S = 3t + 1$ )

In this case,  $d_1 = t \cdot Q_s + Q_1 + (t+1)\bar{Q}_s - \bar{Q}_2 + q_1$ ,  $d_2 = t \cdot Q_s + Q_2 + (t+1)\bar{Q}_s - \bar{Q}_3 + q_2$  and  $d_3 = t \cdot Q_s + Q_3 + (t+1)\bar{Q}_s - \bar{Q}_1 + q_3$ . Accordingly, we have

$$\begin{aligned} d_1 + d_2 &= 2t \cdot Q_s + (2t + 1)\bar{Q}_s + Q_1 + Q_2 + \bar{Q}_1 + q_s - q_3 \\ &\leq D - t(Q_s + \bar{Q}_s) - ((Q_s + \bar{Q}_s) - (Q_1 + Q_2 + \bar{Q}_1)) \end{aligned} \quad (3.69)$$

Similar to (3.61), based on (3.21), (3.22), (3.42) and (3.43), we can get

$$d_i + d_j \leq \begin{cases} (9t + 4)N - (6t + 4)M - (2t + 1)D \\ 3tM - (2t - 1)D \\ (6t + 2)(N + M) - (8t + 2)D \end{cases} \quad (3.70)$$

Then, we derive another bound of  $d_i + d_j$ . Again, since  $d_2 = t \cdot Q_s + Q_2 + (t + 1)\bar{Q}_s - \bar{Q}_3 + q_2$  and  $P_2 = t \cdot (Q_s + \bar{Q}_s) + \bar{Q}_3$ , the following bound can be obtained based on (3.23) and (3.30), (or based on (3.28) with  $j = 2$  and (3.29)).

$$d_i + d_j \leq N \quad (3.71)$$

Next, to derive the bound of  $d_2$ , (3.54) can be expressed as

$$d_2 \leq M - t(Q_s + \bar{Q}_s) - \bar{Q}_3 \quad (3.72)$$

Since  $Q_s + \bar{Q}_s \geq 2D - 3M$  and  $\bar{Q}_3 \geq 0$ , we can get

$$d_2 \leq (3t + 1)M - 2tD \Rightarrow d_i \leq (3t + 1)M - 2tD \quad (3.73)$$

which leads to

$$(2t + 1)d_i + 2td_j + 2td_k \leq (3t + 1)M \quad (3.74)$$

Note that the bound of (3.47) is included in (3.74); and the bound (3.70) is included in (3.48), (3.71) and (3.74) (The proof is in Appendix F). As a result, by combining (3.48), (3.71) and (3.74), the achievable DoF region for  $\frac{3t-1}{3t} \leq \frac{N}{M} < \frac{3t}{3t+1}$  is the same as (3.7).

**Remark 3.4** *In Sections 3.3-3.4, we propose a beamforming scheme and show that the achievable DoF region for 3-user interference channels is (3.5)-(3.7) with  $d_i$  being an integer.*

### 3.5 Achieving Fractional DoF with Symbol Extension

In Sections 3.3-3.4, we have shown that all the integer DoF within the outer bound DoF region can be achieved. In this section, we discuss the achievability of fractional DoF within the outer bound region with symbol extension over time (or frequency). For a given antenna configuration  $(M_R, M_T)$ , its DoF region can be found in (3.5)-(3.7), which would be a 3-dimensional polyhedron. Then, the coordinates of any point in the region can be expressed as  $\{\frac{d'_1}{a_1}, \frac{d'_2}{a_2}, \frac{d'_3}{a_3}\}$ , where  $a_1, a_2, a_3$  are natural numbers and  $d'_1, d'_2, d'_3$  are non-negative integers. In order to achieve DoF  $\{\frac{d'_1}{a_1}, \frac{d'_2}{a_2}, \frac{d'_3}{a_3}\}$ , we perform  $T$  symbol extensions (where  $T$  equals the least common multiple of  $a_1, a_2$  and  $a_3$ ). As a consequence, the system can be equivalent to a new system with antenna configuration  $(T \cdot M_R, T \cdot M_T)$ , and channel matrix is

$$\mathbf{H}'_{ij} = \begin{bmatrix} \mathbf{H}_{ij}(1) & & \\ & \ddots & \\ & & \mathbf{H}_{ij}(T) \end{bmatrix}$$

where  $\mathbf{H}_{ij}(t)$  denote the channel matrix between transmitter  $j$  and receiver  $i$  at time slot  $t$ .

In the equivalent system, the number of signals sent by transmitter  $i$  should be equal to  $\frac{Td'_i}{a_i}$ . Further, since the coordinates of point  $\{\frac{Td'_1}{a_1}, \frac{Td'_2}{a_2}, \frac{Td'_3}{a_3}\}$  are all integers and are inside the outer bound region, a beamforming matrix for each transmitter can be designed based on (3.18). If the desired signals can be linearly decoded on each receiver, transmitter  $i$  will achieve  $\frac{d'_i}{a_i}$  DoF, as  $\frac{Td'_i}{a_i}$  symbols are sent by transmitter  $i$  over  $T$  time slots.

Note that if channel matrices  $\mathbf{H}'_{ij}$  are generic, the signals can be linearly decoded for sure based on previous discussion. However, due to symbol extensions, the equivalent channels are all block diagonal matrices, which may not be generic. Hence, although all the conditions in *Theorem 3.3* are satisfied, it cannot be proved in the

same way as that of in *Theorem 3.3*. While there is not a systematic approach to prove it in general, there are some ways to examine this issue for each individual case. Let  $\mathbf{Y}_i^d$  and  $\mathbf{Y}_i^I$  denote the desired signal space and interference space on receiver  $i$ , respectively. Proving that the desired signals can be linearly decoded on receiver  $i$  is equivalent to showing that  $\mathbf{Y}_i = \begin{bmatrix} \mathbf{Y}_i^d & \mathbf{Y}_i^I \end{bmatrix}$  having full column rank. Since each subspace in  $\mathbf{Y}_i$  is completely determined by randomly generated channels, there are only two possibilities, i.e.,  $\mathbf{Y}_i$  will always or never have full column rank for any group of random channel matrices [22].

Hence, in order to exam whether DoF of  $\{\frac{Td'_1}{a_1}, \frac{Td'_2}{a_2}, \frac{Td'_3}{a_3}\}$  is achievable in the equivalent system, we can first randomly generate a group of generic channel matrices  $\mathbf{H}_{ij}(t)$  to create  $\mathbf{H}'_{ij}$ . Then, the beamforming matrix can be designed accordingly, which will give us  $\mathbf{Y}_i$ . Finally, DoF of  $\{\frac{Td'_1}{a_1}, \frac{Td'_2}{a_2}, \frac{Td'_3}{a_3}\}$  can be proved to be achievable as long as  $\mathbf{Y}_i$  has full column rank. Note that if the channels are time-varying, i.e.,  $\mathbf{H}_{ij}(a)$  and  $\mathbf{H}_{ij}(b)$  are independent of each other, no case has been found that a point inside the DoF region cannot be achieved. This is because under varying channel condition, the property of equivalent channels are very close to generic channel. If the channels are constant, i.e.,  $\mathbf{H}_{ij}(1) = \mathbf{H}_{ij}(2) = \dots = \mathbf{H}_{ij}(T)$ , there are evidences indicating that some DoF inside the region cannot be achieved. (It is shown in [22] that under constant channel conditions, the outer-bound of sum DoF can not be achieved when  $\frac{M}{N} = \frac{p}{p+1}$ .)

In addition to this approach, we can also prove each individual case mathematically. In the following, we use an example to elaborate the application of symbol extensions and explain how to prove that the desired signals are linearly decodable on each receiver.

#### • An Example

In this example, we assume  $M_R = 7$ ,  $M_T = 10$ . We show that DoF of  $\{d_1 = 5, d_2 = \frac{11}{3}, d_3 = \frac{11}{3}\}$  can be achieved with three symbol extensions. The equivalent

channel matrix can be expressed as

$$\mathbf{H}'_{ij} \in \mathbb{C}^{21 \times 30} = \begin{bmatrix} \mathbf{H}_{ij}(1) & & \\ & \mathbf{H}_{ij}(2) & \\ & & \mathbf{H}_{ij}(3) \end{bmatrix} \quad (3.75)$$

As can be seen, the number of dimensions on each transmitter and receiver has been tripled due to symbol extension. Hence, under this equivalent system, transmitter 1, 2, 3 will send 15, 11, and 11 signals, respectively. The beamforming matrix of transmitter  $i$ ,  $\mathbf{B}_i$ , is designed as follows,

$$\begin{aligned} \mathbf{B}_1 &= \begin{bmatrix} \mathbf{V}_{1(1)}^1 & \mathbf{V}_{1(1)}^2 & \mathbf{V}_{1(1)}^3 & \bar{\mathbf{V}}_{1(1)}^1 & \bar{\mathbf{V}}_{1(2)}^1 \end{bmatrix} \\ \mathbf{B}_2 &= \begin{bmatrix} \mathbf{V}_{2(1)}^1 & \mathbf{V}_{2(1)}^2 & \mathbf{V}_{2(1)}^3 & \bar{\mathbf{V}}_{2(1)}^1 \end{bmatrix} \\ \mathbf{B}_3 &= \begin{bmatrix} \mathbf{V}_{3(1)}^1 & \mathbf{V}_{3(1)}^2 & \mathbf{V}_{3(1)}^3 & \bar{\mathbf{V}}_{3(1)}^1 \end{bmatrix} \end{aligned} \quad (3.76)$$

where the notation of  $\mathbf{V}_i^j$  and  $\bar{\mathbf{V}}_i^j$  follows from (3.18). In addition,  $\mathbf{V}_{1(1)}^3$ ,  $\mathbf{V}_{2(1)}^3$  and  $\mathbf{V}_{3(1)}^3$  are  $30 \times 5$  matrix,  $\bar{\mathbf{V}}_{1(1)}^1$ ,  $\bar{\mathbf{V}}_{2(1)}^1$  and  $\bar{\mathbf{V}}_{3(1)}^1$  are  $30 \times 4$  matrix, others are all  $30 \times 1$  vectors.

The design of each subspace can be further expressed as follows,

$$\begin{aligned} \mathbf{V}_{i(1)}^1 &= \mathfrak{V}_{i(1)}^1 \cdot \mathbf{w}, \quad \mathbf{V}_{i(1)}^2 = \mathfrak{V}_{i(1)}^2 \cdot \mathbf{z} \\ \mathbf{V}_{i(1)}^3 &= \mathfrak{V}_{i(1)}^3 \cdot \mathbf{\Pi}, \quad \bar{\mathbf{V}}_{i(1)}^1 = \bar{\mathfrak{V}}_{i(1)}^1 \cdot \mathbf{P}, \quad \bar{\mathbf{V}}_{i(2)}^1 = \bar{\mathfrak{V}}_{i(2)}^1 \cdot \mathbf{P} \end{aligned}$$

where

$$\begin{aligned} \mathfrak{V}_{i(a)}^j &\in \mathbb{C}^{30 \times 6} \triangleq \begin{bmatrix} \mathbf{V}_{i(a)}^j(1) & \mathbf{0}^{10 \times 2} & \mathbf{0}^{10 \times 2} \\ \mathbf{0}^{10 \times 2} & \mathbf{V}_{i(a)}^j(2) & \mathbf{0}^{10 \times 2} \\ \mathbf{0}^{10 \times 2} & \mathbf{0}^{10 \times 2} & \mathbf{V}_{i(a)}^j(3) \end{bmatrix} \\ \bar{\mathfrak{V}}_{i(a)}^j &\in \mathbb{C}^{30 \times 12} \triangleq \begin{bmatrix} \bar{\mathbf{V}}_{i(a)}^j(1) & \mathbf{0}^{10 \times 4} & \mathbf{0}^{10 \times 4} \\ \mathbf{0}^{10 \times 4} & \bar{\mathbf{V}}_{i(a)}^j(2) & \mathbf{0}^{10 \times 4} \\ \mathbf{0}^{10 \times 4} & \mathbf{0}^{10 \times 4} & \bar{\mathbf{V}}_{i(a)}^j(3) \end{bmatrix} \end{aligned}$$

and  $\mathbf{w} \in \mathbb{C}^{6 \times 1}$ ,  $\mathbf{z} \in \mathbb{C}^{6 \times 1}$ ,  $\mathbf{\Pi} \in \mathbb{C}^{6 \times 5}$ ,  $\mathbf{P} \in \mathbb{C}^{12 \times 4}$  are random matrices.

Note that  $\mathbf{V}_{i(a)}^j(t) \in \mathbb{C}^{10 \times 2}$  and  $\bar{\mathbf{V}}_{i(a)}^j(t) \in \mathbb{C}^{10 \times 4}$  are designed according to (3.18), but based on the channel matrices in time slot  $t$ . For example,  $\mathbf{V}_{i(1)}^3(t)$  are designed as

$$\begin{bmatrix} \mathbf{H}_{13}(t) \\ \mathbf{H}_{23}(t) & -\mathbf{H}_{21}(t) \\ & \mathbf{H}_{31}(t) & -\mathbf{H}_{32}(t) \\ & & \mathbf{H}_{12}(t) \end{bmatrix} \begin{bmatrix} \mathbf{V}_{3(1)}^3(t) \\ \mathbf{V}_{1(1)}^3(t) \\ \mathbf{V}_{2(1)}^3(t) \end{bmatrix} = \mathbf{0}$$

and  $\bar{\mathbf{V}}_{i(1)}^1(t)$ ,  $\bar{\mathbf{V}}_{1(2)}^1(t)$  are designed as

$$\begin{bmatrix} \mathbf{H}_{12}(t) \\ \mathbf{H}_{31}(t) & -\mathbf{H}_{32}(t) \\ & \mathbf{H}_{12}(t) & -\mathbf{H}_{13}(t) \\ & & \mathbf{H}_{23}(t) & \mathbf{H}_{21}(t) \\ & & & \mathbf{H}_{31}(t) \end{bmatrix} \begin{bmatrix} \bar{\mathbf{V}}_{1(1)}^1(t) \\ \bar{\mathbf{V}}_{2(1)}^1(t) \\ \bar{\mathbf{V}}_{3(1)}^1(t) \\ \bar{\mathbf{V}}_{1(2)}^1(t) \end{bmatrix} = \mathbf{0}$$

Next, we show that the signals can be linear decoded on each receiver under constant channel conditions. Based on previous discussion, the desired signal space on receiver 1 can be expressed as

$$\mathbf{Y}_1^d = \left[ \mathbf{H}'_{11} \mathfrak{Y}_{1(1)}^1 \cdot \mathbf{w} \quad \mathbf{H}'_{11} \mathfrak{Y}_{1(1)}^2 \cdot \mathbf{z} \quad \mathbf{H}'_{11} \mathfrak{Y}_{1(1)}^3 \cdot \boldsymbol{\Pi} \quad \mathbf{H}'_{11} \bar{\mathfrak{Y}}_{1(1)}^1 \cdot \mathbf{P} \quad \mathbf{H}'_{11} \bar{\mathfrak{Y}}_{1(2)}^1 \cdot \mathbf{P} \right]$$

and the interference space can be expressed as

$$\mathbf{Y}_1^I = \left[ \mathbf{H}'_{12} \mathfrak{Y}_{2(1)}^1 \cdot \mathbf{w} \quad \mathbf{H}'_{12} \mathfrak{Y}_{2(1)}^2 \cdot \mathbf{z} \quad \mathbf{H}'_{12} \bar{\mathfrak{Y}}_{2(1)}^1 \cdot \mathbf{P} \right]$$

Note that  $\mathbf{H}'_{12} \mathfrak{Y}_{2(1)}^j = \mathbf{H}'_{13} \mathfrak{Y}_{3(1)}^j$ .

Since the channels are constant, we have  $\mathbf{H}_{ij}(1) = \mathbf{H}_{ij}(2) = \mathbf{H}_{ij}(3) = \mathbf{H}_{ij}$  and  $\mathbf{V}_{i(a)}^j(1) = \mathbf{V}_{i(a)}^j(2) = \mathbf{V}_{i(a)}^j(3) = \mathbf{V}_{i(a)}^j(\cdot)$ . Then, let

$$\begin{bmatrix} \mathbf{w} & \mathbf{z} \end{bmatrix} = \mathbf{I}_{2 \times 2}, \quad \mathbf{P} = \begin{bmatrix} \mathbf{0}^{4 \times 2} & \mathbf{0} \\ \mathbf{I}_{2 \times 2} & \mathbf{0} \\ \mathbf{0}^{6 \times 2} & \mathbf{I}_{2 \times 2} \end{bmatrix},$$



## 3.6 Summary

In this chapter, the outer bound of DoF region of 3-user MIMO interference channels was shown first. Then, a linear beamforming scheme based on alignment chain was proposed, which can achieve all the integer DoF inside the outer bound DoF region. In addition, we further discussed the achievability of fractional DoF within the outer bound region with the proposed scheme in combination with symbol extension.

## 3.7 Appendix A: Proof of Theorem 3.1

First, we can see that the outer bound DoF region of 3-user interference channel must contain the bound of  $d_1 + d_2 + d_3$ ,  $d_i + d_j$  and  $d_i$ . Further, it has already been proved that  $d_1 + d_2 + d_3 \leq 3DoF^*$  (where  $DoF^*$  is defined in (1.2)) and  $d_i + d_j \leq N$  in [22] and [20], respectively. It is also known that  $d_i \leq M$ . Hence, in the following, we focus on the rest of the bounds in (3.5)-(3.7), which are also in the form of  $L\{d_i, d_j, d_k\} \leq M$  or  $L\{d_i, d_j, d_k\} \leq N$ , where  $L\{d_i, d_j, d_k\}$  means a linear combination of  $\{d_i, d_j, d_k\}$ . For these bounds, we refer to those in the form of  $L\{d_i, d_j, d_k\} \leq M$  and  $L\{d_i, d_j, d_k\} \leq N$  as  $M$ -side bounds and  $N$ -side bounds, respectively.

Next, we show that with some extension of [22], the  $M$ -side bounds and  $N$ -side bounds can be obtained.

We first briefly review some results in [22]. As mentioned before, the outer bound of sum DoF can be expressed as  $D \leq 3DoF^*$ , where  $DoF^* = \min\{\frac{\kappa}{2\kappa-1}M, \frac{\kappa}{2\kappa+1}N\}$ . The two bounds  $\frac{\kappa}{2\kappa-1}M$  and  $\frac{\kappa}{2\kappa+1}N$  are referred to as  $M$ -bound and  $N$ -bound, respectively. Assuming  $M_R > M_T$  ( $N = M_R, M = M_T$ ), the region  $\frac{M}{N} \in (\frac{1}{2}, 1)$  can be divided into small regions as  $\frac{M}{N} \in [\frac{2L-1}{2L}, \frac{2L}{2L+1}]$  and  $\frac{M}{N} \in [\frac{2L}{2L+1}, \frac{2L+1}{2L+2}]$ ,  $L = 1, 2, \dots + \infty$ . The outer-bound of sum DoF is obtained from the following four major results,

1. Any  $\frac{M}{N} \in [\frac{2L-1}{2L}, \frac{2L}{2L+1}] \Rightarrow d \leq \frac{2L}{4L+1}N$  (Appendix A.2.6 of [22])

2. Any  $\frac{M}{N} \in [\frac{2L}{2L+1}, \frac{2L+1}{2L+2}] \Rightarrow d \leq \frac{2L+1}{4L+3}N$  (Appendix A.2.8 of [22])
3. Any  $\frac{M}{N} \geq \frac{2L+1}{2L+2} \Rightarrow d \leq \frac{2L+2}{4L+3}M$  (Appendix A.2.7 of [22])
4. Any  $\frac{M}{N} \geq \frac{2L}{2L+1} \Rightarrow d \leq \frac{2L+1}{4L+1}M$  (Appendix A.2.5 of [22])

where  $d$  can be seen as  $d = \frac{D}{3}$ . Each result contains certain part of the outer-bound of sum DoF, which also implies a certain part of the DoF region.

We first examine the first result, i.e., the  $N$ -bound sum DoF of the region  $[\frac{2L-1}{2L}, \frac{2L}{2L+1}]$ . In [22], the authors provided  $2L$  genie signal sets to each receiver. The genie signal sets are designed in a way such that each receiver is able to decode the messages from all three users. Each genie signal set leads to one inequality.

Without loss of generality, we focus on receiver 1 only, where there are  $2L$  inequalities. The left-hand side of these inequalities are always the sum rate of the network, i.e.,  $nR_\Sigma = n(R_1 + R_2 + R_3)$ , where  $n$  and  $R_i$  denote the time slots and rate of each link, respectively. The right-hand side of the inequalities contain several terms. In one of the inequalities, the terms are  $Nn \log \rho \pm h(\dots) + no(\log \rho) + o(n)$ , where  $\pm$  means  $+$  or  $-$ ;  $h(\dots)$  is the entropy term that is determined by the corresponding genie signal set;  $no(\log \rho) + o(n)$  is the noise distortion. In the other  $2L - 1$  inequalities, the terms are  $Nn \log \rho + nR_j \pm h(\dots) + no(\log \rho) + o(n)$ , where  $j = 2$  or  $3$ . Since the links are interchangeable, by advancing the user indices,  $R_2$  and  $R_3$  can all be denoted as  $R = \frac{R_\Sigma}{3}$ . Consequently, these  $2L$  inequalities can be expressed as

$$\begin{cases} 1 : & nR_\Sigma \leq Nn \log \rho \pm h(\dots) + no(\log \rho) \\ 2L - 1 : & nR_\Sigma \leq Nn \log \rho + nR \pm h(\dots) + no(\log \rho) \end{cases} \quad (3.77)$$

Then, by summing up all  $2L$  inequalities, the entropy terms will be canceled out. Ignoring the noise distortion, the result  $d \leq \frac{2L}{4L+1}N$  can be easily derived since  $d = \frac{R}{n \log \rho}$ .

Next, we show how to get the  $N$ -side bound for  $\frac{M}{N} \in [\frac{2L-1}{2L}, \frac{2L}{2L+1}]$  based on (3.77). The issue is addressed according to the value of  $L \bmod 3$ .

When  $L \bmod 3 = 0$ , we keep two inequalities not advancing the user indices, i.e., as

$$\left\{ \begin{array}{l} 1 : nR_{\Sigma} \leq Nn \log \rho \pm h(\cdots) + no(\log \rho) + o(n) \\ 1 : nR_{\Sigma} \leq Nn \log \rho + nR_2 \pm h(\cdots) + no(\log \rho) \\ 1 : nR_{\Sigma} \leq Nn \log \rho + nR_3 \pm h(\cdots) + no(\log \rho) \\ 2L - 3 : nR_{\Sigma} \leq Nn \log \rho + nR \pm h(\cdots) + no(\log \rho) \end{array} \right.$$

by summing up all  $2L$  inequalities, we have

$$\begin{aligned} 2Ln(3R) &\leq 2LNn \log \rho + nR_2 + nR_3 + (2L - 3)nR + no(\log \rho) \Rightarrow \\ (4L + 3)nR &\leq 2LNn \log \rho + nR_2 + nR_3 + no(\log \rho) \Rightarrow \\ (4L + 3)d &\leq 2LN + d_2 + d_3 \Rightarrow \\ \frac{4L + 3}{3}D - d_2 - d_3 &\leq 2LN \Rightarrow \\ \frac{4L + 3}{3}d_1 + \frac{4L}{3}d_2 + \frac{4L}{3}d_3 &\leq 2LN \end{aligned} \quad (3.78)$$

Since the links are interchangeable, (3.78) can be written as

$$\frac{4L + 3}{3}d_i + \frac{4L}{3}d_j + \frac{4L}{3}d_k \leq 2LN \quad (3.79)$$

where  $i, j, k = 1, 2, 3$  and  $i \neq j \neq k$ .

When  $L \bmod 3 = 1$ , we keep one inequality not advancing the user indices, i.e.,

$$\left\{ \begin{array}{l} 1 : nR_{\Sigma} \leq Nn \log \rho \pm h(\cdots) + no(\log \rho) + o(n) \\ 1 : nR_{\Sigma} \leq Nn \log \rho + nR_3 \pm h(\cdots) + no(\log \rho) + o(n) \\ 2L - 2 : nR_{\Sigma} \leq Nn \log \rho + nR \pm h(\cdots) + no(\log \rho) + o(n) \end{array} \right.$$

By summing up all  $2L$  inequalities, we have

$$\begin{aligned} 2Ln(3R) &\leq 2LNn \log \rho + nR_3 + (2L - 2)nR + no(\log \rho) + o(n) \\ \Rightarrow (4L + 2)d &\leq 2LN + d_3 \Rightarrow \frac{4L + 2}{3}D - d_3 \leq 2LN \\ \Rightarrow \frac{4L + 2}{3}d_1 + \frac{4L + 2}{3}d_2 + \frac{4L - 1}{3}d_3 &\leq 2LN \end{aligned}$$

which leads to

$$\frac{4L+2}{3}d_i + \frac{4L+2}{3}d_j + \frac{4L-1}{3}d_k \leq 2LN \quad (3.80)$$

When  $L \bmod 3 = 2$ , the  $N$ -side bound does not exist.

With the same approach, we can get the  $N$ -side bound of DoF for  $\frac{M}{N} \in [\frac{2L}{2L+1}, \frac{2L+1}{2L+2}]$  based on result (2) (Appendix A.2.8 of [22]), i.e.,

$$\begin{cases} \emptyset & \text{when } l = 0 \\ \frac{4L+5}{3}d_i + \frac{4L+2}{3}d_j + \frac{4L+2}{3}d_k \leq (2L+1)N & \text{when } l = 1 \\ \frac{4L+4}{3}d_i + \frac{4L+4}{3}d_j + \frac{4L+1}{3}d_k \leq (2L+1)N & \text{when } l = 2 \end{cases} \quad (3.81)$$

where  $\emptyset$  means that the  $N$ -side bound does not exist and  $l = L \bmod 3$ .

Hence, by combining (3.79), (3.80) and (3.81), the  $N$ -side bounds for  $\frac{M}{N} \in [\frac{P-1}{P}, \frac{P}{P+1}]$  ( $P = 2, 3, \dots + \infty$ ) can be written as

$$\begin{cases} \frac{2P+3}{3}d_i + \frac{2P}{3}d_j + \frac{2P}{3}d_k \leq P \cdot N & \text{when } p = 0 \\ \emptyset & \text{when } p = 1 \\ \frac{2P+2}{3}d_i + \frac{2P+2}{3}d_j + \frac{2P-1}{3}d_k \leq P \cdot N & \text{when } p = 2 \end{cases} \quad (3.82)$$

where  $p = P \bmod 3$

Similarly, based on the derivation of  $M$ -bound sum DoF (Appendix A.2.7 and A.2.5 of [22]), we can get that for  $\frac{M}{N} \geq \frac{P-1}{P}$ , the  $M$ -side bound is

$$\begin{cases} \frac{2P}{3}d_i + \frac{2P}{3}d_j + \frac{2P-3}{3}d_k \leq P \cdot M & \text{when } p = 0 \\ \frac{2P+1}{3}d_i + \frac{2P-2}{3}d_j + \frac{2P-2}{3}d_k \leq P \cdot M & \text{when } p = 1 \end{cases} \quad (3.83)$$

When  $P \bmod 3 = 2$ , the  $M$ -side bound cannot be obtained directly from the corresponding derivation of  $M$ -bound sum DoF. However, we should note that in the derivation of  $M$ -bound sum DoF, all the result derived from  $\frac{M}{N} \geq \frac{P-1}{P}$  can be applied on  $\frac{M}{N} \geq \frac{P}{P+1}$  because  $\frac{P}{P+1} > \frac{P-1}{P}$ . Taking  $P = 5$  for example, the  $M$ -side bound of DoF cannot be obtained from the derivation of  $\frac{M}{N} \geq \frac{4}{5} \Rightarrow d \leq \frac{5}{9}M$ , but the bound derived from  $\frac{M}{N} \geq \frac{3}{4} \Rightarrow d \leq \frac{4}{7}M$  still hold, which is  $3d_i + 2d_j + 2d_k \leq 4M$ . Hence, the  $M$ -side bound for  $P \bmod 3 = 2$  is

$$\frac{2P-1}{3}d_i + \frac{2P-4}{3}d_j + \frac{2P-4}{3}d_k \leq (P-1) \cdot M \quad (3.84)$$

where  $P \geq 5$ .

As a result, by combining the  $N$ -side bound (3.82), the  $M$ -side bound (3.83)-(3.84), the existing outer-bound of sum DoF, and the 2-user bound derived in [20] ( $d_i + d_j \leq N$ ), the outer-bound DoF region of 3-user interference channels for  $\frac{M}{N} \in [\frac{P-1}{P}, \frac{P}{P+1}]$  can be summarized as (3.5)-(3.7).

### 3.8 Appendix B: Derivation of (3.42)-(3.45)

In Section 3.3 we have shown that each original chain and long chain contain  $S$  and  $S + 1$  subspaces, respectively. In addition, for the original chain and long chain that originate from transmitter  $i$  and  $j$ , respectively, each of their subspaces has  $Q_i$  and  $\bar{Q}_j$  signal dimensions, respectively. Hence, the total number of the transmitted signals, (the sum DoF of the network), can be calculated as

$$D = S \cdot Q_s + (S + 1)\bar{Q}_s + q_s \quad (3.85)$$

where  $q_s = q_1 + q_2 + q_3$  and  $q_1 = q_{21} + q_{31}$ ,  $q_2 = q_{12} + q_{32}$ ,  $q_3 = q_{13} + q_{23}$ .

In addition, from (3.18) we can see that each original chain and long chain generates  $(S - 1)Q_i$  and  $S \cdot \bar{Q}_j$  interference dimensions, respectively, and each signal in  $\mathbf{U}_i$  generates one interference dimension. As a result, the total number of interference dimensions generated by the three users equals  $(S - 1)Q_s + S \cdot \bar{Q}_s + q_s$ . Since there are totally  $3M$  dimensions on the receivers' side and  $D$  desired signals, the number of interference dimensions cannot be larger than  $3M - D$ , which will lead to (3.42), i.e.,  $Q_s + \bar{Q}_s \geq 2D - 3M$ . (Note that (3.42) can also be equivalent to the summation of (3.29)-(3.31).)

Next, we derive (3.43). Taking (3.85) into (3.42), we have

$$D = (2S - 1) \cdot Q_s + (2S + 1)\bar{Q}_s + 2q_s \leq 3M \quad (3.86)$$

Then, we assume all signals are from either the original chains or the long chains, i.e.,  $q_s = 0$ . In that case, we can get  $\bar{Q}_s = \frac{D-S \cdot Q_s}{S+1}$  according to (3.85). By taking this

result into (3.86), with  $q_s = 0$ , we can get

$$\frac{2S+1}{S+1}(D - S \cdot Q_s) + (2S-1)Q_s \leq 3M$$

which leads to (3.43).

Moreover, since  $Q_s = \sum_{i=1}^3 Q_i$  and  $Q_i \leq S \cdot N - (S+1)M$  (according to (3.21)), we can get (3.44) as follows,

$$\begin{aligned} Q_i &= Q_s - (Q_j + Q_k) \geq Q_s - 2(S \cdot N - (S+1)M) \\ &\geq [(2S+1)D - (S+1)M - 2SN]^+ \end{aligned}$$

Next, since  $\bar{Q}_s \geq 2D - 3M - Q_s$  (from (3.42)) and  $Q_s \leq 3(S \cdot N - (S+1)M)$ , we have (3.45) as

$$\bar{Q}_s \geq [2D - 3SN + 3SM]^+$$

### 3.9 Appendix C: Derivation of (3.61)

To get the upper bound of  $d_i$ , we want the right side of (3.60) as large as possible, which is equivalent to minimizing  $Q_s + \bar{Q}_s - (Q_1 + Q_2 + \bar{Q}_1)$ .

Note that  $Q_s + \bar{Q}_s \geq 2D - 3M$ ,  $Q_i \leq (3t-1)N - 3tM$  and  $\bar{Q}_i \leq 3tN - (3t+1)M$ . Hence, if  $2D - 3M > 2((3t-1)N - 3tM) + 3tN - (3t+1)M$ , we can maximize the right side of (3.60) by letting  $Q_s + \bar{Q}_s = 2D - 3M$ ,  $Q_i = (3t-1)N - 3tM$  and  $\bar{Q}_i = 3tN - (3t+1)M$ , which gives the first term of (3.61).

Then, if  $2D - 3M \leq 2((3t-1)N - 3tM) + 3tN - (3t+1)M$ , the value of  $Q_s + \bar{Q}_s - (Q_1 + Q_2 + \bar{Q}_1)$  can be minimized to zero (which leads to the second term) except when  $(6t-1)D - 9tM > 2((3t-1)N - 3tM)$ . The reason is that  $(6t-1)D - 9tM$  is the lower bound of  $Q_s$  (according to (3.43)), if the value of  $Q_1 + Q_2$  is lower than that, the minimum value of  $Q_s + \bar{Q}_s - (Q_1 + Q_2 + \bar{Q}_1)$  should be expressed as  $\min\{Q_s - Q_1 - Q_2\} + \min\{\bar{Q}_s - \bar{Q}_1\}$ . In that case, by letting  $Q_s + \bar{Q}_s = 2D - 3M$ ,  $Q_i = (3t-1)N - 3tM$ ,  $Q_s = (6t-1)D - 9tM$  and  $\bar{Q}_s = \bar{Q}_1 = [(9t-3)M - (6t-3)D]^+$ , we can obtain the third term of (3.61).

### 3.10 Appendix D: Discussion on achievable DoF region for $\frac{3t-2}{3t-1} \leq \frac{M}{N} < \frac{3t-1}{3t}$

In Appendix D, we show that (3.48), (3.52), the first and third terms of (3.61) are included in (3.47), (3.53) and (3.59). First of all, it can be easily proved that (3.48) is included in (3.53). Then, for (3.52), it implies that  $d_i + d_j \leq (3t - 3)M - (2t - 3)D$ , i.e., the outer bound of  $d_i + d_j$ . Note that (3.53) and (3.59) also indicate the outer bound of  $d_i + d_j$ , which are  $d_i + d_j \leq (3t - 1)N - (2t - 1)D$  and  $d_i + d_j \leq N$ , respectively. Hence, for (3.52) to be not trivial, the following two inequalities must be both satisfied in some part of the region,

$$\begin{aligned} (3t - 3)M - (2t - 3)D &< (3t - 1)N - (2t - 1)D \Rightarrow \\ 2D &< (3t - 1)N - (3t - 3)M \end{aligned} \quad (3.87)$$

$$\begin{aligned} (3t - 3)M - (2t - 3)D &< N \Rightarrow \\ D &> \frac{(3t - 3)M - N}{2t - 3} \end{aligned} \quad (3.88)$$

It can be calculated that (3.87) and (3.88) can only be both satisfied in the region of  $\frac{M}{N} < \frac{6t^2 - 11t + 5}{6t^2 - 9t + 3}$ . Note that  $\frac{6t^2 - 11t + 5}{6t^2 - 9t + 3} < \frac{3t-2}{3t-1}$ , which means in the region of  $\frac{3t-2}{3t-1} \leq \frac{M}{N} < \frac{3t-1}{3t}$ , (3.87) and (3.88) can never hold at the same time, i.e., (3.52) is trivial as it is included by (3.53) and (3.59) in the region of  $\frac{3t-2}{3t-1} \leq \frac{M}{N} < \frac{3t-1}{3t}$ .

Lastly, we show that (3.61) are included by (3.47), (3.53) and (3.59). As we can see, (3.53) indicates that  $d_i + d_j \leq (3t - 1)N - (2t - 1)D$ , which also implies that  $d_k = D - (d_i + d_j) \geq 2tD - (3t - 1)N$ . Since the links are interchangeable, we have  $d_k + d_j \geq 4tD - 2(3t - 1)N$ , which leads to

$$d_i = D - (d_i + d_j) \leq 2(3t - 1)N - (4t - 1)D \quad (3.89)$$

It means that the bound (3.53) is not only the outer bound of  $d_i + d_j$ , but also implies the outer bound of  $d_i$ , i.e.,  $d_i \leq 2(3t - 1)N - (4t - 1)D$ . Similarly, the bound  $d_i + d_j \leq N$  also implies

$$d_i \leq 2N - D \quad (3.90)$$

As can be seen, the bounds in (3.61) also indicate the outer bound of  $d_i$ . Hence, if the outer bound in (3.61) is not lower than that of in (3.89) and (3.90), the bound would be trivial, i.e., included by (3.89) and (3.90).

The first term of (3.61) is  $d_i \leq (9t - 2)N - 6tM - 2tD$ . For this bound not to be included in (3.89) and (3.90), the following two inequalities must be both satisfied,

$$\begin{aligned} (9t - 2)N - 6tM - 2tD &< 2(3t - 1)N - (4t - 1)D \Rightarrow \\ (2t - 1)D &< 6tM - 3tN \end{aligned} \quad (3.91)$$

$$\begin{aligned} (9t - 2)N - 6tM - 2tD &< 2N - D \Rightarrow \\ (2t - 1)D &> (9t - 4)N - 6tM \end{aligned} \quad (3.92)$$

which means  $6tM - 3tN > (9t - 4)N - 6tM \Rightarrow \frac{M}{N} > \frac{3t-1}{3t}$ . Hence, in the region of  $\frac{3t-2}{3t-1} \leq \frac{M}{N} < \frac{3t-1}{3t}$ , (3.91) and (3.92) cannot be both satisfied for sure.

The third term of (3.61) is  $d_i \leq (6t - 2)(N + M) - (8t - 3)D$ . For this bound not to be included in (3.89), the following inequality must be satisfied,

$$\begin{aligned} (6t - 2)(N + M) - (8t - 3)D &< 2(3t - 1)N - (4t - 1)D \\ \Rightarrow (2t - 1)D &> (3t - 1)M \end{aligned} \quad (3.93)$$

However, according to (3.47) and  $S = 3t - 1$ , we have  $D \leq \frac{(3t-1)M}{2t-1}$ , which means (3.93) does not hold for sure in the region  $\frac{3t-2}{3t-1} \leq \frac{M}{N} < \frac{3t-1}{3t}$ .

### 3.11 Appendix E: Proof of $\bar{Q}_i \geq 0$

Similar to (3.44), since  $\bar{Q}_i \leq (S + 1)N - (S + 2)M$ , we have

$$\begin{aligned} \bar{Q}_i &\geq \bar{Q}_s - 2((S + 1)N - (S + 2)M) \\ &\geq [2D - (5S + 2)N + (5S + 4)M]^+ \stackrel{a}{=} 0 \end{aligned} \quad (3.94)$$

where the proof of  $a$  is as follows,

*Proof:* According to (3.48), in the region of  $\frac{S-1}{S} \leq \frac{M}{N} < \frac{S}{S+1}$ ,  $D \leq \frac{3S}{2S+1}$ . Hence, for  $[2D - (5S + 2)N + (5S + 4)M]^+$  to be larger than zero, i.e.,  $2D > (5S + 2)N -$

$(5S + 4)M$ , the following must be satisfied,

$$\frac{6S}{2S+1} > (5S+2)N - (5S+4)M \quad (3.95)$$

It can be proved that (3.95) can only be satisfied when  $\frac{M}{N} > \frac{S}{S+1}$ , which means  $2D \leq (5S+2)N - (5S+4)M$  for sure. Therefore, the lower bound of  $\bar{Q}_i$  is equal to zero.

### 3.12 Appendix F: Proof of the redundancy of (3.70)

(3.74) indicates that  $d_i \leq (3t+1)M - 2tD$ , which implies that

$$d_i + d_j \leq (6t+2)M - 4tD \quad (3.96)$$

Hence, there are already two upper bounds for  $d_i + d_j$ , which are (3.96) and  $d_i + d_j \leq N$ .

Next, we show that the upper bounds in (3.70) are all included by (3.96) and  $d_i + d_j \leq N$ .

In the first term,  $d_i + d_j \leq (9t+4)N - (6t+4)M - (2t+1)D$ . For the bound not being included by  $d_i + d_j \leq N$ , the follows must be satisfied,

$$\begin{aligned} (9t+4)N - (6t+4)M - (2t+1)D &< N \\ \Rightarrow (2t+1)D &> (9t+3)N - (6t+4)M \end{aligned} \quad (3.97)$$

Note that  $D \leq \frac{3SN}{2S+1} = \frac{3t+1}{2t+1}N$ , which means it is only possible to satisfy (3.97) when  $\frac{M}{N} > \frac{3t+1}{3t+2}$ , i.e., outside the region of this case.

In the second term,  $d_i + d_j \leq 3tM - (2t-1)D$ . For the bound not being included by (3.96) and  $d_i + d_j \leq N$ , the following two conditions must be satisfied,

$$\begin{aligned} 3tM - (2t-1)D &< (6t+2)M - 4tD \Rightarrow (2t+1)D < (3t+2)M \\ 3tM - (2t-1)D &< N \Rightarrow (2t-1)D > 3tM - N \end{aligned}$$

which means  $\frac{(3t+2)M}{2t+1} > \frac{3tM-N}{2t-1}$ , i.e.,  $\frac{M}{N} < \frac{2t+1}{2t+2}$ . Note that the region of  $S = 3t + 1$  is  $\frac{3t}{3t+1} \leq \frac{M}{N} < \frac{3t+1}{3t+2}$ . Since  $\frac{2t+1}{2t+2} \leq \frac{3t}{3t+1}$ , the conditions cannot be satisfied inside the region.

In the third term,  $d_i + d_j \leq (6t + 2)(N + M) - (8t + 2)D$ . For the bound not being included by (3.96), we have

$$\begin{aligned} (6t + 2)(N + M) - (8t + 2)D &< (6t + 2)M - 4tD \Rightarrow \\ (3t + 1)N &< (2t + 1)D \end{aligned} \quad (3.98)$$

Note that from (3.48) we can derive that  $D \leq \frac{3SN}{2S+1} = \frac{3t+1}{2t+1}N$ , which means (3.98) cannot be satisfied for sure.

# Chapter 4

## Device-to-Device LAN Underlying Cellular Network

### 4.1 Introduction

In future cellular networks, underlying Device-to-Device (D2D) communications are expected to be incorporated into the network for higher spectrum efficiency. In cellular operation, each user equipment (UE) is served by the network via base stations, which are called evolved NodeBs (eNBs) in the LTE architecture. With D2D technologies, UE units may communicate directly with each other without traversing the core network [54, 56], or enable multihop relays in cellular networks [55].

Allowing D2D transmissions on the same time-frequency resources as the cellular uplink/downlink poses two major challenges. First, the interference caused to the eNBs or cellular users (CU) by D2D devices could critically affect the performance of cellular devices. Second, the quality-of-service (QoS) requirements of D2D devices need to be guaranteed. Since both problems are caused by the mutual interference between cellular links and D2D links, an effective interference coordination mechanism is needed. Currently, most works deal with the problems from the aspects of resource scheduling and power control. Many schemes are proposed to jointly allocate the

physical resource blocks (in both time domain and frequency domain) and perform power control for D2D links subject to interference constraints for cellular operations and QoS demands of D2D links [57–62]. In addition, in D2D networks, since the D2D devices can compete or cooperate with each other to reuse the resources, the resource allocation and access for D2D communication can be treated as games [62–65].

MIMO has been identified as a key enabling technology to improve performance of communications. In modern cellular networks, devices are usually equipped with multiple antennas [66, 67]. Thanks to such setup, beamforming has been shown as an effective technique for interference management, i.e., the direction of transmitted signals is steered so that their negative effect on receivers can be minimized [1, 2]. Moreover, beamforming is performed in spatial domain, which can be used as a complement of existing resource allocation schemes and further improve the spectrum efficiency. In [68], a downlink MIMO beamforming scheme was proposed for eNB to transmit signals in the nullspace of the interference between eNB and D2D receiver (DR). In [69], two beamforming schemes for eNB were proposed. The first one is similar to [68], where eNB uses beamforming to cancel the interference to DR. In the second one, the eNB aims at serving its cellular user rather than dealing with interference. The capacity performance of these two cases were evaluated in [69]. The same system model was also studied in [70], where jointly precoding on both eNB and D2D transmitter is used to maximize the signal-to-leakage-noise ratio (SLNR) or signal-to-interference-noise ratio (SINR). The precoding vectors in [70] are selected from predefined codebooks. In [68–70], each CU shares resources with only one D2D link in the cellular network. In [71], a beamforming scheme based on interference alignment (IA) was proposed for three D2D links, but their effects on cellular network were not studied. In [72], IA was adopted to improve the energy efficiency for both D2D and cellular links.

IA is a type of beamforming that has been extensively studied in a variety of networks such as interference channel [3], X channel [4], and cellular networks [42, 73], etc. In this paper, we explore the possibility of integrating IA techniques into D2D

communication systems. We consider a D2D local area networks (LAN) underlaying a cellular uplink, where multiple DUs intend to communicate with a D2D receiver. This model can be found in many practical scenarios. For example, some context-aware applications (on cell phone) allow nearby devices to discover each other and exchange messages directly. In some occasions, there are many devices with same application gathering together, and they need to communicate with a common DU. Two D2D communication schemes based on IA are proposed to manage the interference between the two networks for different scenarios. The first scheme is referred to as ‘interference-free’ IA scheme, which can be applied in the scenarios where some sub-channels of eNB are not occupied by CUs. In this scheme, the interference signals from DUs are aligned in the orthogonal space of cellular links at the eNB. Hence, the links of CUs are completely free from interference. Note that if all the sub-channels of eNB are used by CUs, the orthogonal space of cellular links may not exist. In case of such scenarios, we propose another scheme which is referred to as ‘interference-limiting’ IA scheme. In this scheme, the DUs’ signals are allowed to occupy some links of CUs, but the peak interference power on each of the ‘interfered’ links is kept under a certain threshold  $\gamma$ . It is shown that the ‘interference-limiting’ IA scheme is most efficient for the scenarios where there are a large number of DUs. The explicit design frameworks and feasibility conditions of the two schemes are provided. Performance analysis shows that based on the proposed schemes, the interference generated on the cellular links is eliminated or well controlled, while the QoS of the D2D LAN can also be guaranteed.

The rest of the paper is organized as follows. In Section 4.2, system model is introduced. In Section 4.3, the ‘interference-free’ IA-based D2D communication scheme is proposed, followed by the performance analysis of the networks. In Section 4.4, the ‘interference-limiting’ IA-based D2D communication scheme is proposed, followed by the performance analysis of the networks. In Section 4.5, simulation results are presented and discussed. Section 4.6 concludes the paper.

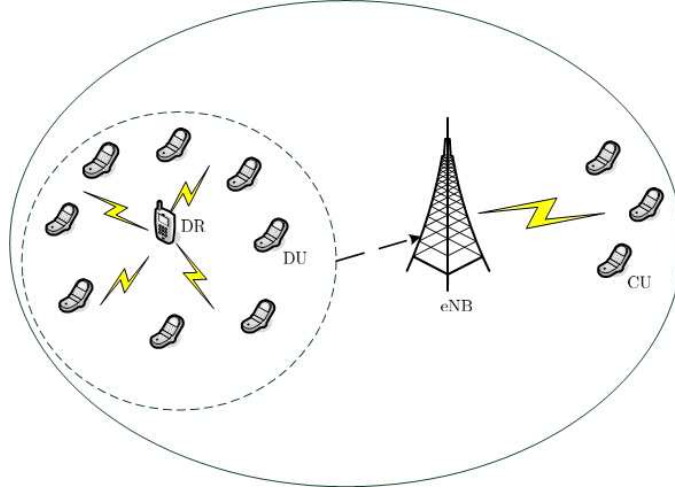


Figure 4.1 D2D LAN underlaying a cellular uplink network

## 4.2 System Model

We consider a D2D LAN underlaying a cellular uplink in a single cell setting, where multiple DUs intend to communicate with a DR, as shown in Fig. 4.1. The eNB receives both desired signals and interference signals from CUs and DUs, respectively. The eNB and DR are equipped with  $N$  and  $N_d$  antennas, respectively. The CU and DU each are equipped with  $M$  and  $M_d$  antennas, respectively.

Let  $\mathbf{H}_{CU,i}^e$  denote the channel from  $CU_i$  to eNB, and  $\mathbf{u}_i$  denote the precoding vector of  $CU_i$ . The received signals on eNB at the absence of interference can be expressed as

$$\begin{aligned} \mathbf{y}'_e &= \mathbf{D}_e \mathbf{y}_e = \mathbf{D}_e \sum_{i=1}^s \mathbf{H}_{CU,i}^e \mathbf{u}_i P_c^{\frac{1}{2}} m_i + \mathbf{D}_e \mathbf{z}_e \\ &= P_c^{\frac{1}{2}} \mathbf{D}_e \begin{bmatrix} \mathbf{H}_{CU,1}^e \mathbf{u}_1 & \cdots & \mathbf{H}_{CU,s}^e \mathbf{u}_s \end{bmatrix} \begin{bmatrix} m_1 \\ \vdots \\ m_s \end{bmatrix} + \mathbf{D}_e \mathbf{z}_e \end{aligned}$$

where  $\mathbf{D}_e \in \mathbb{C}^{s \times N}$  denotes the post-processing matrix of eNB,  $s$  denotes the number of links of CU and  $s \leq N$ ,  $m_i$  denotes the message of  $CU_i$ ,  $P_c$  denotes the transmit power of CU,  $\mathbf{z}_e$  denotes the noise on eNB with unit variance. The design of  $\mathbf{D}_e$  is

different in two schemes, which will be explained later.

Then,  $\mathbf{u}_i$  can be designed to lie in the null space of  $\overline{\mathbf{D}_e \mathbf{H}_{CU,i}^e(i)}$ , i.e.,

$$\overline{\mathbf{D}_e \mathbf{H}_{CU,i}^e(i)} \cdot \mathbf{u}_i = \mathbf{0} \quad (4.1)$$

where  $\overline{\mathbf{D}_e \mathbf{H}_{CU,i}^e(i)}$  denotes the matrix  $\mathbf{D}_e \mathbf{H}_{CU,i}^e$  without the  $i$ th row.

As a result, the links from CUs to eNB can be transformed to  $s$  parallel links, i.e.,

$$\mathbf{y}'_e = P_c^{\frac{1}{2}} \underbrace{\begin{bmatrix} \lambda_1 & & \\ & \ddots & \\ & & \lambda_s \end{bmatrix}}_{\Lambda \in \mathbb{C}^{s \times s}} \begin{bmatrix} m_1 \\ \vdots \\ m_s \end{bmatrix} + \mathbf{z}'_e \quad (4.2)$$

where  $\lambda_i = \mathbf{D}_e \mathbf{H}_{CU,i}^e(i) \mathbf{u}_i$  denotes the equivalent channel gain of the  $i$ -th link of CU, and  $\mathbf{D}_e \mathbf{H}_{CU,i}^e(i)$  denotes the  $i$ -th row of  $\mathbf{D}_e \mathbf{H}_{CU,i}^e$ . Since there are totally  $N$  antennas on eNB, there will be  $r = N - s$  dimensions left 'unused' by CUs.

Let  $\mathbf{H}_{DU,i}^e$  denote the channel from  $DU_i$  to eNB and  $\mathbf{v}_i$  denote the beamforming vector of  $DU_i$ . Assuming there are  $l$  active DUs, the received signal on eNB in the presence of interference becomes

$$\mathbf{y}_e = P_c^{\frac{1}{2}} \Lambda \mathbf{m} + \mathbf{D}_e \sum_{i=1}^l \mathbf{H}_{DU,i}^e \mathbf{v}_i P_d^{\frac{1}{2}} t_i + \mathbf{z}'_e \quad (4.3)$$

where  $\mathbf{m} = [m_1 \ \cdots \ m_s]^T$ ,  $t_i$  denotes the message of  $DU_i$  and  $P_d$  denotes the power of  $t_i$ , and the design of  $\mathbf{v}_i$  is specified in different schemes.

Then, the received signal on DR is given by

$$\mathbf{y}_r = \sum_{i=1}^l \mathbf{H}_{DU,i}^r \mathbf{v}_i P_d^{\frac{1}{2}} t_i + \sum_{i=1}^s \mathbf{H}_{CU,i}^r \mathbf{u}_i P_c^{\frac{1}{2}} m_i + \mathbf{z}_r \quad (4.4)$$

where  $\mathbf{H}_{DU,i}^r$  and  $\mathbf{H}_{CU,i}^r$  denote the channels from  $DU_i$  and  $CU_i$  to DR, respectively.

Further,  $DU_i$  only knows the channel  $\mathbf{H}_{DU,i}^e$ . All the channel matrices are sampled from continuous complex Gaussian distributions and each entry is independent and identically distributed (i.i.d.) with zero mean and unit variance. The channels are assumed to undergo block fading.

Finally, from (4.3) we should note that if  $s < M_d$ , then  $\mathbf{D}_e \mathbf{H}_{DU,i}^e \in \mathbb{C}^{s \times M_d}$  is a ‘fat’ matrix, which means  $\mathbf{v}_i$  can be found to null the interference at eNB almost surely, regardless of the choice of  $\mathbf{D}_e$ . Hence, in the following, we only focus on the case of  $s \geq M_d$ .

### 4.3 Interference-Free IA Scheme

In this section, we introduce the ‘interference free’ IA scheme for D2D communications. We first elaborate the design process of the scheme. Then, the performance analysis of both D2D LAN and cellular link is provided. Finally, the advantage and limitation of this scheme are discussed.

#### 4.3.1 Design Process

Four steps are involved in the design process of D2D transmission. In **Step 1**, the eNB select  $l$  DUs for D2D communications, where  $l < \frac{N \cdot r}{N - M_d}$  and  $l \leq N_d$ . In **Step 2**, the eNB designs and broadcasts the post-processing matrix  $\mathbf{D}_e$  through physical downlink control channels. In **Step 3**, each DU designs the precoding vectors  $\mathbf{v}_i$  according to the received  $\mathbf{D}_e$ . Each CU also designs precoding vector  $\mathbf{u}_i$  as described in Section 4.2. In **Step 4**, the D2D receiver (DR) designs the receiving filter to decode transmitted signals.

- **Step 1:** The  $l$  DUs can be selected randomly, or according to some protocols or preference of DR. To ensure that the signals from DUs can be linearly decoded at DR, it must have  $l \leq N_d$ . Further, we have following result.

**Theorem 4.1** *In a cellular uplink network underlying a D2D LAN, where there are  $s$  links of CUs and  $l$  active DUs, the interference on eNB can be nulled while the desired signals can still be linearly decoded as long as  $l < \frac{N \cdot r}{N - M_d}$ , where  $r = N - s$ .*

*Proof:* The eNB receives  $s$  desired signals and  $l$  interference signals. Since the desired signals occupy  $s$  dimensions, the  $l$  interference signals must be aligned to

$r = N - s$  dimensions. To do so, we should align each of the last  $l - r$  interference signals within the interference space that spanned by the first  $r$  interference signals, i.e.,

$$\underbrace{\begin{bmatrix} a \cdot \mathbf{H}_{DU,1}^e & b \cdot \mathbf{H}_{DU,2}^e & f \cdot \mathbf{H}_{DU,r}^e & -\mathbf{H}_{DU,r+1}^e & 0 & 0 & 0 \\ g \cdot \mathbf{H}_{DU,1}^e & \epsilon \cdot \mathbf{H}_{DU,2}^e & q \cdot \mathbf{H}_{DU,r}^e & 0 & -\mathbf{H}_{DU,r+2}^e & 0 & 0 \\ \vdots & \vdots & \dots & \vdots & \vdots & \ddots & \vdots \\ \gamma \cdot \mathbf{H}_{DU,1}^e & \kappa \cdot \mathbf{H}_{DU,2}^e & \lambda \cdot \mathbf{H}_{DU,r}^e & 0 & 0 & 0 & -\mathbf{H}_{DU,l}^e \end{bmatrix}}_{\mathbf{H}' \in \mathbb{C}^{N \cdot (l-r) \times M_d \cdot l}} \cdot \left[ \begin{array}{c} (\mathbf{v}'_1)^T \quad \dots \quad (\mathbf{v}'_r)^T \\ \vdots \\ (\mathbf{v}'_{r+1})^T \quad \dots \quad (\mathbf{v}'_l)^T \end{array} \right]^T = \mathbf{0} \quad (4.5)$$

where  $a \dots \lambda$  are all arbitrary complex parameters.

As we can see, the non-zero solution for  $\left[ \mathbf{v}'_1 \quad \dots \quad \mathbf{v}'_l \right]^T$  can be found if  $\mathbf{H}'$  is a ‘fat’ matrix, i.e.,

$$M_d \cdot l > N \cdot (l - r) \quad (4.6)$$

which is equivalent to

$$l < \frac{N \cdot r}{N - M_d} \quad (4.7)$$

Moreover, since all the channels are generic, there are at least  $M_d \cdot l + 1$  non-zero entries in  $\left[ \mathbf{v}'_1 \quad \dots \quad \mathbf{v}'_l \right]^T$ . Hence, each of the  $l$  precoding vectors can be guaranteed to be non-zero vector almost surely.

• **Step 2:** After selecting the potential DUs, the eNB needs to design a proper post processing matrix  $\mathbf{D}_e$ , which should be orthogonal to the interference space. Since the eNB knows all the receiving channels, it can formulate equation (4.5) with the channel matrices between selected DUs and eNB. Hence, the interference space that formed by DUs’ signals is  $\text{span}\left\{ \left[ \mathbf{H}_{DU,1}^e \mathbf{v}'_1 \quad \dots \quad \mathbf{H}_{DU,r}^e \mathbf{v}'_r \right] \right\} \in \mathbb{C}^{N \times r}$ . Then,  $\mathbf{D}_e \in \mathbb{C}^{(N-r) \times N}$  can be designed as follows,

$$\mathbf{D}_e \cdot \left[ \mathbf{H}_{DU,1}^e \mathbf{v}'_1 \quad \dots \quad \mathbf{H}_{DU,r}^e \mathbf{v}'_r \right] = \mathbf{0} \quad (4.8)$$

Moreover, we assume that eNB will send  $\mathbf{D}_e$  to all users (DUs and CUs) through the physical downlink control channels. Specifically, the matrix  $\mathbf{D}_e$  can be sent in an unquantized uncoded version based on the analog channel state information (CSI) feedback scheme proposed in [74, 75]. Alternatively,  $\mathbf{D}_e$  can also be transmitted with conventional CSI feedback mechanism based on quantization codebooks [76–78]. First, a common codebook can be stored in eNB and users. Then,  $\mathbf{D}_e$  can be quantized by using the codebook. Each time, the eNB will only broadcast the index of the corresponding codeword of  $\mathbf{D}_e$ .

• **Step 3:** After receiving  $\mathbf{D}_e$ , each DU can design the precoding vector accordingly.

The  $\text{DU}_i$  first calculates  $\mathbf{P}_i \in \mathbb{C}^{(N-r) \times M_d} = \mathbf{D}_e \mathbf{H}_{DU,i}^e$  (Note that  $\mathbf{H}_{DU,i}^e$  is known by  $\text{DU}_i$ ). Then, the precoding vector  $\mathbf{v}_i$  is determined by calculating the null space of  $\mathbf{P}_i$ , i.e.,

$$\mathbf{P}_i \mathbf{v}_i = \mathbf{0} \quad (4.9)$$

Since  $N - r = s \leq M_d$ ,  $\mathbf{P}_i$  is either a square or ‘thin’ matrix, which means its null space does not exist if  $\mathbf{P}_i$  is full rank.

If the  $\text{DU}_i$  is one of DUs that are selected by the eNB in **Step 1**,  $\mathbf{H}_{DU,i}^e$  is one of the channel matrices in (4.5), which means

$$\mathbf{H}_{DU,i}^e \mathbf{v}'_i = \begin{bmatrix} \mathbf{H}_{DU,1}^e \mathbf{v}'_1 & \cdots & \mathbf{H}_{DU,r}^e \mathbf{v}'_r \end{bmatrix} \begin{bmatrix} a_1 \\ \vdots \\ a_r \end{bmatrix}. \quad (4.10)$$

If  $r + 1 \leq i \leq l$ ,  $a_1 \cdots a_r$  are all random complex numbers; if  $1 \leq i \leq r$ ,  $a_1 \cdots a_r$  are all zeros except  $a_i = 1$ .

Hence, based on (4.8), we can see that  $\mathbf{P}_i$  must not be full rank and its null space is  $\mathbf{v}_i = \text{span}\{\mathbf{v}'_i\}$ . Therefore, by calculating (4.9),  $\text{DU}_i$  can find the precoding vector as  $\mathbf{v}_i = \text{span}\{\mathbf{v}'_i\}$ .

On the other hand, if the  $\text{DU}_i$  is not selected by the eNB, then  $\mathbf{P}_i$  is just a random matrix that has full rank almost surely. Therefore, since a non-zero solution

of  $\mathbf{v}_i$  that satisfies (4.9) does not exist, those unselected DUs will not start the D2D transmission.

• **Step 4:** Finally, DR designs its post processing matrix  $\mathbf{U}_r$  to decode signals from DUs. Let  $\mathbf{g}_i \in \mathbb{C}^{N_d \times 1} = \mathbf{H}_{DU,i}^r \mathbf{v}_i$  be the equivalent channel from DU $_i$  to DR, and  $\mathcal{G} = \begin{bmatrix} \mathbf{g}_1 & \cdots & \mathbf{g}_l \end{bmatrix}$ , (4.4) can be written as

$$\mathbf{y}_r = P_d^{\frac{1}{2}} \mathcal{G} \mathbf{t} + \mathcal{G}_{-i} (\mathbf{t}_{-i})^T + \mathcal{H} P_c^{\frac{1}{2}} \mathbf{m} + \mathbf{z}_r \quad (4.11)$$

where  $\mathbf{t} = \begin{bmatrix} t_1 & \cdots & t_l \end{bmatrix}$ ,  $\mathbf{m} = \begin{bmatrix} m_1 & \cdots & m_s \end{bmatrix}^T$ , and  $\mathcal{H} = \begin{bmatrix} \mathbf{H}_{CU,1}^r \mathbf{u}_1 & \cdots & \mathbf{H}_{CU,l}^r \mathbf{u}_s \end{bmatrix}$ .  $\mathcal{G}_{-i}$  denotes the matrix  $\mathcal{G}$  without the  $i$ -th column.

Then,  $\mathbf{U}_r$  is designed to cancel the interference from other DUs, while treating the interference from cellular links as noise. Specifically, let  $\mathbf{u}_j \in \mathbb{C}^{1 \times N_d}$  denotes the  $j$ -th row of  $\mathbf{U}_r$ , i.e.,  $\mathbf{U}_r = \begin{bmatrix} \mathbf{u}_1^T & \cdots & \mathbf{u}_l^T \end{bmatrix}^T$ .  $\mathbf{u}_j$  is designed as the null-space of  $\mathcal{G}_{-j} \in \mathbb{C}^{N_d \times (l-1)}$ , i.e.,

$$\mathbf{u}_j \cdot \mathcal{G}_{-j} = \mathbf{0} \quad (4.12)$$

Since  $l \leq N_d$ , we have  $l-1 < N_d$  for sure, which means  $\mathbf{u}_j$  can be found for sure.

As a result, the received signal of DU $_j$  can be expressed as

$$y_j = \omega_j P_d^{\frac{1}{2}} t_j + P_c^{\frac{1}{2}} \mathbf{u}_j \mathcal{H} \mathbf{m} + \mathbf{u}_j \mathbf{z}_r, \quad j = 1, \cdots, l \quad (4.13)$$

where  $\omega_j = \mathbf{u}_j \mathbf{g}_j$ .

### 4.3.2 Performance of Cellular Network

We first study the performance of cellular links. Specifically, we investigate the outage probability of each cellular link, which is defined as the probability of event that  $\rho_i$  is lower than a predetermined threshold  $\alpha$ , where  $\rho_i$  denotes the signal-to-noise ratio (SNR) of the link of CU $_i$ . Note that based on the proposed scheme, the interference signals from DUs are all aligned in the orthogonal space of cellular links, which means there is no interference at each cellular link.

**Theorem 4.2** *In a cellular uplink network underlaying a D2D LAN, based on the proposed ‘interference-free’ IA scheme, the outage probability of each cellular link is*

$$P_{out} = Pr[\rho_i \leq \alpha] = 1 - \frac{1}{\frac{\alpha}{P_c} + 1} \quad (4.14)$$

*Proof:* Since the interference is completely nulled, the received signals on eNB can be written as (4.2). Hence, the SNR of CU<sub>i</sub>, ρ<sub>i</sub> can be expressed as

$$\rho_i = \frac{P_c |\lambda_i|^2}{|\mathbf{z}'_e(i)|^2} = P_c \frac{|\mathbf{D}_e \mathbf{H}_{CU,i}^e \mathbf{u}_i(i)|^2}{|\mathbf{D}_e \mathbf{z}_e(i)|^2} \quad (4.15)$$

where  $\mathbf{D}_e \mathbf{H}_{CU,i}^e \mathbf{u}_i(i)$  and  $\mathbf{D}_e \mathbf{z}_e(i)$  denotes the  $i$ -th row of vector  $\mathbf{D}_e \mathbf{H}_{CU,i}^e \mathbf{u}_i$  and  $\mathbf{D}_e \mathbf{z}_e$ , respectively.

Let  $y_i = \mathbf{D}_e \mathbf{z}_e(i)$ . Since both  $\mathbf{D}_e$  and  $\mathbf{u}_i$  are unitary (each of them is the null space of a matrix),  $\lambda_i$  and  $y_i$  follow the same distribution as the elements in  $\mathbf{H}_{CU,i}^e$  and  $\mathbf{z}_e$ , respectively. Hence, both  $\lambda_i$  and  $y_i$  have complex normal distribution with zero mean and unit variance, which means both  $|\lambda_i|^2$  and  $|y_i|^2$  have exponential distributions, i.e.,  $|\lambda_i|^2 \sim \exp(1)$  and  $|y_i|^2 \sim \exp(1)$ . Therefore, the probability density function (pdf) of  $Z = \frac{|\lambda_i|^2}{|y_i|^2}$  is

$$f_Z(z) = \frac{1}{(z+1)^2}, \text{ for } z \geq 0 \quad (4.16)$$

Accordingly, the pdf of  $\rho_i = P_c \cdot Z$  is

$$f_{\rho_i}(z) = \frac{1}{P_c \left(\frac{z}{P_c} + 1\right)^2}, \text{ for } z \geq 0 \quad (4.17)$$

Finally, the outage probability of CU<sub>i</sub> can be calculated as

$$P_{out} = Pr[\rho_i \leq \alpha] = \int_0^\alpha f_{\rho_i}(z) dz = 1 - \frac{1}{\frac{\alpha}{P_c} + 1} \quad (4.18)$$

### 4.3.3 Performance of D2D LAN

Next, we examine the outage probability of each D2D link. Let  $\rho_j^D$  denote the SINR of the link of DU<sub>j</sub>. The outage probability of the D2D link is  $Pr[\rho_j^D \leq \beta]$ .

**Theorem 4.3** *In a cellular uplink network underlaying a D2D LAN, based on the proposed ‘interference-free’ IA scheme, the outage probability of each D2D link is*

$$P_{out} = Pr[\rho_j^D \leq \beta] = 1 - \frac{1}{\left(\frac{\beta P_c}{P_d} + 1\right)^s} \quad (4.19)$$

*Proof:* Let  $\mathbf{p}_j \in \mathbb{C}^{1 \times s} = \mathbf{u}_j \mathcal{H}$ . According to (4.13), the SINR at DR with a high SNR approximation can be expressed as

$$\begin{aligned} \rho_j^D &= \frac{P_d |\omega_j|^2}{P_c \mathbf{p}_j \mathbf{p}_j^* + |\mathbf{z}'_r|^2} = \frac{P_d |\omega_j|^2}{P_c \sum_{k=1}^s |p_k|^2 + |\mathbf{z}'_r|^2} \\ &\approx \frac{P_d |\omega_j|^2}{P_c \mathbf{p}_j \mathbf{p}_j^* + |\mathbf{z}'_r|^2} = \frac{P_d |\omega_j|^2}{P_c \sum_{k=1}^s |p_k|^2} \end{aligned} \quad (4.20)$$

where  $p_k$  denotes the  $k$ -th element of  $\mathbf{p}_j$ .

Since  $\omega_j$  and  $p_k$  all follow independent complex Gaussian distribution, based on the results in [60], the pdf of  $\rho_j^D$  can be expressed as

$$f_{\rho_j^D}(x) = \frac{P_c}{P_d} \frac{s}{\left(x \frac{P_c}{P_d} + 1\right)^{(s+1)}}, \text{ for } x \geq 0 \quad (4.21)$$

The outage probability of the link of DU <sub>$j$</sub>  is calculated as

$$P_{out} = Pr[\rho_j^D \leq \beta] = \int_0^\beta f_{\rho_j^D}(x) dx = 1 - \frac{1}{\left(\frac{\beta P_c}{P_d} + 1\right)^s} \quad (4.22)$$

#### 4.3.4 Discussion

The main advantage of this scheme is that the interference from DUs is completely nulled at the eNB, and hence both cellular and D2D links can achieve the desired performance by simply adjusting the power. As can be seen from (4.14), the outage probability of each link of CU is only related to the power of CU,  $P_c$ . Further, in D2D LAN, (4.19) implies that the outage probability of the link of DU will decrease if the power of DU is increased. Hence, the DUs can adjust the power  $P_d$  to obtain the required QoS without considering its impact on cellular links.

On the other hand, we should also note that this scheme may not be applicable if the value of  $\frac{N \cdot r}{N - M_d}$  is small. For example, if  $\frac{N \cdot r}{N - M_d} \leq 1$ , then the D2D LAN will not be active according to *Theorem 1*.

## 4.4 Interference-limiting IA scheme

In this scheme, the DUs' signals are allowed to occupy some links of CUs. However, the peak interference power on each of the 'interfered' links must be under a certain threshold  $\gamma$ .

### 4.4.1 Design Process

Three steps are involved in the design process. In **Step 1**, the eNB designs and broadcasts the post-processing matrix  $\mathbf{D}_e$ . In **Step 2**, each DU designs the precoding vectors  $\mathbf{v}_i$  according to the received  $\mathbf{D}_e$ . Each CU also designs precoding vector  $\mathbf{u}_i$  as described in Section 4.2. In **Step 3**, some DUs are scheduled for transmission according to some user selection criterion.

- **Step 1:** We simply design  $\mathbf{D}_e$  as an antenna selection matrix i.e.,

$$\mathbf{D}_e = \begin{bmatrix} \mathbf{I}_{s \times s} & \mathbf{0}_{s \times (N-s)} \end{bmatrix} \quad (4.23)$$

where  $\mathbf{I}_{s \times s}$  denotes the  $s \times s$  identity matrix and  $\mathbf{0}_{s \times (N-s)}$  denotes the  $s \times (N-s)$  matrix with all zeros. Then, the  $\text{CU}_i$  can design  $\mathbf{u}_i$  accordingly to realize the parallel channels on the first  $s$  antennas of eNB as shown in (4.2).

- **Step 2:** We describe the design of  $\mathbf{v}_i$  for  $\text{DU}_i$ . From (4.3) we can see that the  $j$ -th row of  $\mathbf{D}_e \mathbf{H}_{DU,i}^e$  represents interference from  $\text{DU}_i$  added on the  $j$ -th link of CUs. Since  $\mathbf{v}_i \in \mathbb{C}^{(M_d \times 1)}$ , it can be designed as the null space of at most  $M_d - 1$  rows of  $\mathbf{D}_e \mathbf{H}_{DU,i}^e$ , so as to keep the corresponding links free from interference.

Assume that we want the first  $M_d - 1$  links to be interference free,  $\mathbf{v}_i$  can be designed by satisfying

$$\mathbf{D}_e(M_d - 1) \mathbf{H}_{DU,i}^e \cdot \mathbf{v}_i = \mathbf{0} \quad (4.24)$$

where  $\mathbf{D}_e(M_d - 1)$  denotes the first  $M_d - 1$  rows of  $\mathbf{D}_e$ .

- **Step 3:** Since all DUs design their signals to avoid interfering the first  $M_d - 1$  links of CUs, it is equivalent to aligning the interference on to the rest  $s - M_d + 1$

links of CUs. The received signal from DU<sub>*i*</sub> on eNB can be written as

$$\begin{aligned} & \mathbf{D}_e \mathbf{H}_{DU,i}^e \mathbf{v}_i P_d^{\frac{1}{2}} t_i \\ &= \left[ \mathbf{0}_{1 \times (M_d-1)} \quad \vartheta_{M_d}^i \quad \cdots \quad \vartheta_s^i \right]^T P_d^{\frac{1}{2}} t_i \end{aligned} \quad (4.25)$$

where  $\vartheta_k^i$  is a complex number that represents the interference from DU<sub>*i*</sub> on the *k*-th link of eNB. Accordingly, the interference power generated on eNB's *k*th link by DU<sub>*i*</sub> can be calculated as  $|\vartheta_k^i|^2 P_d$ .

Let  $\gamma$  denote the interference constraint on each link of CU, which can be determined according to the requirement of cellular network. The DU<sub>*i*</sub> will become a qualified DU if the following condition is satisfied,

$$|\vartheta_k^i|^2 P_d \leq \frac{\gamma}{N_d}, \quad \forall k = M_d, \dots, s \quad (4.26)$$

Then, DR will select  $l \leq N_d$  qualified DUs to start transmission. When there are a large number of DUs, the active DUs can be selected based on their equivalent channels with the semi-orthogonal user selection (SUS) algorithm introduced in [37].

#### 4.4.2 Performance of Cellular Network

We first examine the performance of cellular network. Note that with this scheme, the first  $M_d - 1$  links of CUs are free from interference. Therefore, they have the same performance as 'interference-free' IA scheme. Next, we focus on those 'interfered' links of CUs. Let  $\phi_k$  denote the SINR of the *k*-th links of CUs, where  $k \geq M_d$ , we have the following Theorem,

**Theorem 4.4** *In a cellular uplink network underlaying a D2D LAN, based on the proposed 'interference-limiting' IA scheme, the outage probability of each 'interfered' cellular link is*

$$\begin{aligned} P_{out} &= Pr[\phi_k \leq \alpha] \\ &= 1 - \left(1 + \frac{\alpha}{P_c}\right)^{-1} \cdot (1 - e^{-\gamma'})^{-N_d} \cdot \\ &\quad \left(1 + \frac{P_d \alpha}{P_c}\right)^{-N_d} (1 - e^{-\gamma'(\frac{P_d \alpha}{P_c} + 1)})^{N_d} \end{aligned} \quad (4.27)$$

where  $\gamma' = \frac{\gamma}{P_d N_d}$ .

The proof is given in Appendix A.

### 4.4.3 Performance of D2D LAN

Note that in this scheme, only those DUs who can satisfy (4.26) are qualified to start D2D transmission. Hence, we first examine the number of qualified DUs for a certain threshold of a cellular link.

**Proposition 4.1** *For the D2D LAN with  $K$  DUs underlying a cellular uplink, given the interference constraint  $\gamma$  at each link of CU, the number of qualified DUs is*

$$N_q = K \cdot p_q \approx K \cdot (1 - e^{-\gamma'})^{(s - M_d + 1)} \quad (4.28)$$

where  $p_q$  denotes the probability of a DU being qualified.

The proof is in Appendix B.

As can be seen, the value of  $N_q$  is related to  $\gamma$  and  $s - M_d$ . First, it is obvious that when the interference threshold is increased, more DUs will be allowed to transmit. In addition, we can see that with less links of CUs in the network (smaller  $s$ ), more DUs are qualified for transmission.

Next, we study the performance of D2D LAN. Let  $\mathbf{g}_i \in \mathbb{C}^{N_d \times 1} = \mathbf{H}_{DU,i}^r \mathbf{v}_i$  denote the equivalent channel from DU <sub>$i$</sub>  to DR, the received signals on DR can be expressed as

$$\mathbf{y}_r = \underbrace{\begin{bmatrix} \mathbf{g}_1 & \cdots & \mathbf{g}_l \end{bmatrix}}_{\mathcal{G} \in \mathbb{C}^{N_d \times l}} P_d^{\frac{1}{2}} \mathbf{t} + \mathbf{q}_c + \mathbf{z}_r \quad (4.29)$$

where  $\mathbf{t} = [t_1 \ \cdots \ t_l]^T$ ,  $\mathbf{q}_c = \sum_{i=1}^s \mathbf{H}_{CU,i}^r \mathbf{u}_i P_c^{\frac{1}{2}} m_i$ , and  $\mathbf{z}_r$  denotes the noise on DR.

Since  $l \leq N_d$ , the signal  $\mathbf{t}$  can be decoded with a zero-forcing filter  $\mathcal{G}^{-1}$ , which leads to

$$\mathbf{y}'_r = P_d^{\frac{1}{2}} \mathbf{t} + \mathcal{G}^{-1}(\mathbf{q}_c + \mathbf{z}_r) \quad (4.30)$$

Then, the rate of D2D LAN can be expressed as

$$R_r = \log_2 \det(\mathbf{I} + \frac{\mathcal{G}\mathcal{G}^*}{(\mathbf{q}_c + \mathbf{z}_r)(\mathbf{q}_c + \mathbf{z}_r)^*}) \quad (4.31)$$

Note that the equivalent model in (4.29)-(4.31) is the same as that of in [38]. Hence, it can be proved in the same way as in [38] that the sum rate of D2D LAN scales as  $N_d \log_2(1 + \log(N_q))$ , which means the performance of the network can be improved by taking advantage of multiuser diversity.

#### 4.4.4 Discussion

As we can see, in this scheme, the number of active DUs is limited by  $l \leq \min\{N_d, N_q\}$ . Hence, as long as  $N_q \geq N_d$ , the number of active DUs can reach maximum. In addition, if there are a large number of DUs, this scheme can take advantage of multiuser diversity to improve the performance of D2D LAN.

## 4.5 Simulation Results

In this section, we examine the simulation performance of the networks.

Fig. 4.2 and Fig. 4.3 show the theoretical and simulation results of outage probabilities of each link of CU and DU with the use of ‘interference-free’ IA scheme, respectively, where the x-axis is the threshold of SINR in dB. We set  $N = 5$ ,  $N_d = 4$ , and  $M = M_d = 3$ . Three CUs communicate with eNB, i.e.,  $s = 3$ . Meanwhile, four DUs communicate with DR, whose signals are aligned in the two-dimensional orthogonal space of links of CUs at eNB. In addition, the transmitting power of CU is set to 10dB or 15dB and the power of DU is set to 20dB or 25dB. The theoretical results are obtained from (4.14) and (4.19) for cellular link and D2D link, respectively. We can see that the simulation results are matched almost perfectly with theoretical results. The outage probability of each link decreases when their transmitting power is increasing. Moreover, the outage probability of the link of CU remains the same

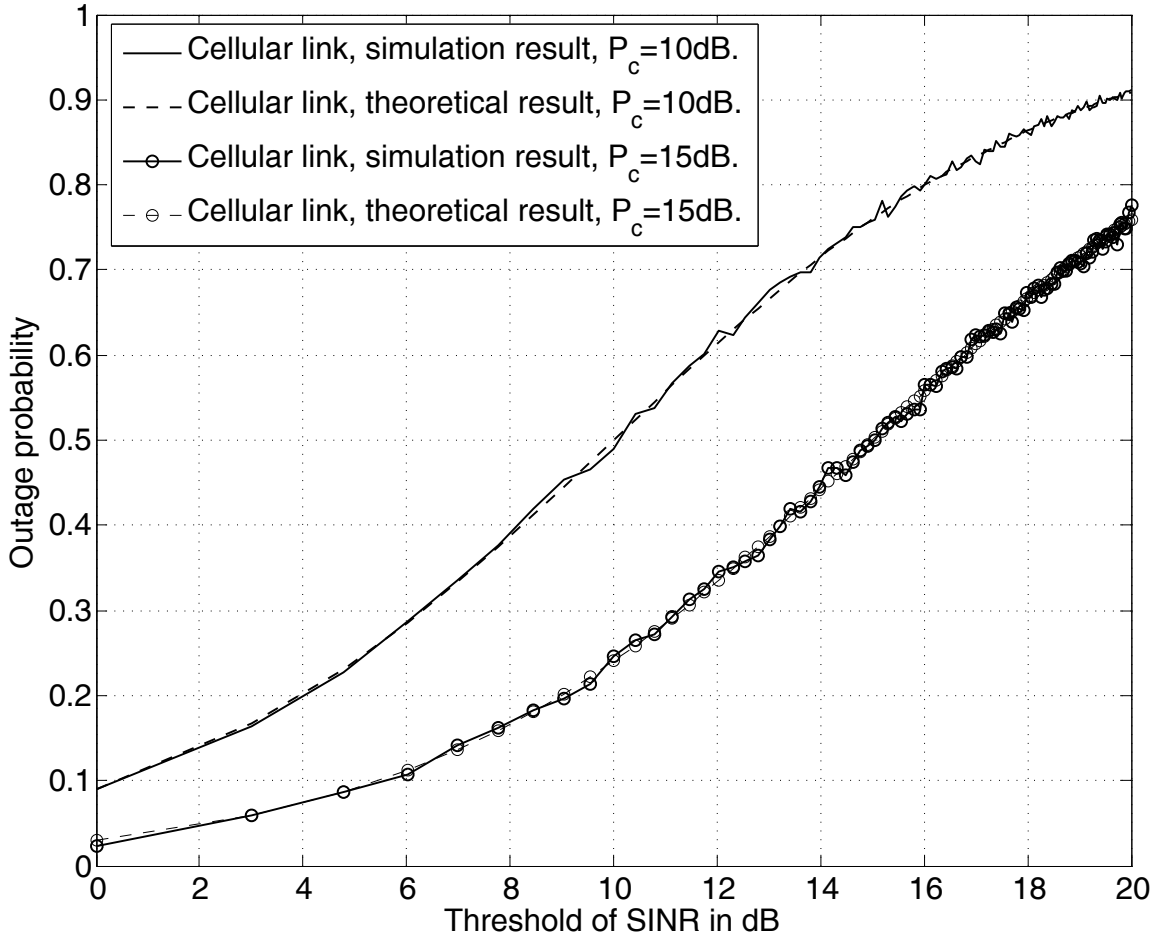


**Figure 4.2** Outage probability of cellular link with ‘interference-free’ IA scheme.

for different transmitting power on DU. This is because the interference signals from DU are completely nulled at links of CUs.

Fig. 4.4 shows the number of qualified DUs in the application of ‘interference-limiting’ IA scheme. Specifically, it depicts the growth of the number of qualified DUs with an increase of total DUs, under different threshold  $\gamma$ . In the simulation, we set three CUs communicating with eNB, i.e.,  $s = 3$ . In addition, each DU designs the precoding vector such that the interference signal does only affect the third link of CU. Then, the DU who can satisfy (4.26) is selected as a qualified user. The theoretical results are obtained from (4.28). As we can see, the theoretical results are

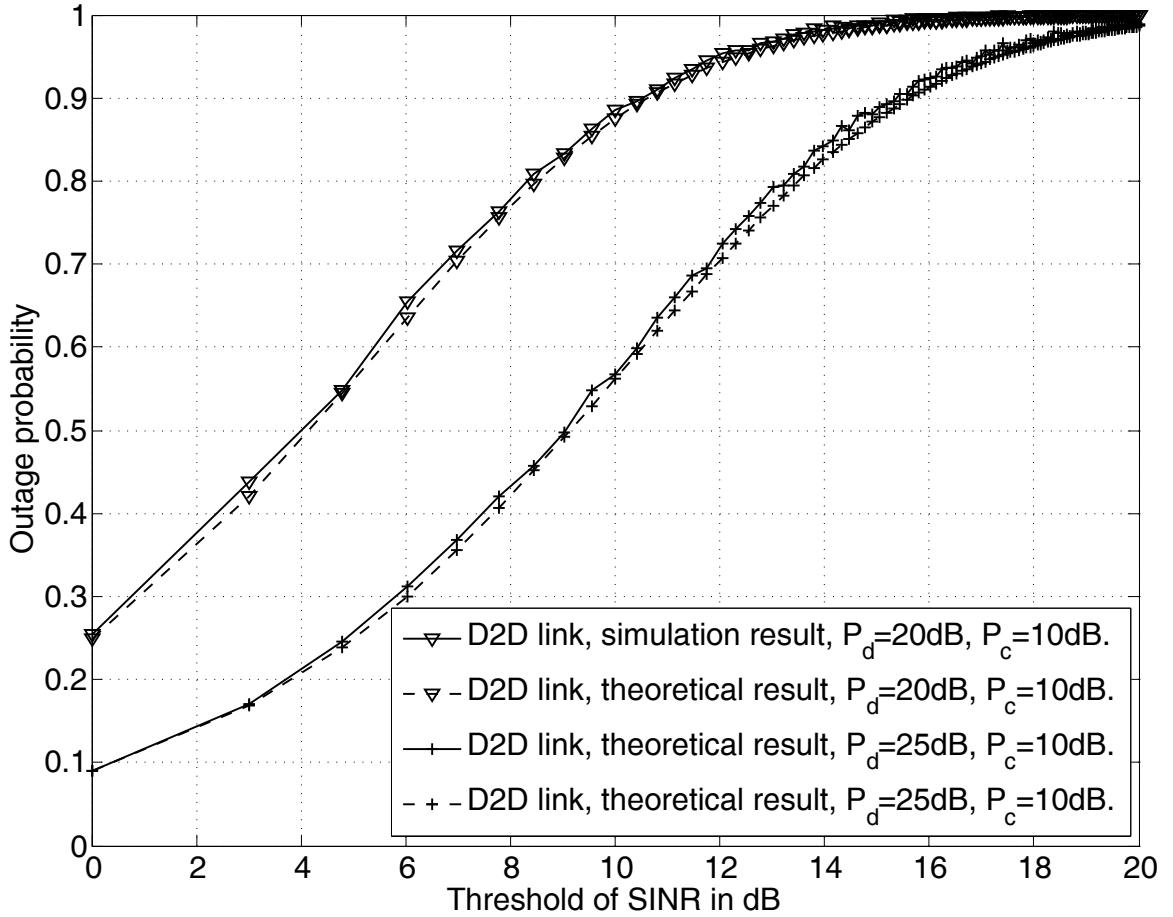


**Figure 4.3** Outage probability of D2D link with ‘interference-free’ IA scheme.

matched with simulation results perfectly. Hence, *Proposition 4.1* is verified in the figure. For instance, the number of qualified users increases almost linearly with the increase of total number of DUs. In addition, higher threshold leads to more qualified DUs because the probability of a DU satisfying (4.26) becomes higher.

Fig. 4.5 shows the simulation results and theoretical results of the outage probability of each interfered cellular link with ‘interference-limiting’ IA scheme, under different interference threshold  $\gamma$ . The system model in this simulation is the same as that in Fig. 4.4. The theoretical result is obtained according to (4.27). As we can see, the outage probability of the interfered cellular link increases when the interference threshold increases. This is because more interference power is allowed on the cellular

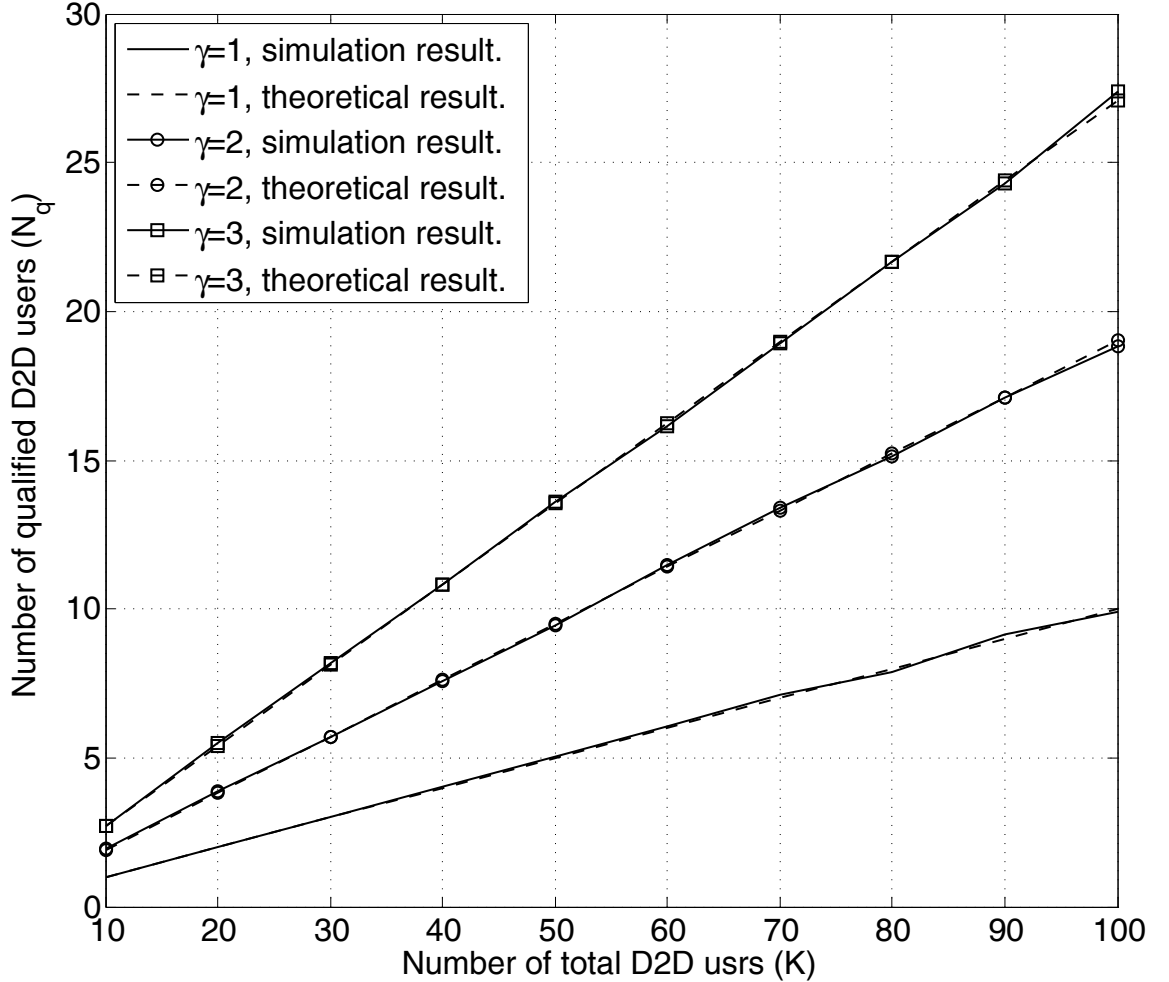


Figure 4.4 Number of qualified D2D users.

link.

Finally, in Fig. 4.6 we study the sum rate of the D2D LAN achieved with ‘interference-limiting’ schemes, under different transmitting power of DU and different number of DUs. We set  $M = M_d = 3$  and  $N = N_d = 4$ . Three CUs communicate with the eNB, i.e.,  $s = 3$ . In ‘interference-limiting’ IA scheme, SUS algorithm [37] is used to select active DUs from qualified DUs. Hence, the sum rate of D2D LAN can be calculated according to (4.31). Note that with ‘interference-limiting’ IA scheme, at most four DUs can be selected. As can be seen, ‘interference-limiting’ IA scheme can take advantage of multiuser diversity. When there are a large number of DUs,

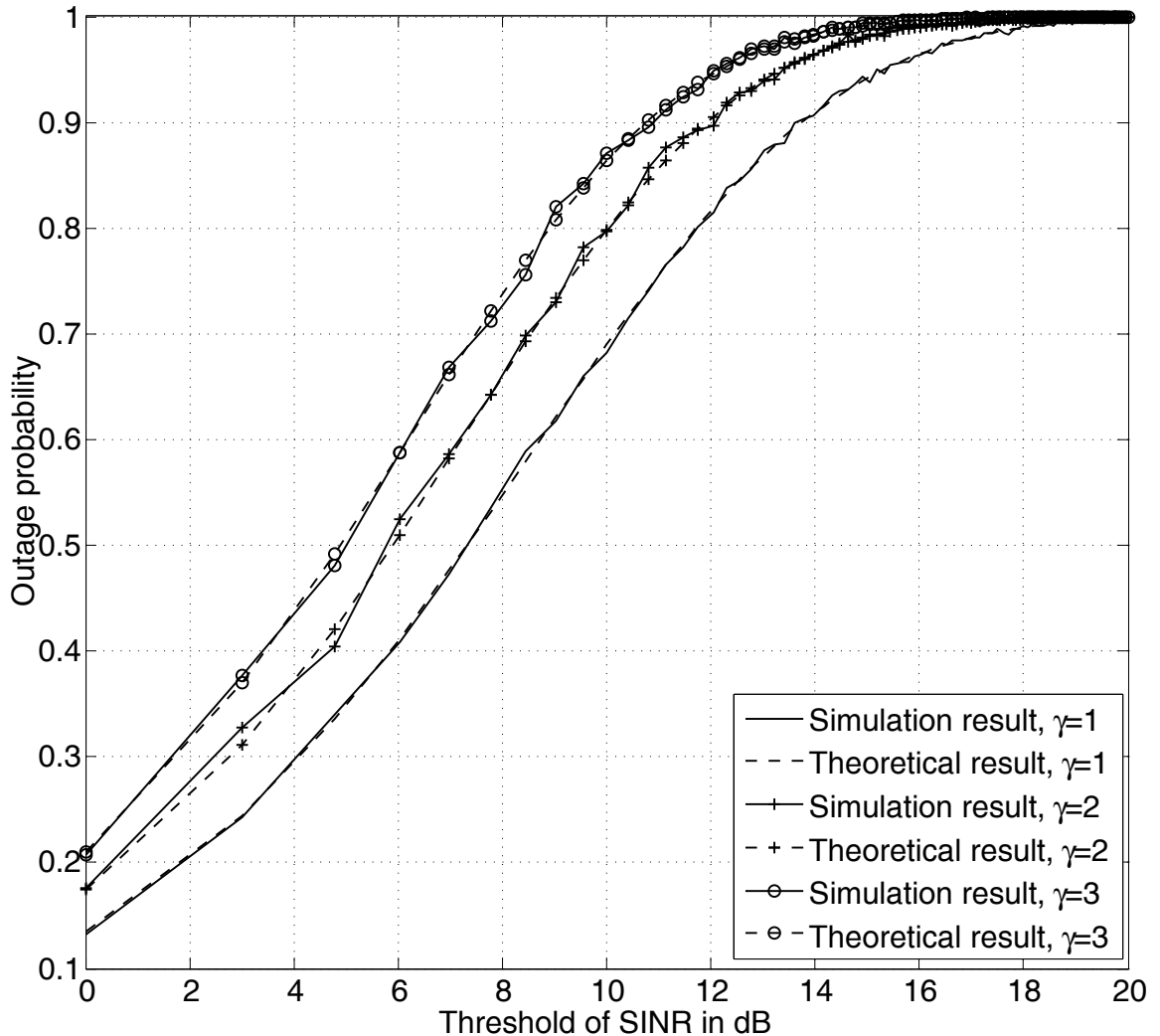


Figure 4.5 Outage probability of each interfered cellular link.

the performance of D2D LAN can be largely improved.

## 4.6 Summary

In this paper, we investigated IA in D2D LAN underlying a cellular uplink, where multiple DUs intend to communicate with a D2D receiver. Two schemes were proposed to effectively manage the mutual interference between the two networks for different scenarios. ‘Interference-free’ IA scheme is applicable when the number of

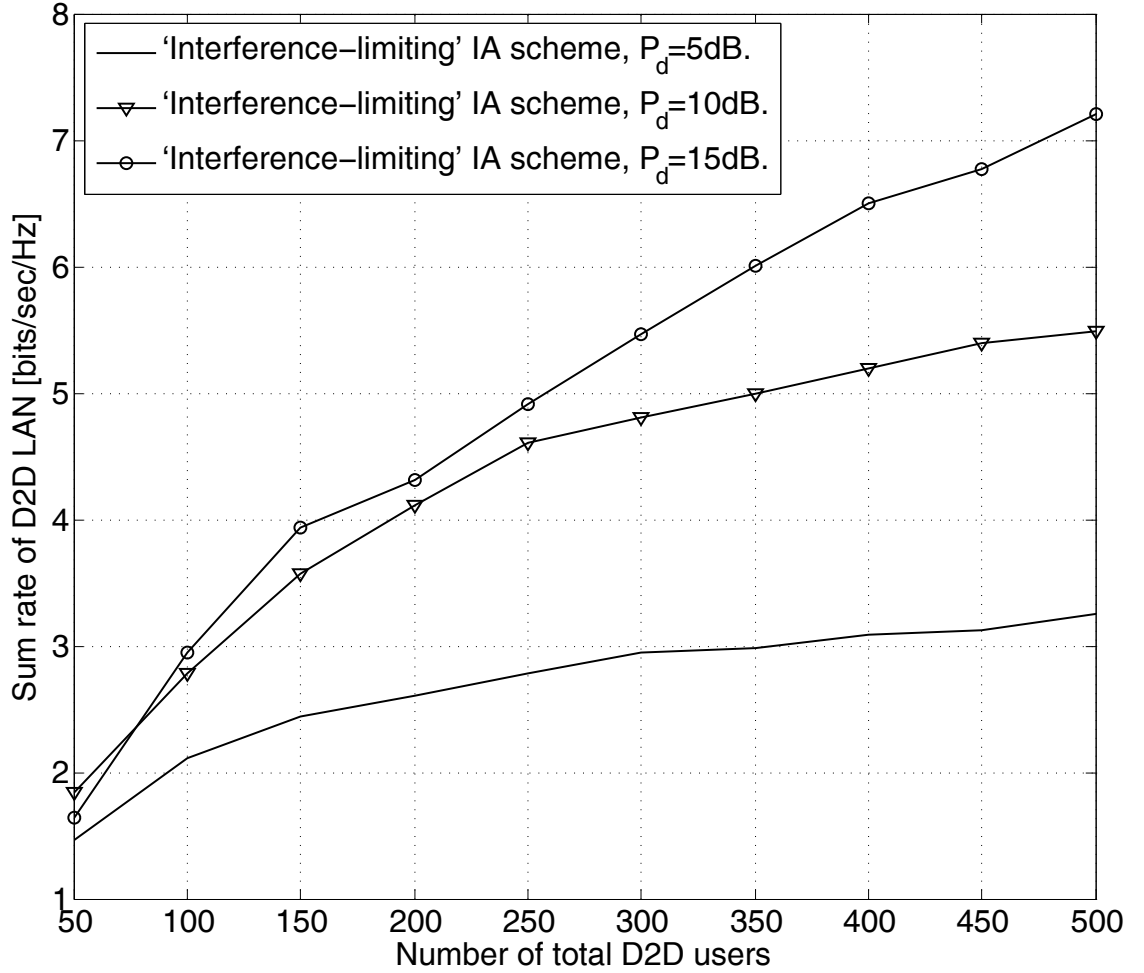


Figure 4.6 Achievable sum rate of D2D LAN.

DUs is small and the cellular links are not fully occupied, whereas ‘Interference-limiting’ IA scheme can be used in other cases. The performance of cellular and D2D networks with both schemes were analyzed. The theoretical results were corroborated by simulations.

## Appendix A: Proof of Theorem 4.4

The SINR of the  $k$ -th link of CUs can be expressed as

$$\phi_k = \frac{P_c |\lambda_k|^2}{|\mathbf{z}'_e(k)|^2 + P_d \sum_{i=1}^{N_d} |g_k^i|^2} \quad (4.32)$$

First, we let  $\Lambda$ ,  $Z$ , and  $\Theta_i$  denote  $|\lambda_k|^2$ ,  $|\mathbf{z}'_e(k)|^2$  and  $|\vartheta_k^i|^2$ , respectively, where their PDF is regardless of index  $k$ . In other words, they are i.i.d. for all  $k$ . Hence, (4.32) can be written as

$$\phi_k = \frac{P_c \Lambda}{Z + P_d \sum_{i=1}^{N_d} \Theta_i} \quad (4.33)$$

Accordingly, the outage probability of the  $k$ -th 'interfered' link of CUs can be expressed as follows,

$$\begin{aligned} P_{out} &= Pr[\phi_k \leq \alpha] \\ &= Pr[\Lambda \leq \frac{\alpha}{P_c} (Z + P_d \sum_{i=1}^{N_d} \Theta_i)] \\ &= 1 - Pr[\Lambda > \frac{\alpha}{P_c} (Z + P_d \sum_{i=1}^{N_d} \Theta_i)] \end{aligned} \quad (4.34)$$

Since  $\Lambda$  has exponential distribution, i.e.,  $\Lambda \sim \exp(1)$ , (4.34) can be further written as

$$\begin{aligned} P_{out} &= 1 - \mathbb{E}\{e^{-\frac{\alpha}{P_c} (Z + P_d \sum_{i=1}^{N_d} \Theta_i)}\} \\ &= 1 - \mathbb{E}\{e^{-\frac{\alpha}{P_c} Z}\} \cdot \prod_{i=1}^{N_d} \mathbb{E}\{e^{-\frac{\alpha P_d}{P_c} \Theta_i}\} \end{aligned} \quad (4.35)$$

$$= 1 - \int_0^{+\infty} e^{-\frac{\alpha}{P_c} z} f_Z(z) dz \cdot \prod_{i=1}^{N_d} \int_0^{\gamma'} e^{-\frac{\alpha P_d}{P_c} \theta} f_{\Theta_i}(\theta) d\theta \quad (4.36)$$

where  $\gamma' = \frac{\gamma}{P_d N_d}$ .

(4.35) is due to the fact that the variables  $Z$  and  $\Theta_i$  for  $i = 1, \dots, N_d$  are independent of each other. In addition,  $f_Z(z)$  and  $f_{\Theta_i}(\theta)$  denote the PDF of variables  $Z$  and  $\Theta_i$ , respectively. Based on *Theorem 4.2*, it can be shown that  $Z$  has exponential distribution, i.e.,  $Z \sim \exp(1)$ , which means

$$f_Z(z) = e^{-z} \text{ for } z \geq 0 \quad (4.37)$$

Next, we derive  $f_{\Theta_i}(\theta)$ . Since  $\Theta_i$  are i.i.d for  $i = 1, \dots, N_d$ , the index  $i$  of  $\Theta_i$  is omitted in the following discussions. Note that  $\Theta$  is from 0 to  $\gamma'$ , the CDF of  $\Theta$  is

$$F_{\Theta}(\theta) = \frac{1}{1 - e^{-\gamma'}}(1 - e^{-\theta}) \text{ for } 0 \leq \theta \leq \gamma' \quad (4.38)$$

which leads to

$$f_{\Theta}(\theta) = F'_{\Theta}(\theta) = \frac{e^{-\theta}}{1 - e^{-\gamma'}} \quad (4.39)$$

Then, by taking (4.37) and (4.39) into (4.36), we can obtain (4.27).

## Appendix B: Proof of Proposition 4.1

The interference constraint on each link is  $\gamma$ , which can be surely guaranteed by limiting the interference generated by each DU to be less than  $\frac{\gamma}{l}$ . Further, since  $l \leq N_d$ , we have (4.26) as the condition that should be satisfied for each selected DU, which is equivalent to

$$|\vartheta_{k'}^i|^2 \leq \gamma', \quad \forall k' = M_d, M_d + 1, \dots, s \quad (4.40)$$

where  $\gamma' = \frac{\gamma}{F_d N_d}$ .

Hence, the DU who can satisfy (4.40) is qualified for D2D communications with DR. Let  $p_i$  denote the probability of  $\text{DU}_i$  satisfying (4.40), we have  $p_1 = p_2 = \dots = p_K = p_q$ , which is equal to the probability of  $|\vartheta_{k'}^i|^2 \leq \gamma', \quad \forall k' = M_d, M_d + 1, \dots, s$ .

Further, since the CDF of  $|\vartheta_{k'}^i|^2$  is given in (4.38) as  $F_{\vartheta}(x)$ , we have

$$p_q = [F_{\vartheta}(\gamma')]^{s-M_d+1} = (1 - e^{-\gamma'})^{s-M_d+1} \quad (4.41)$$

Finally, the average number of qualified users satisfying the interference constraint is  $N_q \approx K(1 - e^{-\gamma'})^{s-M_d+1}$ .

# Chapter 5

## Conclusion and Future Work

### 5.1 Thesis Conclusion

Interference alignment techniques have been extensively studied from both theoretical and practical perspectives. In the field of information theory, IA has been known as a powerful tool to characterize the DoF of a variety of networks, which is an important metric that can be used to approximate the capacity of network. In practical field, IA can serve as an effective interference coordination mechanism to improve the performance of communications. However, many problems still remain open in theoretical research. In addition, it is challenging to integrate IA schemes into newly emerged communication technologies. This thesis aims to solve some open problems in the DoF characterization of MIMO X channels and interference channels, as well as design IA-based interference management schemes.

In Chapter 2, a linear interference alignment framework in combination with asymmetric complex signaling is proposed for MIMO X channels. It is shown that based on the proposed scheme, the DoF of  $\lfloor D_{outer} \rfloor + \frac{1}{2}$  can be achieved if  $D_{outer} - \lfloor D_{outer} \rfloor \geq \frac{1}{2}$ , and  $\lfloor D_{outer} \rfloor$  can be achieved otherwise, without the use of symbol extensions in time, frequency, or space. Note that with conventional linear schemes that based on spatial beamforming, the maximum achievable DoF equals  $\lfloor D_{outer} \rfloor$ . Our result shows

that the technique of asymmetric complex signaling, which was originally proposed for single-antenna systems, can provide DoF benefit for MIMO systems as well when symbol extensions are not allowed.

In Chapter 3, the DoF region of three-user MIMO interference channel is investigated, where each transmitter and each receiver is equipped with  $M_T$  and  $M_R$  antennas. The outer bound of DoF region was shown first. Then, a linear beamforming scheme based on alignment chain was proposed, which can achieve all the integer DoF inside the outer bound DoF region. This work completely solved the problem of feasibility of IA in such three-user interference channels, Further, it provides a DoF region that is tight in terms of integer DoF. Finally, the achievability of fractional DoF within the outer bound region with the proposed scheme in combination with symbol extension is also addressed.

In Chapter 4, IA techniques is investigated in the context of D2D LAN underlaying a cellular uplink, where multiple DUs intend to communicate with a D2D receiver. Two schemes were proposed to effectively manage the mutual interference between the two networks for different scenarios. ‘Interference-free’ IA scheme is applicable when the number of DUs is small and the cellular links are not fully occupied, while ‘Interference-limiting’ IA scheme can be used in other cases. The performance of two networks with both schemes were analyzed. The advantages and limitations of two schemes were discussed. The theoretical results were corroborated with simulations. Performance analysis shows that based on the proposed schemes, the interference generated on the cellular links is eliminated or well controlled, while the quality of service of the D2D LAN can also be guaranteed.

## 5.2 Future Work

Apart from the problems addressed in this thesis, there are some interesting and challenging topics to be investigated in the future.

- In this thesis, an outer bound DoF region of three-user interference channel is

derived and further shown to be tight in terms of integer DoF. However, as mentioned in Chapter 3, there is lack of a method to prove that all fractional DoF in the region is achievable, we cannot claim that the region is tight. In order to achieve fractional DoF, symbol extension must be used, which will make the equivalent channel into a block diagonal form. The challenge is to show that the equivalent channels with block diagonal form behave the same as generic channels, especially under block fading channel conditions.

- Most IA techniques take advantage of distinct channel rotations by beamforming at transmitters, which means the channel state information (CSI) is required at transmitters. If we are only interested in the optimal DoF in theory, we can simply assume that each transmitter has perfect CSI. However, in practice, the CSI is usually estimated at receivers and then fed back to the transmitters [80], which means the CSI at transmitters must be imperfect. Hence, it is interesting and necessary to investigate the impact of imperfect CSI on the performance of IA. In fact, there has been some works focusing on the scenarios where the CSI at transmitters is perfect but outdated due to the channel variations [81–85]. On the other hand, we should note that the feedback of CSI is usually expressed with a sequence of binary bits, which means the received CSI is quantized instead of original [86]. Hence, such quantized feedback of CSI can certainly bring inaccuracy to the alignment, and hence lead to interference leakage [75, 87]. In the future work, we will investigate the impact of quantized feedback on IA for various communication networks, such as D2D communications.

# Bibliography

- [1] R. Zhang and S. Cui, "Cooperative interference management with MISO beamforming," *IEEE Trans. on Signal Processing*, vol. 58, no. 10, pp. 5450-5458, Oct. 2010.
- [2] A. shaverdian and M. Nakhai, "Robust distributed beamforming with interference coordination in downlink cellular networks," *IEEE Trans. Communications*, vol. 62, no. 7, pp. 2411-2421, July 2014.
- [3] V. Cadambe and S. Jafar, "Interference alignment and degrees of freedom of the  $K$ -user interference channel," *IEEE Trans. Inf. Theory*, vol. 54, no. 8, pp. 3425-3441, Aug. 2008.
- [4] M. Maddah-Ali, A. Motahari, and A. Khandani, "Communication over MIMO X channels: interference alignment, decomposition, and performance analysis," *IEEE Trans. Inf. Theory*, vol. 54, no. 8, pp. 3457-3470, Aug. 2008.
- [5] L. Zheng and D. Tse, "Communication on the grassmann manifold: a geometric approach to the noncoherent multiple-antenna channel" *IEEE Trans. Inf. Theory*, vol. 48, no. 2, pp. 359-383, Feb. 2002.
- [6] L. Zheng and D. Tse, "Diversity and multiplexing: a fundamental tradeoff in multiple antenna channels" *IEEE Trans. Inf. Theory*, vol. 1, no. 8, pp.2-25, Aug. 2002.
- [7] D. Tse and P. viswanath, "*Fundamentals of wireless communications*," Cambridge university press, 2005.
- [8] M. Maddah-Ali, A. Motahari, and A. Khandani, "Signaling over MIMO multi-base systems: combination of multiaccess and broadcast schemes," *Proc. IEEE International Symposium on Information Theory (ISIT)*, Seattle, USA, July 9-14, 2006, pp. 2104-2108.
- [9] S. Jafar and S. Shamai, "Degrees of freedom region for the MIMO X channel," *IEEE Trans. Inf. Theory*, vol. 54, no. 1, pp. 151-170, Jan. 2008.

- [10] K. Gomadam, V. Cadambe, and S. Jafar, "A distributed numerical approach to interference alignment and applications to wireless interference networks" *IEEE Trans. Inf. Theory*, vol. 57, no. 6, pp. 3309-3322, June 2011.
- [11] S. Avestimehr, S. Diggavi, and D. Tse, "Deterministic approach to wireless relay networks," *Proc. Allerton Conf. on Commun., Control, and Computing*, Monticello, IL, Sep, 2007.
- [12] G. Bresler, A. Parekh, and D. Tse, "The approximate capacity of the many-to-one and one-to-many Gaussian interference channel," *IEEE Trans. Inf. Theory*, vol. 56, no. 9, pp. 4566-4580, Sep. 2010.
- [13] V. Cadambe, S. Jafar, and S. Shamai, "Interference alignment on the deterministic channel and application to Gaussian networks," *IEEE Trans. Inf. Theory*, vol. 55, no. 1, pp. 269-274, Jan. 2009.
- [14] A. Motahari, S. Oveis-Gharan, M. Maddah-Ali, and A. Khandani, "Real interference alignment: exploiting the potential of single antenna systems," *IEEE Trans. Inf. Theory*, vol. 60, no. 8, pp. 4799-4810, Aug. 2014.
- [15] S. Mahboubi, A. Motahari, and A. Khandani, "Layered interference alignment: achieving the total DoF of MIMO X-channels," *Proc. IEEE International Symposium on Information Theory (ISIT)*, Austin, USA, June 13-18, 2010.
- [16] M. Maddah-Ali, "On the degrees of freedom of the compound MIMO broadcast channels with finite states," in <http://arxiv.org/abs/0909.5006v3>.
- [17] R. Etkin and E. Ordentlich, "The degrees of freedom of the  $K$ -user Gaussian interference channel is discontinuous at rational channel coefficients" *IEEE Trans. Inf. Theory*, vol. 55, no. 11, pp. 4932-4946, Nov. 2009.
- [18] V. Cadambe and S. Jafar, "Interference alignment and degrees of freedom of wireless X networks," *IEEE Trans. Inf. Theory*, vol. 55, no. 9, pp. 3893-3908, Sep. 2009.
- [19] H. Sun, T. Gou and S. Jafar, "Degrees of freedom of MIMO X networks: spatial scale invariance and one-sided decomposability," *IEEE Trans. Inf. Theory*, vol. 59, no. 12, pp. 2432-2479, May 2014.
- [20] S. Jafar and M. Fakhereddin, "Degrees of freedom for the MIMO interference channel" *IEEE Trans. Inf. Theory*, vol. 53, no. 7, pp.2637-2641, July 2007.
- [21] T. Gou and S. Jafar, "Degree of freedom of the  $K$ -user  $M \times N$  MIMO interference channel," *IEEE Trans. Inf. Theory*, vol. 56, no. 12, pp. 6040-6057, Dec. 2010.
- [22] C. Wang, T. Gou and S. Jafar, "Subspace alignment chains and the degree of freedom of the three-user MIMO interference channel" *IEEE Trans. Inf. Theory*, vol. 60, no. 5, pp. 2432-2479, May 2014.

- 
- [23] M. Torrellas, A. Agustin, J. Vidal and O. Munoz, "The DoF of the 3-user  $(p,p+1)$  MIMO interference channel," *IEEE Trans. Communications*, vol. 62, no. 11, pp. 3842-3853, Sept. 2014.
- [24] V. Cadambe, S. Jafar, and C. Wang, "Interference alignment with asymmetric complex signaling—setting the Host-Madsen-Nosratinia conjecture," *IEEE Trans. Inf. Theory*, vol. 56, no. 9, pp. 4552-4565, Sep. 2010.
- [25] C. Yetis, T. Gou, S. Jafar and A. Kayran, "On feasibility of interference alignment in MIMO interference network," *IEEE Trans. Signal Processing*, vol. 58, no. 9, pp. 4771-4782, Sept. 2010.
- [26] M. Razaviyayn, G. Lyubeznik and Z. Luo, "On the Degrees of freedom achievable through interference alignment in a MIMO interference channel," *IEEE Trans. Signal Processing*, vol. 60, no. 2, pp. 812-821, Feb. 2012.
- [27] M. Razaviyayn, M. Sanjabi and Z. Luo, "Linear transceiver design for interference alignment: complexity and computation," *IEEE Trans. Inf. Theory*, vol. 58, no. 5, pp. 2896-2910, May 2012.
- [28] G. Bresler, D. Cartwright and D. Tse, "Feasibility of interference alignment for the MIMO interference channel", *IEEE Trans. Inf. Theory*, vol. 60, no. 9, pp. 5573-5587, Sep. 2014.
- [29] G. Bresler, D. Cartwright, and D. Tse "Geometry of the 3-user MIMO interference channel," *Proc. Allerton Conf. on Commun., Control, and Computing*, 2011, pp. 1264-1271.
- [30] C. Suh and D. Tse, "Interference alignment for cellular network," *Proc. 46th Annual Allerton Conf. on Commun., Control, and Computing*, Sep. 23-26, 2008, pp. 1037-1044.
- [31] B. C. Jung, D. Park, and W. Shin, "Opportunistic interference mitigation achieves optimal degrees-of-freedom in wireless multi-cell uplink networks" *IEEE Trans. Communication*, vol. 60, no.7, pp.1935-1944, July 2012.
- [32] L. Yang and W. Zhang, "Opportunistic interference alignment in heterogeneous two-cell uplink network," *Proc. IEEE International Conference on Communications*, (ICC 2013), Budapest, Hungary, June 9-13, 2013, pp. 5448-5452.
- [33] W. Shin, N. Lee, J. Lim, C. Shin, and K. Jang, "On the design of interference alignment scheme for two-cell MIMO interference broadcast channels," *IEEE Trans. Wireless Commun.*, vol. 10, no. 2, pp. 437-442, Feb. 2011.
- [34] C. Suh, M. Ho, J. Lim, and D. Tse, "Downlink interference alignment," *IEEE Trans. Commun.*, vol. 59, no. 9, pp. 2616-2626, Sep. 2011.

- [35] S. M. Perlaza, N. Fawaz, S. Lasaulce, and M. Debbah, "From spectrum pooling to space pooling: opportunistic interference alignment in MIMO cognitive networks," *IEEE Trans on Signal Processing*, vol. 58, No.7, pp. 3728-3741, July 2010.
- [36] M. Amir, A El-Keyi, and M. Nafle, "Opportunistic interference alignment for multiuser cognitive radio," *Proc. IEEE Information Theory Workshop*, Cairo, Egypt, Jan. 6-8, 2010.
- [37] T. Yoo and A. Goldsmith, "On the optimality of multiantenna broadcast scheduling using zero-forcing beamforming," *IEEE Journal. Selected Areas in Communications*, vol. 24, no. 3, pp. 528-541, Mar. 2006.
- [38] L. Yang, W. Zhang, N. Zheng, and P. C. Ching, "Opportunistic user scheduling in MIMO cognitive radio networks," *Proc. IEEE International Conference on Acoustics, Speech and Signal Processing*, (ICASSP 2014), Florence, Italy, May 4-9, 2014, pp. 7303-7307.
- [39] T. Gou, S. Jafar, C. Wang, S. Jeon, and S. Chung, "Aligned interference neutralization and the degrees of freedom of the  $2 \times 2 \times 2$  interference channel," *IEEE Trans. Inf. Theory*, vol. 58, no. 7, pp. 4381-4395, July 2012.
- [40] Z. Wang, M. Xiao, C. Wang and M. Skoglund, "Degrees of freedom of multi-hop MIMO broadcast networks with delayed CSIT" *IEEE Comm. Letter*, vol. 2, no. 2, pp. 207-210, April 2013.
- [41] L. Yang and W. Zhang, "Degrees of freedom of relay-assisted MIMO interfering broadcast channels," *Proc. IEEE Globe Communications Conference* (Globecom), Austin, TX, USA, Dec. 8-12, 2014.
- [42] N. Lee and R. Heath Jr, "Degrees of freedom for the two-cell two-hop MIMO interference channel: interference-free relay transmission and spectrally efficient relaying protocol," *IEEE Trans. Inf. Theory*, vol. 59, no. 5, pp. 2882-2896, May 2013.
- [43] V. Cadambe, S. Jafar, H. Maleki, K. Ramchandran, and C. Suh, "Asymptotic interference alignment for optimal repair of MDS codes in distributed storage," *IEEE Trans. Inf. Theory*, vol. 59, no. 5, pp. 2974-2987, May 2013.
- [44] O. Ayach, S. Peters, and R. Heath Jr, "Feasibility of Interference Alignment of Measured MIMO-OFDM Channels," *IEEE Trans. on Veh. Tech.*, vol. 59, no. 9, pp. 4309-4321, Nov. 2010.
- [45] O. Ayach, S. Peters, and R. Heath Jr, "The Practical Challenges of Interference Alignment," *IEEE Trans. Wireless Comm.*, vol. 20, no. 1, pp. 35-42, Feb. 2013.
- [46] N. Lee and R. Heath Jr, "Space-time physical-layer network coding," *IEEE Journal on Selected Areas in Comm.*, accepted for publication, 2014.

- [47] S. Gollakota, S. Perli, and D. Katabi, "Interference alignment and cancellation," *ACM SIGCOMM Computer Communication Review*, vol. 39, no. 4, ACM, 2009.
- [48] J. Angreus, S. Buzzi, W. Choi, S. Hanly, A. Lozano, A. Soong, and J. Zhang, "What will 5G be," *IEEE Journal on Selected Areas in Comm.*, vol. 32, no. 6, pp. 1065-1082, June 2014.
- [49] M. Marcus and B. Pattan, "Millimeter wave propagation: spectrum management implications," *IEEE Microwave Magazine*, vol. 6, no. 2, pp. 54-62, June 2005.
- [50] W. Roh, J. Seol, J. Park, B. Lee, J. Lee, Y. Kim, J. Cho, K. Cheun, and F. Aryanfar, "Millimeter-wave beamforming as an enabling technology for 5G cellular communications: theoretical feasibility and prototype results," *IEEE Comm. Magazine*, vol. 52, no. 2, pp. 106-113, Feb. 2014.
- [51] S. Rangan, T. Rappaport, and E. Erkip, "Millimeter-wave cellular wireless networks: potentials and challenges," *Proceedings of IEEE*, vol. 102, no. 3, pp. 366-385, Mar. 2014.
- [52] T. Marzetta, "Noncooperative cellular wireless with unlimited numbers of base station antennas," *IEEE Trans. Wireless Commun.*, vol. 9, no. 11, pp. 3590-3600, Nov. 2010.
- [53] F. Rusek, D. Persson, B. Lau, E. Larsson, T. Marzetta, O. Edfors and F. Tufveson, "Scaling up MIMO: opportunities and challenges with very large arrays," *IEEE Signal Processing Magazine*, vol. 30, no. 1, pp. 40-60, Jan. 2013.
- [54] K. Doppler, M. Rinne, C. Wijting, C. B. Ribeiro, and K. Hugl, "Device-to-device communication as an underlay to LTE-advanced networks," *IEEE Communications Magazine*, vol. 47, no. 12, pp. 42-49, Dec. 2009.
- [55] Y. Lin and Y. Hsu, "Multihop cellular: a new architecture for wireless communications," in *Proc. IEEE INFOCOM*, Israel, pp. 1273-1282, Mar. 26-30, 2000.
- [56] A. Asadi, Q. Wang, and V. Mancuso, "A survey on device-to-device communication in cellular networks," *IEEE Communications Surveys and Tutorials*, accepted.
- [57] C.-H. Yu, K. Doppler, C. B. Ribeiro, and O. Tirkkonen, "Resource Sharing Optimization for Device-to-Device Communication Underlying Cellular Networks," *IEEE Trans. Wireless Commun.*, vol. 10, no. 8, pp. 2752-2763, August 2011.
- [58] P. Phunchongharn, E. Hossain, and D. I. Kim, "Resource allocation for device-to-device communications underlying LTE-advanced networks," *IEEE Wireless Communications Magazine*, vol. 20, no. 4, pp. 91-100, Aug. 2013.

- [59] D. Feng, L. Lu, Y. Wu, G. Y. Li, G. Feng, and S. Li, "Device-to-device communications underlying cellular networks," *IEEE Trans. Communications*, vol. 61, no. 8, pp. 3541-3551, Aug. 2013.
- [60] H. Min, J. Lee, S. Park and D. Hong, "Capacity enhancement using an interference limited area for device-to-device uplink underlying cellular networks," *IEEE Trans. Wireless Commun.*, vol. 10, no. 12, pp. 3995-4000, Dec. 2011.
- [61] H. Min, W. Seo, J. Lee, S. Park, and D. Hong, "Reliability improvement using receive mode selection in the device-to-device uplink period underlying cellular networks" *IEEE Trans. Wireless Commun.*, vol. 10, no. 2, pp. 413-418, Feb. 2011.
- [62] L. Song, D. Niyato, Z. Han, and E. Hossain, "Game-theoretic Resource Allocation Methods for Device-to-Device (D2D) Communication," *IEEE Wireless Comm. Magazine*, pp. 136-144, June 2014.
- [63] T. Wang, L. Song, and Z. Han, "Coalitional graph games for popular content distribution in cognitive radio VANETs," *IEEE Trans. Veh. Technology*, vol. 62, no. 8, pp. 4010-4019, Oct. 2013.
- [64] T. Wang, L. Song, Z. Han, and B. Jiao, "Dynamic popular content distribution in vehicular networks using coalition formation games," *IEEE Journal on Selected Areas in Communications*, vol. 31, no. 9, pp. 538-547, Sep. 2013.
- [65] F. Pantisano, M. Bennis, W. Saad, M. Debbah, and M. Latva-aho, "Interference alignment for cooperative femtocell networks: a game theoretic approach," *IEEE Trans. on Mobile Computing*, vol. 12, no. 11, pp. 2233 - 2246, Nov. 2013.
- [66] F. Boccardi, B. Clerckx, A. Ghosh, E. Hardouin, G. Jongren, K. Kusume, E. Onggosanusi, and Y. Tang, "Multiple antenna techniques in LTE-Advanced," *IEEE Communications Magazine*, vol. 50, no. 3, pp. 114-121, Mar. 2012.
- [67] C. Lim, T. Yoo, B. Clerckx, B. Lee, and B. Shim, "Recent trend of multiuser MIMO in LTE-Advanced," *IEEE Communications Magazine*, vol. 51, no. 3, pp. 127-135, Mar. 2013.
- [68] P. Janis, V. Koivunen, C. Riberiro, K. Doppler, and K. Hugl, "Interference-avoiding MIMO schemes for device-to-device radio underlying cellular network," in *Proc. IEEE Pers. Indoor and Mobile Radio Communications Symp.(PIMRC)*, Tokyo, Japan, Sept.13-16, 2009.
- [69] W. Xu, L. Liang, H. Zhang, S. Jin, J. Li, and M. Lei, "Performance enhanced transmission in device-to-device communications: beamforming or interference cancellation?" in *Proc. IEEE Global Communications Conference (GLOBECOM 2012)*, Anaheim, California, USA, Dec. 3-7, 2012.

- [70] H. Tang, C. Zhu, and Z. Ding, "Cooperative MIMO precoding for D2D underlay in cellular networks," in *Proc. IEEE Int. Conf. on Communications (ICC)*, Budapest, Hungary, June 9-13, 2013.
- [71] H. Elkotby, K. Elsayed, and M. H. Ismail, "Exploiting interference alignment for sum rate enhancement in D2D-enabled cellular networks," in *Proc. IEEE Wireless Communications and Networking Conference*, Paris, France, April 1-4, 2012.
- [72] J. Jiang, M. Peng, W. Wang, and K. Zhang, "Energy efficiency optimization based on interference alignment for device-to-device MIMO downlink underlaying cellular network," in *Proc. IEEE Global Communications Conference (Globecom 2013)-International Workshop on Device-to-Device (D2D) Communication With and Without Infrastructure*, Atlanta, GA, USA, Dec. 9-13, 2013, pp. 585-590.
- [73] L. Yang and W. Zhang, "Opportunistic interference alignment in heterogeneous two-cell uplink network," in *Proc. IEEE International Conference on Communications (ICC 2013)*, Budapest, Hungary, June 9-13, 2013, pp. 5448-5452.
- [74] O. Ayach and R. Heath Jr., "Interference alignment with analog channel state feedback," *IEEE Trans. Wireless Commun.*, vol. 11, no. 2, pp. 626-636, Feb. 2012.
- [75] O. Ayach, A. Lozano, and R. Heath Jr., "On the overhead of interference alignment: training, feedback, and cooperation," *IEEE Trans. Wireless Commun.*, vol. 11, no. 11, pp. 4192-4203, Nov. 2012.
- [76] N. Jindal, "MIMO broadcast channels with finite-rate feedback," *IEEE Trans. Inf. Theory*, vol. 52, no. 11, pp. 5045-5060, Nov. 2006.
- [77] D. Love, R. Heath Jr., V. K. N. Lau, D. Gesbert, B. D. Rao, and M. Andrews, "An overview of limited feedback in wireless communication systems," *IEEE Journal on Selected Areas in Communications*, vol. 26, no. 8, pp. 1341-1365, Oct. 2008.
- [78] S. Cho, K. Huang, D. Kim, V. K. N. Lau, H. Chae, H. Seo, and B. Kim, "Feedback-topology designs for interference alignment in MIMO interference channels," *IEEE Trans. Sig. Processing*, vol. 60, no. 12, pp. 6561-6575, Dec. 2012.
- [79] I. S. Gradshteyn and I. M. Ryzhik, "Tables of integrals, series, and products," San Diego, CA: Academic Press, Inc, 1994.
- [80] D. Love, R. Heath Jr, V. Lau, D. Gesbert, B. Rao, and M. Andrews, "An overview of limited feedback in wireless communication systems," *IEEE Journal on Selected Areas in Comm.*, vol. 26, no. 8, pp. 1341-1365, Oct. 2008.
- [81] H. Maleki, S. Jafar, and S. Shamai, "Retrospective interference alignment over interference networks," *IEEE Journal on Selected Topics in Signal Processing*, vol. 6, no. 3, pp. 228-240, May 2012.

- 
- [82] M. Maddah-Ali and D. Tse, "Completely Stale Transmitter Channel State Information is Still Very Useful," *IEEE Trans. Inf. Theory*, vol. 58, no. 7, pp.4418-4431, July 2012.
- [83] C. Vaze and M. Varanasi, "The degrees of freedom region and interference alignment for the MIMO interference channel with delayed CSIT," *IEEE Trans. on Inf. Theory*, vol. 58, no. 7, pp.4396-4416, July 2012.
- [84] C. Vaze and M. Varanasi, "The degrees of freedom region of the MIMO interference channel with Shannon feedback," *IEEE Trans. Inf. Theory*, vol. 59, no. 8, pp.4798-4810, Aug. 2013.
- [85] N. Lee and R. Heath Jr, "Distributed space time interference alignment with moderately-delayed CSIT," *IEEE Trans. on Wireless Commun.*, early access, Oct. 2014.
- [86] N. Jindal, "MIMO broadcast channel with finit-rate feedback," *IEEE Trans. on Inf. Theory*, vol. 52, no. 11, pp.5045-5060, Nov. 2006.
- [87] R. Krishnamachari and K. Varanasi, "Interference alignment under limited feedback for MIMO interference channels," *IEEE Trans. on Signal Processing*, vol. 61, no. 15, pp. 3908-3917, Aug. 2013.